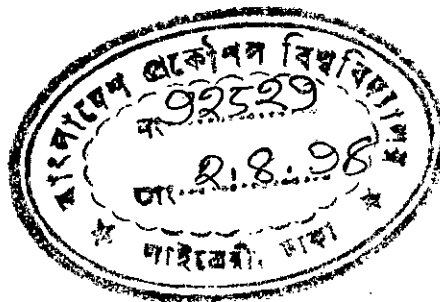


IMPACT OF FIBRE CHROMATIC DISPERSION ON THE PERFORMANCE OF A WDM OPTICAL RING NETWORK

A Thesis submitted to the Electrical and Electronic Engineering
Department of BUET, Dhaka, in partial fulfillment of the requirements
for the degree of Master of Science in Engineering
(Electrical & Electronic)



MD. RAFIQUUL ISLAM

May 1998



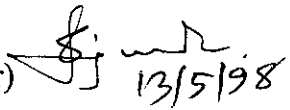
DEDICATED TO
THE DEPARTED SOUL OF MY MOTHER

APPROVAL

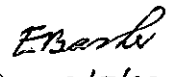
The thesis titled “Impact of Fibre Chromatic Dispersion on the Performance of a WDM Optical Ring Network” submitted by Md. Rafiqul Islam , Roll No. 9406228F, Session 1993-94-95 to the Electrical and Electronic Engineering Department of BUET has been accepted as satisfactory for partial fulfillment of the requirements for the degree of Master of Science in Engineering (Electrical and Electronic)

Board of Examiners

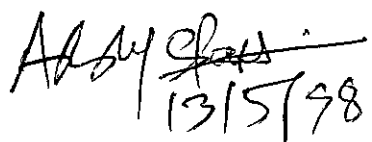
1. Dr. Satya Prasad Majumder
Professor
Department of EEE
BUET, Dhaka-1000.

Chairman
(Supervisor) 
13/5/98

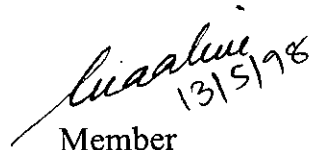
2. Dr. Enamul Basher
Professor and Head
Department of EEE
BUET, Dhaka-1000.

Member 
(Ex-officio) 13/5/98

3. Dr. A.B.M. Siddique Hossain
Professor
Department of EEE
BUET, Dhaka-1000.

Member 
13/5/98

4. Md. Ashraful Alim
Divisional Engineer
Bangladesh T & T Board
37/E Eskaton Garden, Dhaka-1000.

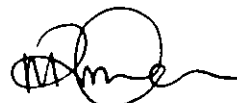

13/5/98
Member
(External)

DECLARATION

This work has been done by me and it has not been submitted elsewhere the award of any degree or diploma.

Countersigned

 13.5.98
(Dr. Satya Prasad Majumder)

 13.5.98
(Md. Rafiqul Islam)

Supervisor

CONTENTS

ACKNOWLEDGMENTS	vii
ABSTRACT	viii
LIST OF FIGURES	ix
LIST OF PRINCIPAL SYMBOLS	xiii
LIST OF ABBREVIATIONS	xiv
1.1 INTRODUCTION	1
1.2 Overview of Optical Fibre Communication System	3
1.3 Present Status and Future Prospects of Optical Fibre Communication in Bangladesh.	8
1.3.1 Present Status	8
1.3.2 Proposed Dhaka-Chittagong Optical fibre link	9
1.3.3 Future Prospect	9
1.4 Limitations of Optical Fibre Communications	10
1.5 Review of Previous Works	11
1.6 Objective of the Study	13
1.7 Brief Introduction to this Thesis	14
2. Performance analysis of a WDM Optical Ring Network	15
2.1 Introduction	15
2.2 Network Architecture	16
2.3 The Receiver Model	22
2.3.1 Mach-Zehnder Interferometer (MZI)	22

2.3.2	MZI Characteristics	24
2.4	Theoretical Analysis of Optical Direct Detection FSK	27
2.4.1	The Optical Signal	27
2.4.2	Receiver Output of the FPF	28
2.4.3	The Crosstalk Signal	30
2.4.4	The Receiver Output Signal	31
2.4.5	Bit Error Rate Expression	34
3.	RESULTS AND DISCUSSIONS	36
4.	CONCLUSION AND SUGGESTIONS FOR FUTURE WORKS	70
4.1	Conclusion	70
4.2	Suggestions for Future Works	73
	REFERENCES	74
APPENDIX-A	Output of PD	A-1

ACKNOWLEDGMENTS

The author would like to express deepest gratitude to his advisor, Dr. Satya Prasad Majumder, Professor, Department of Electrical and Electronic Engineering, BUET, who patiently gave many invaluable advises, proper guidance, constant encouragement, constructive suggestions and kind co-operation throughout the entire progress of this research work.

Special thanks to Dr. Saifur Rahman, Associate Professor, Department of EEE, BUET, for his co-operation and constant encouragement specially in computer programming related works.

The author takes this opportunity to express his deepest appreciation to Dr. Enamul Basher, Professor and Head of the department of EEE, BUET, for providing departmental facilities.

Grateful acknowledgment is also made to Md. Aklas Ali Sheikh, Electronic Assistant, Telecommunication Laboratory, for giving enough time to use computer facilities in this Laboratory to complete the research work.

Finally, author would like to give thanks to them who have directly or indirectly helped in this research work, specially to Dr. Abdur Rahim Mollah, Professor and Head department of EEE BIT Khulna, and my wife for their encouragement to complete this research.

ABSTRACT

A theoretical analysis is provided for a WDM optical ring network that connects a set of offices with cascaded EDFA's and add drop multiplexers (ADM) using direct detection FSK with Mach-Zehnder Interferometer (MZI) as an optical frequency discriminator. The analysis is carried out taking in to account the combined effect of laser phase noise, chromatic dispersion of optical fibre, ASE noise due to cascaded EDFA's, photodetector shot noise and receiver noise. The single mode fibre is modeled as a bandpass filter with flat amplitude response and linear group delay over the optical bandwidth of the modulated optical signal. The statistics of the signal phase fluctuations at the output of the fibre caused by non linear filtering due to fibre chromatic dispersion are determined in terms of its moments and the probability density function (pdf). The random phase fluctuation due to laser phase noise and cascaded filtering effect on the signal magnitude is evaluated.

Using the noise statistics and moments, the bit error rate (BER) performance of the receiver is then evaluated for several values of FP filter bandwidth, channel spacing and different number of nodes at a bit rate of 10Gb/s. The penalty suffered by the network due to dispersion and phase noise is then determined at a bit error rate (BER) of 10^{-9} by changing fibre lengths between nodes. The minimum power penalty at optimum filter bandwidth is evaluated for different number of nodes and fibre lengths. For a specified power penalty of 1 dB, the maximum allowable fibre lengths and number of nodes are then determined.

LIST OF FIGURES

- Fig. 1 Generalized block diagram of an optical communication system.
- Fig. 2.1 WDM interoffice ring network configuration showing ring interconnecting a HUB and N local offices.
- Fig. 2.2 Grating based WDM component as a drop and add filter.
- Fig. 2.3 A simple four-port filter with optical drop and add capability.
- Fig. 2.4 Acousto optic tunable filter as a add and drop filter.
- Fig. 2.5 Amplifier output signals and forward noise power with 15 input signals each at -10 dBm.
- Fig. 2.6 The connection of 2x2 optical switch for normal operations.
- Fig. 2.8 Optical equipment at each local office for the network in Fig. 2.7.
- Fig. 2.9 Optical equipment at the hub for the network in Fig. 2.7.
- Fig. 2.10 Block diagram of an FSK direct detection receiver with Mach-Zehnder Interferometer (MZI) as an optical frequency discriminator (OFD).
- Fig. 2.11 (a) An MZI with large ΔL or narrow wavelength spacing, (b) Transmittance characteristics of an MZI and (c) Differential output of the balanced receiver.
- Fig. 3.1 The bit error rate (BER) performance of a WDM optical ring network using direct detection optical FSK system at a bit rate 10 Gb/s with fibre chromatic dispersion $D_c = 15$ ps/km.nm , fibre length $L=40$ km, number of node $N=2$, channel spacing $\Delta F=1.0$ nm at an wavelength of 1550 nm and modulation index $h=1.0$ for several values of FP filter bandwidth.
- Fig. 3.2 The bit error rate (BER) performance of a WDM optical ring network using direct detection optical FSK system at a bit rate 10 Gb/s with fibre chromatic dispersion $D_c = 15$ ps/km.nm , fibre length $L=120$ km, number of node $N=2$, channel spacing $\Delta F=1.0$ nm at an wavelength of 1550 nm and modulation index $h=1.0$ for several values of FP filter bandwidth.

- Fig. 3.3 The bit error rate (BER) performance of a WDM optical ring network using direct detection optical FSK system at a bit rate 10 Gb/s with fibre chromatic dispersion $D_c = 15 \text{ ps/km.nm}$, fibre length $L=40 \text{ km}$, number of node $N=8$, channel spacing $\Delta F=1.0 \text{ nm}$ at an wavelength of 1550 nm and modulation index $h=1.0$ for several values of FP filter bandwidth.
- Fig. 3.4 The bit error rate (BER) performance of a WDM optical ring network using direct detection optical FSK system at a bit rate 10 Gb/s with fibre chromatic dispersion $D_c = 15 \text{ ps/km.nm}$, fibre length $L=40 \text{ km}$, number of node $N=8$, channel spacing $\Delta F=1.0 \text{ nm}$ at an wavelength of 1550 nm and modulation index $h=0.5$ for several values of FP filter bandwidth.
- Fig. 3.5 The bit error rate (BER) performance of a WDM optical ring network using direct detection optical FSK system at a bit rate 10 Gb/s with combined effect of fibre chromatic dispersion $D_c = 15 \text{ ps/km.nm}$ and laser phase noise $\Delta \nu T=0.001$, fibre length $L=40 \text{ km}$, number of node $N=4$, channel spacing $\Delta F=1.0 \text{ nm}$ at an wavelength of 1550 nm and modulation index $h=1.0$ for several values of FP filter bandwidth.
- Fig. 3.6 The bit error rate (BER) performance of a WDM optical ring network using direct detection optical FSK system at a bit rate 10 Gb/s with fibre chromatic dispersion $D_c = 15 \text{ ps/km.nm}$, fibre length $L=40 \text{ km}$, number of node $N=4$, channel spacing $\Delta F=1.0 \text{ nm}$ at an wavelength of 1550 nm and modulation index $h=1.0$ for several values of FP filter bandwidth.
- Fig. 3.7 Plots of penalty in signal power due to fibre chromatic dispersion at $\text{BER}=10^{-9}$ versus FP filter bandwidth (nm) with fibre length $L=40 \text{ km}$, number of node $N=2$ and modulation index $h=1.0$ for several values of channel spacing ΔF (nm).
- Fig. 3.8 Plots of penalty in signal power due to fibre chromatic dispersion at $\text{BER}=10^{-9}$ versus FP filter bandwidth (nm) with fibre length $L=120 \text{ km}$, number of node $N=2$ and modulation index $h=1.0$ for several values of channel spacing ΔF (nm).
- Fig. 3.9 Plots of penalty in signal power due to fibre chromatic dispersion at $\text{BER}=10^{-9}$ versus FP filter bandwidth (nm) with fibre length $L=40 \text{ km}$, number of node $N=4$ and modulation index $h=1.0$ for several values of channel spacing ΔF (nm).

- Fig. 3.10 Plots of penalty in signal power due to fibre chromatic dispersion at $BER=10^{-9}$ versus FP filter bandwidth (nm) with fibre length $L=120$ km, number of node $N=4$ and modulation index $h=1.0$ for several values of channel spacing ΔF (nm).
- Fig. 3.11 Plots of penalty in signal power due to fibre chromatic dispersion at $BER=10^{-9}$ versus FP filter bandwidth (nm) with fibre length $L=80$ km, number of node $N=8$ and modulation index $h=1.0$ for several values of channel spacing ΔF (nm).
- Fig. 3.12 Plots of penalty in signal power due to fibre chromatic dispersion at $BER=10^{-9}$ versus FP filter bandwidth (nm) with fibre length $L=120$ km, number of node $N=8$ and modulation index $h=1.0$ for several values of channel spacing ΔF (nm).
- Fig. 3.13 Plots of penalty in signal power due to fibre chromatic dispersion at $BER=10^{-9}$ versus FP filter bandwidth (nm) with fibre length $L=40$ km, number of node $N=10$ and modulation index $h=1.0$ for several values of channel spacing ΔF (nm).
- Fig. 3.14 Plots of penalty in signal power due to fibre chromatic dispersion at $BER=10^{-9}$ versus FP filter bandwidth (nm) with fibre length $L=80$ km, number of node $N=10$ and modulation index $h=1.0$ for several values of channel spacing ΔF (nm).
- Fig. 3.15 Plots of penalty in signal power due to combined effect of laser phase noise and fibre chromatic dispersion at $BER=10^{-9}$ versus FP filter bandwidth (nm) with fibre length $L=40$ km, number of node $N=4$, normalized laser linewidth $\Delta\nu T=0.001$ and modulation index $h=1.0$ for several values of channel spacing ΔF (nm).
- Fig. 3.16 Plots of penalty in signal power due to fibre chromatic dispersion at $BER=10^{-9}$ versus FP filter bandwidth (nm) with fibre length $L=40$ km, number of node $N=4$ and modulation index $h=0.5$ for several values of channel spacing ΔF (nm).
- Fig. 3.17 Plots of penalty in signal power due to fibre chromatic dispersion at $BER=10^{-9}$ versus FP filter bandwidth (nm) with fibre length $L=80$ km, number of node $N=8$ and modulation index $h=0.5$ for several values of channel spacing ΔF (nm).
- Fig. 3.18 Variation of power penalty in signal power due to fibre chromatic dispersion at $BER=10^{-9}$ versus channel spacing ΔF (nm) with fibre length $L=40$ km, number of node $N=2$ and modulation index $h=1.0$ for several values of FP filter bandwidth (nm).

- Fig. 3.19 Variation of power penalty in signal power due to fibre chromatic dispersion at $BER=10^{-9}$ versus channel spacing ΔF (nm) with fibre length $L=120$ km, number of node $N=2$ and modulation index $h=1.0$ for several values of FP filter bandwidth (nm).
- Fig. 3.20 Variation of power penalty in signal power due to fibre chromatic dispersion at $BER=10^{-9}$ versus channel spacing ΔF (nm) with fibre length $L=40$ km, and $L=80$ km at FP filter bandwidth $B=2.0$ nm and modulation index $h=1.0$ for different number of nodes.
- Fig. 3.21 Variation of power penalty in signal power due to fibre chromatic dispersion at $BER=10^{-9}$ versus channel spacing ΔF (nm) with fibre length $L=40$ km, and $L=80$ km at FP filter bandwidth $B=3.0$ nm and modulation index $h=1.0$ for different number of nodes
- Fig. 3.22 Variation of power penalty in signal power due to fibre chromatic dispersion at $BER=10^{-9}$ versus channel spacing ΔF (nm) with fibre length $L=40$ km, and $L=80$ km at FP filter bandwidth $B=2.0$ nm and modulation index $h=0.5$ for different number of nodes $N=4$ and $N=8$.
- Fig. 3.23 Variation of minimum power penalty in signal power due to fibre chromatic dispersion at $BER=10^{-9}$ versus fibre length (km) with modulation index $h=0.5$ and $h=1.0$ for different number of nodes.
- Fig. 3.24 Variation of minimum power penalty in signal power due to fibre chromatic dispersion at $BER=10^{-9}$ versus number of nodes with channel spacing $\Delta F=2$ nm and modulation index $h=0.5$ and $h=1.0$ for several values of fibre length (km).
- Fig. 3.25 Plots of allowable channel spacing (nm) corresponding to 1dB penalty at $BER=10^{-9}$ as a function of FP filter bandwidth (nm) for modulation index $h=1.0$ number of nodes $N=2$ and fibre length $L=40$ km.
- Fig. 3.26 Plots of allowable channel spacing (nm) corresponding to 1.5 dB penalty at $BER=10^{-9}$ as a function of FP filter bandwidth (nm) for modulation index $h=0.5$ and 1.0 , number of nodes $N=4$ and fibre length $L=40$ km.

LIST OF PRINCIPAL SYMBOLS

B_r	Bit rate
σ^2	Noise variance
$n(t)$	Complex additive Gaussian noise
Δf	Frequency deviation of FSK signal
ϕ_k	Angle modulation of kth channel
ϕ_{nk}	Phase noise of transmitting laser of kth Channel
ϕ_i	Angle modulation of ith channel
ϕ_{in}	Phase noise of transmitting laser of ith Channel
h	Modulation index
R_d	Photon responsivity
P_s	Input optical signal power
f_c	Optical carrier frequency
$H(f)$	Optical fibre transfer function
$H_f(f)$	Fabry-Perot filter transfer function
λ	Optical wavelength
ν	Frequence of optical carrier
$\Delta\nu$	Normalized linewidth of transmitting laser
τ	Delay occurred due to path difference in MZI
l_1, l_2	Lengths of arms I and II of MZI
T_I, T_{II}	Transmittance of arms I and II of MZI
ΔL	Path difference of MZI
η_{eff}	Effective refractive index of MZI
$D(\lambda)$	Fibre Chromatic Dispersion
$I(t)$	Modulating signal
F	Fourier transform
F^{-1}	Inverse fourier transform
c	Velocity of light

k	Boltzman's constant
$\delta(t)$	Delta function of time
$P(\Delta\theta_n)$	PSD of $\Delta\theta_n$
G_a	ASE factor
N_{sp}	Spontaneous emission factor
N_{s-sp}	Signal spontaneous noise power
N_{sp-sp}	Spontaneous spontaneous noise power
N_{c-sp}	Crosstalk noise power
S_{pd}	Photo-detector shot noise
S_{pdi}	Interferometric noise
S_{th}	Receiver thermal noise
$G_{FSK-PN}(f)$	PSD of the FSK signal corrupted by noise
$G_{FSK}(f)$	PSD of FSK signal
$G_{PN}(f)$	PSD of laser phase noise
B	Optical bandwidth
B_e	Electrical bandwidth

LIST OF ABBREVIATIONS

ASK	Amplitude shift keying
APD	Avalanche photo diode
ADMS	Add-drop multiplexers
AOTF	Acousto optic tunable filter
ASE	Accumulated spontaneous emission
BER	Bit error rate
BTTB	Bangladesh telegraph & telephone board
CPFSK	Continuous phase FSK
dBm	Decibel relative to 1 mw
DFB	Distributed feedback
EDFAs	Erbium doped fibre amplifiers
erfc	Complimentary error function
FM	Frequency modulation
FP	Fabry Perot
FSK	Frequency shift keying
FDM	Frequency division multiplexing
FWM	Four wave mixing
GEC	General electric company
GVD	Group velocity dispersion
IF	Intermediate frequency
IM/DD	Intensity modulation direct detection
ISI	Inter-symbol interference
LASER	Light amplification by stimulated emission of radiation
LD	Laser diode
LED	Light emitting diode
LO	Local oscillator
LW	Linewidth
MSK	Minimum shift keying

MZI	Mach-Zehnder interferometer
NEC	Nippon electric company
NRZ	Non-return to zero
OOK	On-off keying
OFD	Optical frequency discriminator
OFDM	Optical frequency division multiplexing
OTDM	Optical time division multiplexing
PDF	Probability density function
PIN	Positive intrinsic negative
PSD	Power spectral density
SNR	Signal to noise ratio
SONET	Synchronous optical network
WADMs	Wavelength add-drop multiplexers
WDM	Wavelength division multiplexing

CHAPTER-1



1.1 Introduction :

The idea of using lightwaves for communication can be traced far back as 1880 when Graham Bell invented the photophone. In this remarkable experiment speech was transmitted by modulating a light beam which traveled through air to the receiver. Guided light wave communication in its present form is due to another remarkable invention by Kao and Hockham in 1965 who produced for the first time a multimode optical fibre of loss about 1000 dB/km. The invention of Light Amplification by Stimulated Emission of Radiation (LASER) in 1960 made the enormous developments in the optical fibre communication system. Since then the technology has been continuously improving and the current state of the art fabricated fibres have loss around 0.2 dB/km at 1.55 micron wavelength. The optical fibre communication system has the following advantages by virtue of its characteristics :

- (i) High bandwidth (10 MHz-Km to over 1 THz-Km).
- (ii) Low attenuation (0.1 dB/km to 3 dB/km).
- (iii) Electrical immunity (no RFI, EMI interference).
- (iv) Security (can not be easily tapped, no cross talk).
- (v) Flexibility (can be bent of a radii of few cms).
- (vi) Falling cost (less than \$ 100/km of cabled fibre).
- (vii) Long repeater spacing (more than 100 km).
- (viii) Higher bit rate (100 Mb/s to 10 Gb/s).

Due to these and other features led today to have around 50 million kilometers of optical fibre installed world wide [1-2].

The generalized block diagram of an optical communication system is shown in Fig. 1.

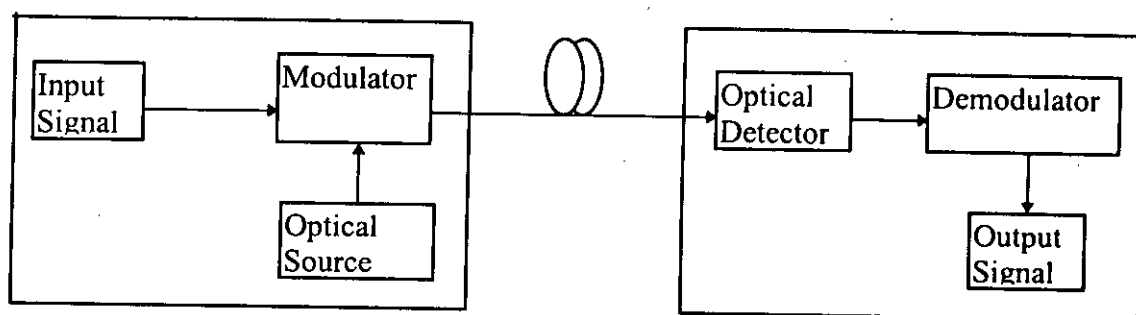


Fig. 1. Generalized block diagram of an optical communication system.

The main components are :

- (i) The optical source.
- (ii) A means to modulate the optical carrier from the source with the information signal to be transmitted.
- (iii) The transmission medium.
- (iv) The photo detector which converts the received optical power to electrical waveform.
- (v) A means to demodulate the electrical waveform and recover the information signal.

There are two conventional light sources used in optical fibre communications are Light emitting diodes (LEDs) and Laser diodes (LDs). The advantages of LED are (i) low sensitivity to retroreflection (ii) no interference problem (iii) low sensitivity to temperature (iv) high reliability (v) simple electronic excitation and (vi) low cost. But main disadvantages are (i) low coupling efficiency between an LED and a fibre (ii) low modulation bandwidth, typically limited 100 MHz to 200 MHz (iii) wide spectrum around 50 nm.

The advantages of LD are (i) high conversion gain i.e. with small bias current relatively high power output (ii) low numerical aperture, as a result, coupling efficiency is high (iii) high modulation bandwidth (GHz) (iv) narrow spectrum. Main disadvantages of LD are (i) high sensitivity to temperature (ii) produce supplementary to return reflected power (iii) less reliable (iv) more costly.

In summary, for short links (< 10 km) LED is suitable, but for medium and long links LD is suitable.

Two types of photodetectors are frequently used in optical fibre communication system i) PIN(Positive-Intrinsic-Negative) photodiode and ii) Avalanche photodiode (APD). For short links Ge PIN is used. For medium links Ge III/V PIN or Ge APD is used and for long links III/V APD is used.

1.2 Overview of optical fibre communication system :

The typical characteristics of optical communication systems during various stages of development is given below [1]

Type	Bit rate	Year of operation	Fibre	Loss	Repeater Spacing
First generation 850 nm to 900 nm	45 Mb/s	1977	Multimode Graded Index	3 dB/Km	10 Km
2nd generation 1310 nm	45 Mb/s	1981	Multimode Graded index	1 dB/Km	30 Km
3rd generation 1310 nm	1 Gb/s	1990	Single mode	< 1 dB/Km	40 Km
4th generation 1550 nm	10 Gb/s	1995	Single mode	<0.3 dB/Km	100 Km
Futuristic 2000 nm	> 10 Gb/s 150,000 Tel. lines		IR fibre	<0.01 dB/Km	1000 Km

It is evident that most of the earlier optical fibre communication system installed were based on multimode fibre. There are few significant disadvantages in the use of multimode fibre.

- (i) High bandwidth (e.g. 4-10 GHz-Km) multimode fibre are not easy to make since modal dispersion is large and difficult to control.
- (ii) Modal noise causes significant system penalty.
- (iii) Loss due to attenuation can not be lowered significantly.

Attenuation in optical fibre is minimum (0.2 dB/km) at wavelength of 1550 nm. Repeater spacing would be determined by the loss and operation at zero dispersion wavelength (1310 nm) of the fibre. Since lowest loss occur at 1550 nm, if one can shift the zero dispersion from 1310 nm, then an ideal situation will arrive. The shifting of zero dispersion at 1550 nm is accomplished by changing the fibre parameters and they are known as dispersion shifted fibre. The refractive index profile of single mode fibre is suitably tailored to achieve extremely small dispersion over the wavelength range of 1300 nm to 1600 nm. These fibres are called dispersion flattened fibres.

Shortly after 1980, there was a clear trend to use single mode optical fibre in long haul systems. The specifications of a typical fibre optic communication system in 1985 in the research (AT & T) laboratory are as follows [1]

	Commercial System	Laboratory System
Bit rate	280 Mb/s	4 Gb/s
Repeater spacing	40 Km to 50 Km	75 Km to 120 Km
Wavelength	1310 nm	1550 nm
Source	InGaAsP/InP Laser diode	DFB laser diode
Detector	Ge-APD	InGaAs-APD
Fibre	Single mode, 1dB/Km	Single mode 0.2 dB/Km
System Life	25 years	

One of the futuristic systems would be the infrared fibre at 2000 nm using fluoride glass which can have loss around 0.01 dB/Km. This is being used into a repeaterless system of 1000 Km. In addition there is ongoing research in soliton transmission [2]. A soliton is a non dispersive pulse that makes use of nonlinearity in a fibre to cancel out chromatic dispersion effects. Experimental demonstration at AT & T laboratory was possible to transmit solitons at 4 Gb/s over 136 km of conventional optical fibre having approximately 15 ps/nm-km of dispersion [3].

After optical signal has been launched into fibre, it becomes progressively attenuated and distorted with increasing distance because of scattering, absorption, dispersion in the fibre. At the receiver the attenuated and distorted optical power is detected by the photodiode. The figure of merit for a fibre is the attenuation and distortion which should be minimum and for a receiver there is a minimum optical power necessary at the desired data rate to attain either a given error probability for a digital system or a specified signal to noise ratio for an analog system.

In lightwave communication system, there are two important detection techniques are normally employed i) direct detection ii) coherent detection. In direct detection, a photodetector only responds to changes in the power level (the intensity) of an optical signal, and not to its frequency and phase content. So this is known as intensity modulation (IM). At the receiving end, one then uses direct detection (DD) to convert the optical signal into an electrical signal. The IM/DD systems are simple and relatively less costly but they suffer from limited sensitivity and do not take full advantage of the tremendous bandwidth capabilities of optical fibres due to relatively low optical power output of semiconductor laser diode (LD). To increase the data rate throughput of all semiconductor free space optical channels, extensive research for bandwidth, power efficient coding and modulation schemes were carried out in the last decade[4-8]. Direct detection optical communication systems were found very

promising for future deep space applications, inter satellite links and terrestrial line of sight communications [3-5].

Coherent light wave communication systems are becoming more attractive for long haul transmission and wide band data distribution. Two major advantages that coherent systems offer are (i) improved receiver sensitivity (up to 20 dB) relative to direct detection so that either the bit rate or the repeater spacing can be greatly increased. ii) a high degree of frequency selectivity on optical wavelength division multiplexing (WDM) system. In coherent optical communication system, information can be impressed on the optical carrier in one of the three ways i) phase shift keying (PSK) ii) frequency shift keying (FSK) iii) amplitude shift keying (ASK). Depending on the specific application various modulation and demodulation formats, similar to those of traditional radio frequency communication, are also employed in coherent lightwave transmission [6]. These include binary PSK (BPSK), quadrature PSK (QPSK), orthogonal QPSK (OQPSK), continuous phase FSK (CPFSK), discontinuous phase FSK (DPFSK), binary pulse position modulation (BPPM) etc. Each of the modulation schemes viz. ASK, FSK, DPFSK etc. and combinations thereof, with homodyne, heterodyne or diversity receivers has its own merits and demerits and none has emerged as absolutely preferable. However, FSK systems are more promising than ASK or PSK due to several reasons. First, modulation can be easily performed using direct modulation of laser diode (LD) through its injection current [7,8]. FSK is flexible enough to allow generation of either compact spectra, which is advantageous in multichannel WDM or two lobe spectra which allows for receiver envelope detection by properly selecting the modulation index. Further, a laser FM transmitter and a receiver front-end can easily be converted to encompass subcarrier modulation scheme, such as MSK-FM for instance and subcarrier multiplexing [7].

Actually, the huge transmission capacity of single mode fibres can be exploited efficiently by accessing the fibre bandwidth in the wavelength domain rather than in the time domain. Among WDM systems, High Density Wavelength Division multiplexing (HD-WDM) (in which the channels spacing is a few times the bit rate) allow the possibility of transmitting many channels simultaneously, increasing the transport capacity. A sharp cut-off filter and a modulation scheme with a compact spectrum are necessary to construct densely spaced multiplexing systems utilizing a direct detection scheme.

In recent years, significant research efforts have been devoted to the design of high capacity, flexible, cost-effective, reliable, transparent, scalable multiwavelength optical networks [9]. A wavelength add-drop multiplexer (WADM) is one of the key network element which is used for selectively dropping and inserting optical signals into WDM network. Within currently envisioned ring networks multiwavelength signals traverse a cascade of erbium-doped fibre amplifiers (EDFAs) each followed by WADM [10]. Amplified spontaneous emission (ASE) noise due to the erbium-doped fibre amplifiers (EDEAs) is filtered inside each WADM by the MUX/DMUX pair. However, the part of amplified spontaneous emission (ASE) noise inside the passband of the MUX/DMUX pair accumulates and eventually degrades the optical signal to noise ratio (SNR) at the drop location. A periodic filter that consists of an anti-symmetric Mach-Zehnder Interferometer (MZI) is promising because it can MUX/DMUX optical carrier with channel spacing of the order of GHz. Moreover, a MZI is 3dB more power efficient compared to Fabry-Perot Filter (FPF). The periodic filter which consists of anti-symmetric MZI, also functions as a channel selective filter and optical frequency discriminator (OFD). When it is used as an OFD, 'mark' and 'space' are differentially detected with two outputs from OFD. Recently an experiment employing 10 Gbit/s modulation using a III-IV semiconductor MZI has been reported [11].

1.3 Present Status and Future Prospects of Optical Fibre Communication in Bangladesh :

1.3.1 Present Status :

In Bangladesh, for the first time optical fibre communication system was introduced in Bangladesh Railway. It was implemented by GEC Telecommunication Ltd. in the year 1987 and Dhaka-Chittagong link was commissioned on January 10, 1989 funded by NORAD aided project. The total length of the whole railway optical link is about 1450km. The maximum distance between repeaters is around 68 km and the minimum is 8 km. Laser diodes (LDs) are used mainly as optical sources, but LEDs are used for shorter distances. Single mode fibre is used for transmission at wavelength of 1310nm. Number of transmitted channels is 30, 60 or 120 which depend on requirement and the speed of transmission is 8 Mb/s.

In the year 1989-90 Bangladesh T & T Board (BTTB) introduced it's first optical fibre communication system. It is first installed with the digital exchange in Dhaka city. These links are connected mainly among the digital telephone exchanges of the city. The system was implemented by NEC, Japan with transmission speed of 140 Mb/s.

BTTB then adopted Fujitsu system with it's Dhaka-Khulna digital microwave project. It has two links, Moghbazar-Ramna link and Jessore-Rajarhat link with transmission speed of 140 Mb/s and 34 Mb/s respectively.

The exchanges in chittagong city were also then connected by optical fibre link with transmission speed of 140 Mb/s under 30,000 telephone project implemented by Alcatel, France.

BTTB connected one optical fibre link (4.5 km) between Mohakhali and Moghbazar at the end of 1994, after the installation of satellite earth station and international switching centre at Mohakhali. It was implemented by NEC, Japan with transmission speed of 140 Mb/s .

Under the 1,50,000 telephone lines project, BTTB implemented optical fibre links in Dhaka, Khulna, Rajshahi and Sylhet. This project implemented by Alcatel, France has transmission speeds of 34 Mb/s, 140 Mb/s and 560 Mb/s.

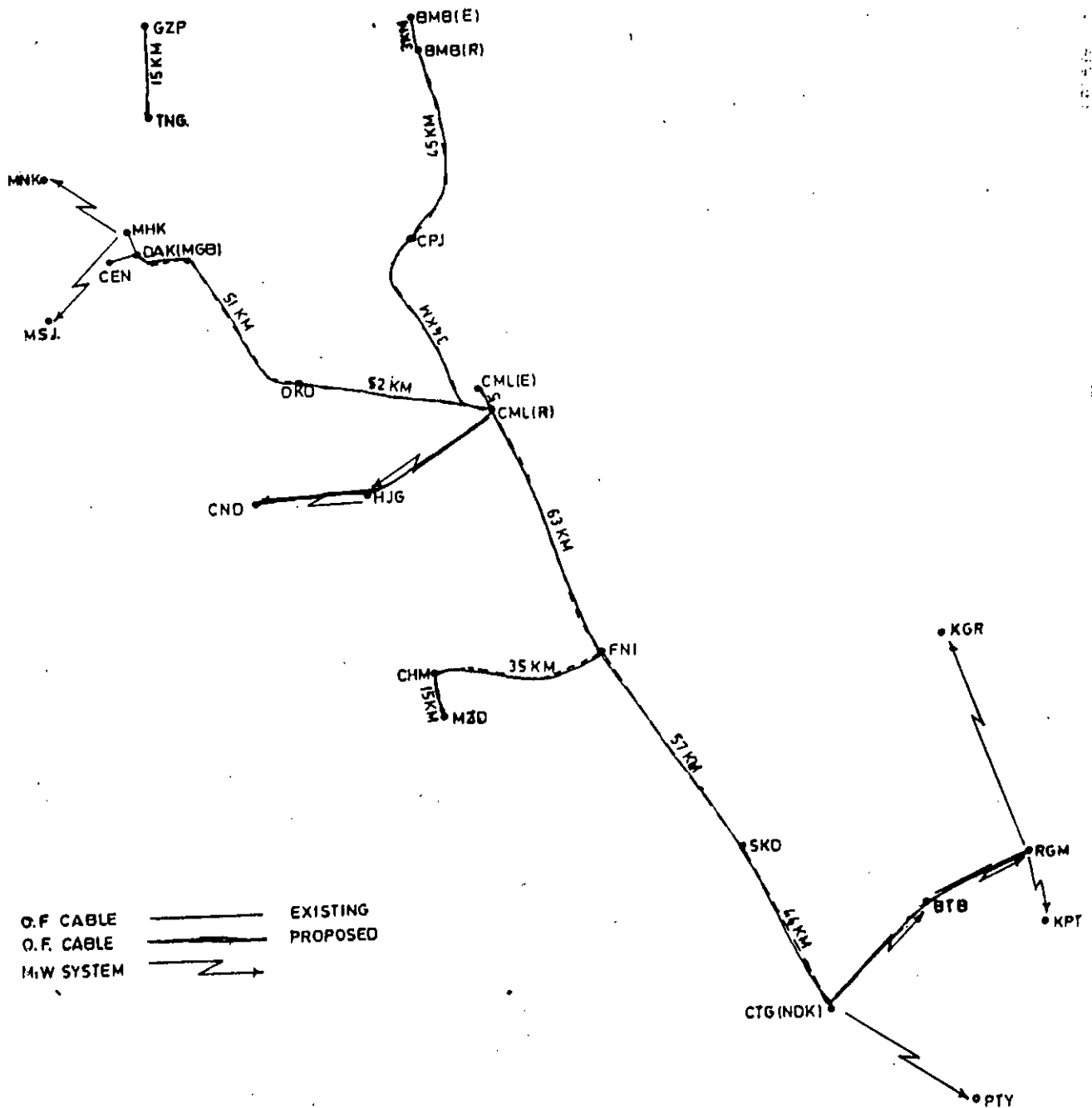
LDs and APDs are used as optical sources and photodetectors for all the systems of BTTB. Each of the system uses single mode fibre with intensity modulation direct detection (IM/DD) with transmission at an wavelength of 1310 nm.

Bangladesh Railway installed only one pair of fibre with no standby or spare fibres, whereas BTTB's has 8 to 12 fibres in every links. One pair is reserved always as hot-standby and in most cases spare fibres are also kept for additional safety.

1.3.2 Proposed Dhaka-Chittagong Optical Fibre link

At present, five lakh telephone lines of BTTB are in service throughout Bangladesh and there are proposals of four to five lakh more telephone lines to be installed under the Five Year Plan. Moreover private operators will also install considerable amount of telephone lines in city and rural areas. As a result, National and International calls (NWD & ISD) between the cities specially between Dhaka and Chittagong will increase two or three times. Now, only an old

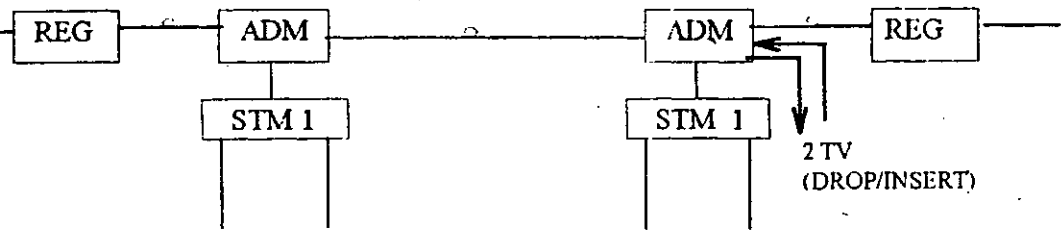
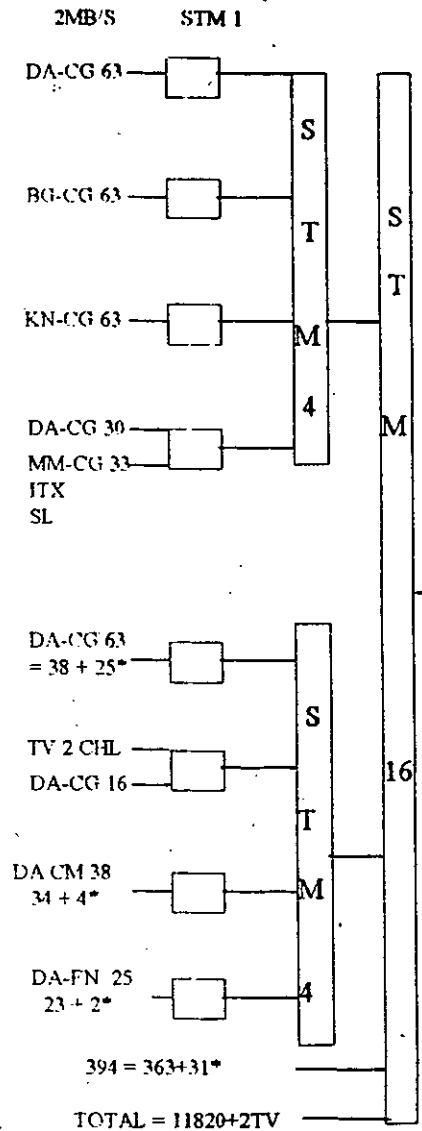
TRANSMISSION SYSTEM IN THE PROJECT.



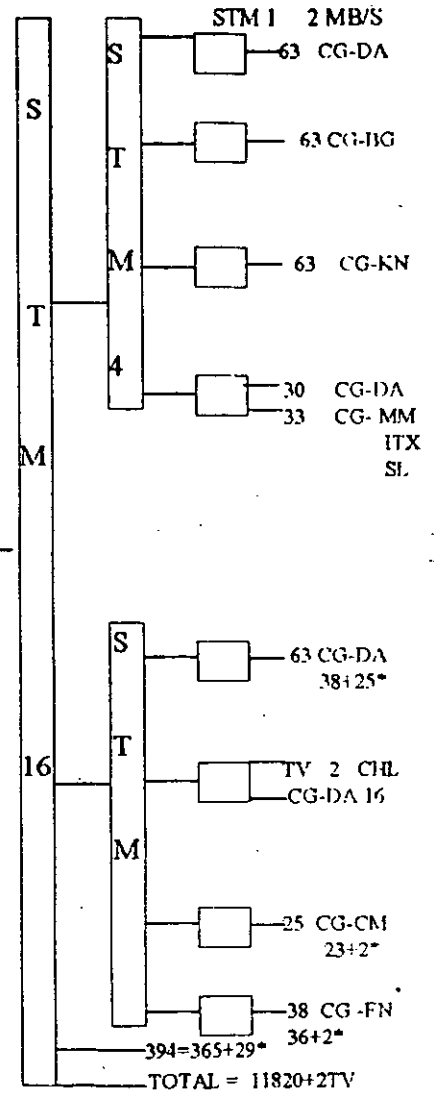
O.F. CABLE ———— EXISTING
 O.F. CABLE - - - - - PROPOSED
 M.W. SYSTEM ————

LEGENDS:

- | | |
|-------------------|------------------------|
| PTY — PATYA | CML(IR) — COMILLA (MW) |
| CTG — CHITTAGONG | CML(E) — " (EXCH) |
| KPT — KAPTAI | HJG — HA JIGANJ |
| BTB — BETBUNIA | CNO — CHANOPUR |
| RGM — RANGAMATI | DKO — DAUDKANDI |
| KGR — KHAGRACHARI | MNK — MANIKGANJ |
| SKO — SITAKUNDO | MSJ — MUNSHIGANJ |
| FNI — FENI | CPJ — COMPANYGANJ |
| CMH — CHOUMAHANI | BMB — BRAHMANBARIA |
| MZO — MAIZDI | CEN — CENTRAL (RAMNA) |
| GZP — GAZIPUR | MGB. — MOGHBAZAR |
| TNG. — TONGI | MHK. — MOHAKHALI |



DA-CM 16 = 14 + 2*	12 = 8 + 4*	CM-CG	DA-FN 10 = 8 + 2*	8 = 6 + 2*	FN-CG
DA-BM 10	9	BM-CG	DA-BL 9	7	BL-CG
DA-CD 4	4	CD-CG	DA-LX 2	6	CH-CG
KL-CM 4 = 3 + 1*			DA-MZ 2	8	MZ-CG
BG-CM 4 = 3 + 1*			DA-CG 2	9	LX-CG
<hr/>			<hr/>		
38 = 34 + 4*	25 = 23 + 2*		25 = 23 + 2*	38 = 36 + 2*	
				+ 2 TV	



Channel plan for DA-CG optical fibre Tx on 2.5 G.Bit/S system.

analog microwave link of 1800 channel capacity has been working for more than 15 years in between the above two cities which is already become congested. As a result subscribers in Dhaka Chittagong routes either fail to get call connection or it takes time to get calls connected. Proposed optical fibre link of latest SDH technology will be the high capacity telecommunication high way by replacing the old and obsolete analog link and will cater the existing congestion as well as future demand. Dhaka-Chittagong optical fibre (18 fibre) will be 2.488 Gb/s system on 1+1 configuration having add-drop multiplexer (ADM) at Comilla and Feni and regenerators at Daudkandi and Sitakunda. This link will start from Dhaka Moghbazar to Comilla microwave station through Daudkandi with total lengths of 103 km. This link will be divided into three routes from Comilla microwave station. One link extended up to Comilla exchange of 5 km lengths. Another link will connect Brahmanbaria exchange to Comilla exchange through Brahmanbaria microwave station and Companygang. The total length of the link is 81 km. From Comilla microwave station another link will go to Chittagong through Feni and Sitakundo, with total lengths of 164 km. From Feni another optical link will connect Maizdi and Choumahani with total lengths of 50 km.

1.3.3 Future Prospect

Bangladesh Railway has a plan to upgrade it's transmission speed from 8 Mb/s to 140 Mb/s in the near future. Public or private companies may be used increased channels due to this upgradation.

Most of the links of BTTB are now digital microwave links connecting it's main cities. BTTB is now preparing for network complementary to the existing links and thus turning almost it's whole network into digital. It is expected that main parts of this network will be optical fibre and extended up to Cox's Bazar.

Telecommunication sector is now open for private investment and on the other hand all sorts of telecommunication services including cable TV and computer networks LAN/WAN are becoming popular in Bangladesh. Private telephone companies are planning to have their own optical fibre telecommunication networks. Optical fibre networks are becoming popular, as a result copper networks are being replaced by the optical fibre networks specially for computer networking.

So, it is expected that optical fibre will soon play an important role in solving future requirements and bring the world to the hands of the citizens of Bangladesh.

1.4 Limitations of Optical Fibre Communications :

There exists a rich collection of non-linear optical effects in fused silica fibres, each of which manifests itself in a unique way [12-15]. Stimulated Raman scattering, an interaction between light and vibrations of silica molecules, causes attenuation of short wavelength channels in wavelength-multiplexed systems. Stimulated Brillouin scattering, an interaction between light and sound waves in the fibre, causes frequency conversion and reversal of the propagation direction of light [13]. Four-photon mixing or four wave mixing (FWM) is analogous to third order intermodulation distortion whereby two or more optical waves at different wavelengths mix to produce new waves at other wavelengths [12]. Self phase modulation is the process of change in signal phase due to change in intensity of the signal due to group-velocity dispersion [16]. Cross-phase modulation is an interaction, via the non-linear refractive index, between the intensity of one light wave and the optical phase of other light waves [17]. Optical non linear effects,

such as stimulated Brillouin scattering (SBS) [14] and four wave mixing (FWM) [15] processes are likely to impose severe restrictions on transmitter power in frequency division multiplexing (FDM) systems employing narrow linewidth single frequency lasers (18,19).

Some other limitations of optical fibre communications are fibre chromatic dispersion, laser phase noise, relative intensity noise etc. The various colors contained in an optical impulse travel at different speeds causing widening of the impulses at the end of the fibre [20,21]. Thus, widening of the impulse depends on the spectral width of the source. This effect is known as chromatic dispersion. If the bit rate increases i.e. if bit period decreases the impulses will overlap and can no longer be distinguished from each other, thus limiting the transmittable bit rate. Further, dispersion is directly proportional to fibre length. As a consequence, dispersion limits the bandwidth distance product of the optical link. Further, chromatic dispersion results in limiting of the fibre transmission capability, due to variation in propagation time as a function of the wavelength. So, limitation due to this phenomenon can be alleviated by using a narrower spectrum laser like DFB laser and by using dispersion compensating fibres.

1.5 Review of previous works :

There is an increasing interest in optical fibre transmission systems which operate at and above 10 Gb/s to meet future demand for higher transmission capacity in exchange networks. Wavelength Division Multiplexing (WDM) techniques will allow for greater transmission capacity and network flexibility compared to the single channel optical transmission systems. The transmission of many WDM channels over a ring network consisting of N local offices can be limited by a variety of phenomena including the effect of amplifier's spontaneous emission (ASE) of Erbium Doped Fibre Amplifiers (EDFAs), the non linear interactions between channels and the noise accumulation along the chain of amplifiers in

terms of the size and capacity of the network. A key problem for high speed (> 5 Gbit/s) light wave systems at 1550 nm wave length is high chromatic dispersion of conventional single mode fibres which are optimized for transmission at 1310 nm [20,21].

The detection performance of a coherent lightwave transmission link can also be sharply degraded by laser phase noise and chromatic dispersion. These problems have been the focus of many recent studies, a representative sampling of which is given by [22-30]. Recent advances in optical signal transmission have already reached several thousands of kilometers in the gigabit-per-second range due to use of in-line amplifier in different stages of light wave communication system. The theoretical and experimental results have been reported at 4 Gbit/s with coherent and direct detection receivers with in-line optical amplifiers [31]. The limitations of cascaded in-line amplifier systems are recently reported experimentally taking into considerations the effects of linear ASE accumulation [32]. The transmission capacity requirement for optical communication system is increasing to meet the future demands of multimedia services which can be achieved by Optical Time Division Multiplexing (OTDM), Wavelength Division Multiplexing (WDM) and / or combination thereof .

Recently, considerable works have been reported on optical networks with the use of WDM technology in long distance optical transmission [33,34]. A computer simulation of an optical IM/DD system is evaluated [34] with a cascade of wavelength add-drop multiplexers (WADMs) each consisting of optical amplifiers, a multiplexer/demultiplexer, gain equalizing attenuators and 2x2 optical switches by considering only the effect of amplifier's spontaneous emission. In this scheme, one of the eight wavelengths can propagate through more than 50 equidistant WADMs before its optical signal to noise ratio SNR drops below acceptable levels. The maximum number of channels in a WDM system is essentially limited by the amplifier bandwidth, by the four wave

mixing (FWM) effect, which may result in a sensitive crosstalk among the channels. A lot of theoretical and experimental works has been reported on crosstalk due to space switch as well as cross-talk induced by FWM effect in WDM networks in many recent studies [33-36].

The performance of a WDM network which utilizes cascaded optical amplifiers and cascaded Fabry-Perot filters has been presented in Ref. [37]. A new architecture for implementing unidirectional and bi-directional self-healing interoffice ring networks using WDM technology has been proposed in Ref. [38]. In Ref. [39], performance results of a WDM ring network is evaluated using a new restorable ring architecture with simple add/drop circuitry. All of the above studies have been carrier out without considering the effect of fibre chromatic dispersion, laser phase noise, self phase modulation (SPM) and cross-phase modulation (XPM). Self phase modulation and chromatic dispersion have a great influence on the performance of optical networks in terms of degradation of receiver sensitivity due to dispersion induced cross-talk and intersymbol interference (ISI), accumulated ASE, and several beat noise components arising out of the beating of the signal and crosstalk with ASE. It is of great importance to analyze WDM ring networks taking into considerations the combined effects of above mentioned system imperfections.

1.6 Objectives of the present study:

The main objective of this research is to analyze an optical WDM ring network with cascaded Erbium doped fibre amplifiers (EDFAs) and Fabry-Perot filters taking into account the effects of laser phase noise and fibre chromatic dispersion and

- (i) to determine analytically the statistics of the resultant phase fluctuations due to chromatic dispersion and laser phase noise at the receiver outputs;

- (ii) to determine the expression for the bit error rate of CPFSK direct detection receiver using MZI as an OFD considering the effects of chromatic dispersion, accumulated ASE, laser phase noise and the effect of cascaded optical filtering;
- (iii) to evaluate the Bit Error Rate (BER) performance of the WDM ring network for NRZ data at a bit rate of 10 Gb/s for several receiver and system parameters;
- (iv) to evaluate the power penalty suffered by the system due to above system imperfections at $BER=10^{-9}$ and to determine optimum system parameters for a specified system penalty.

1.7 Brief introduction to this thesis :

A brief introduction to communication system is presented in Chapter-1 with an emphasis on optical communication and a review of the research works currently going on in this field.

Chapter-2 presents performance analysis of a WDM ring network with cascaded EDFAs and Fabry-Perot filters with optical CPFSK modulation and Mach-Zehnder Interferometer (MZI) based direct detection receiver in the presence of group-velocity dispersion (GVD) and laser phase noise.

The results and discussions are presented in Chapter-3 with a summary of the future scope of works.

CHAPTER-2

Performance analysis of a WDM optical ring network

2.1 Introduction:

Wavelength division multiplexing (WDM) provides enormous capacity enhancement in telecommunication networks. Within currently envisioned ring networks, multiwavelength signals traverse a cascade of Erbium-doped fibre amplifiers each followed by drop-add filter [37]. The amplifier's nonflat gain spectra limits the size and capacity of ring networks. It has been found, however, that Erbium-doped fibre amplifier cascades are capable of supporting 15 wavelengths and 11 offices without requiring gain equalization for closed rings and up to 14 offices with open rings [37]. There is an increasing interest in optical fibre transmission systems which operate at and above 10 Gb/s to meet the future demand for higher transmission capacity in the exchange networks. But fibre chromatic dispersion is the key problem for lightwave transmission at 10 Gb/s of conventional single mode fibres which are optimized for transmission at 1310 nm. When distributed feedback lasers are frequency modulated for direct detection systems, producing significant wavelength chirp as well as intensity modulation, the resulting broad optical spectral width causes severe system degradation when fibre dispersion is present. Nearly all of the presently deployed fibres are optimized for 1310 nm operation and have a high dispersion of about 15 ps/nm.km in the low loss window near 1550 nm. Although several experimental demonstrations and computer simulation are reported [21,22], theoretical analysis taking into account the effect of fibre chromatic dispersion and laser phase noise on optical WDM ring networks is yet to be reported.

In this chapter, performance analysis of an wavelength division multiplexed optical network is presented considering a ring architecture. The analysis is

carried out to evaluate the impact of fibre chromatic dispersion on multiwavelength optical transmission system with CPFSK modulation and direct detection reception using a Mach-Zehnder Interferometer (MZI) as an optical frequency discriminator (OFD). The analysis includes the effect of dispersion induced crosstalk, accumulated amplifiers spontaneous emission (ASE) noise, beat noise components arising out of the beating of the channel signals with ASE and crosstalk, e.g. signal ASE beat noise, crosstalk ASE beat noise, ASE-ASE beat noise etc., laser phase noise and receiver noises. Then single mode fibre is modeled as a band-pass filter with flat amplitude response and linear group delay over optical bandwidth of the modulated optical signal [21]. The statistics of the phase fluctuations due to chromatic dispersion in the presence of filtering effect and laser phase noise are determined analytically and the expression for the bit error probability of the direct detection FSK receiver is developed. Following is the theoretical analysis the Bit Error Rate (BER) performance of the WDM ring network is evaluated for NRZ data at a bit rate of 10 Gb/s for several receiver and system parameters. The power penalty suffered by the system due to above system imperfections at $BER=10^{-9}$ is then determined for several channel separation and number of nodes. The optimum system parameters for a specified system penalty is then determined.

2.2 Network Architecture :

A self-healing ring is a network architecture shown in Fig. 2.1 that connects a set of cascaded offices (including MUX/DMUX and EDFA's with each office) in a physical ring topology by bandwidth sharing and a self-healing capability to mitigate network failures. Several self-healing ring architectures using electronic add-drop multiplexers (ADMS) have been proposed for telecommunications applications [38]. The self-healing ring architectures can generally be divided into two categories, uni-directional and bi-directional self-healing rings. The uni-directional ring requires only one working fibre to carry a duplex channel, and a bi-directional ring requires two working fibres to carry

duplex channel. A uni-directional ring requires two fibres (one working and one protection fibre) and a bi-directional ring may use four fibres (i.e. two working and two protection fibres). In our study we have used only uni-directional ring architecture.

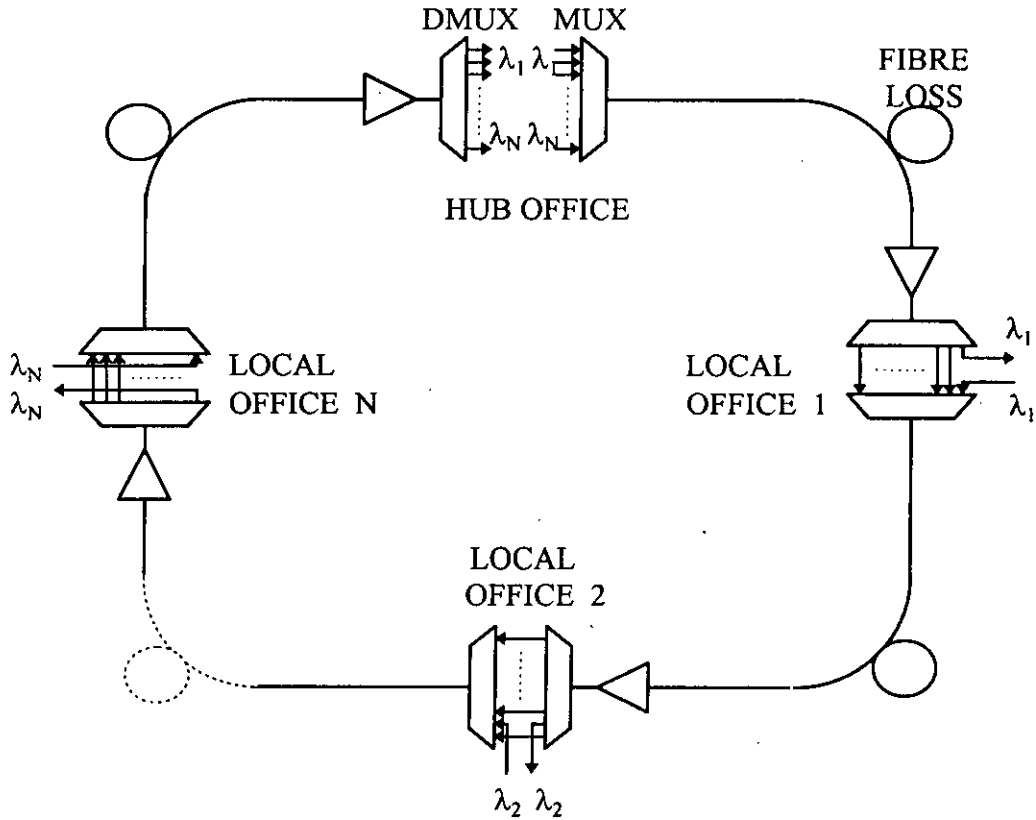


Fig. 2.1 WDM interoffice ring network configuration showing ring interconnecting a HUB and N local offices.

Optical drop and add filters are critical technologies for WDM ring networks. Grating based WDM components shown in Fig. 2.2 pass a discrete set of predetermined wavelengths and filter the remainder of spectrum.

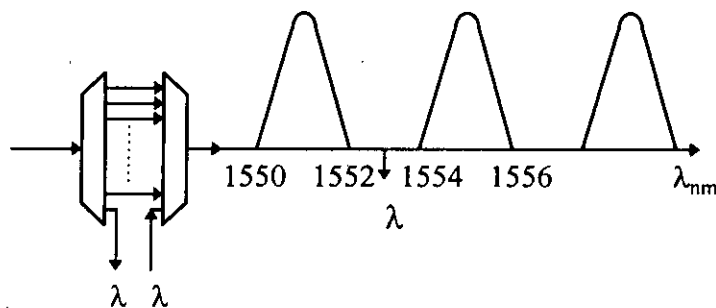


Fig. 2.2 Grating based WDM component as a drop and add filter.

This may prevent the possibility of amplifier gain saturation due to cumulative ASE noise. A simple four-port filter with optical drop and add capability is shown in Fig. 2.3. These filters reflect a specific wave length while transmitting all others.

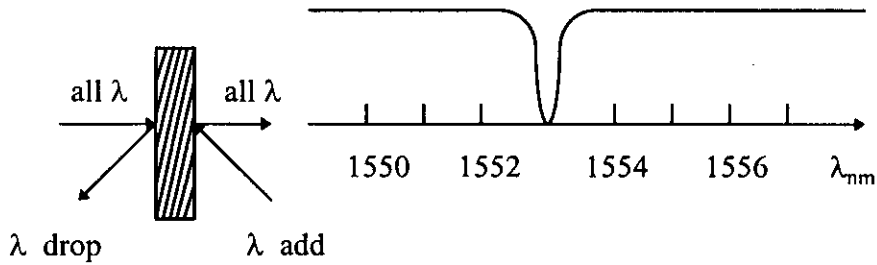


Fig. 2.3 A simple four-port filter with optical drop and add capability.

Another attractive component that can be used to perform the optical drop and add function is the acousto optic tunable filter shown in Fig. 2.4 which can be successfully used with a large number of input optical channels separated by 2 nm. This filter is tunable and can drop and add multiple channels by adjusting the amplitude and frequency of its electric driving signal.

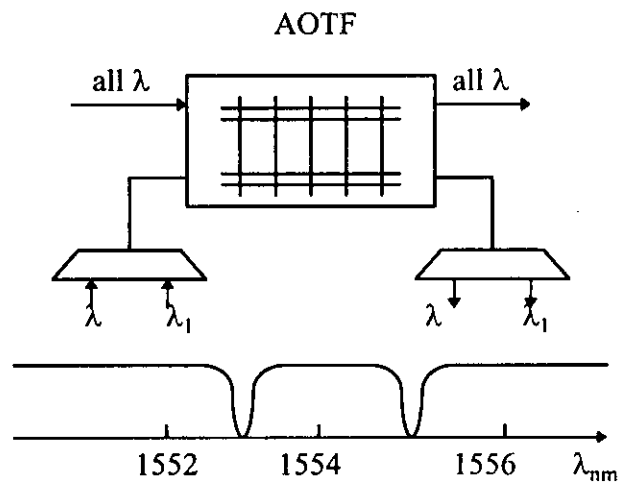


Fig. 2.4 Acousto optic tunable filter as a add and drop filter.

Erbium doped fibre amplifiers (EDFAs) are important essential elements for WDM ring networks. The amplifier is required at every office on the ring to compensate for fibre loss and the excess loss of WDM components. The amplifier has a nearly flat gain spectrum in the range of 1540 nm to 1570 nm as shown in Fig. 2.5.

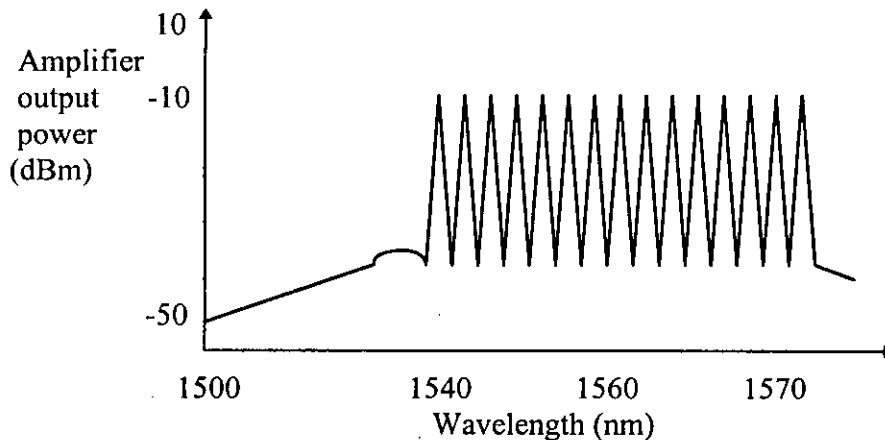


Fig. 2.5 Amplifier output signals and forward noise power with 15 input signals each at -10 dBm.

Optical switches are must be required for the protection path of bi-directional WDM ring networks. The connection of 2x2 optical switch for normal operation shown in Fig 2.6

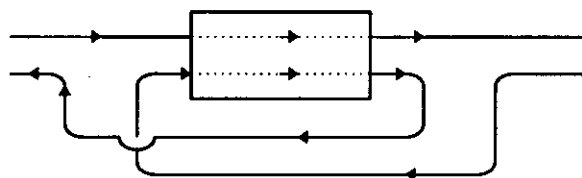


Fig. 2.6 The connection of 2x2 optical switch for normal operations.

High speed protection switching (microsecond range) could be needed for some services requiring highly reliable real time operations like video and high speed LAN/MAN. Photonics switching technologies to be considered for high speed

protection switching include directional couplers and probably liquid crystal devices.

Fig. 2.7 illustrates a two-fibre uni-directional WDM ring network supporting switch consolidation where N local offices are originating homing traffic flow converging to a single hub.

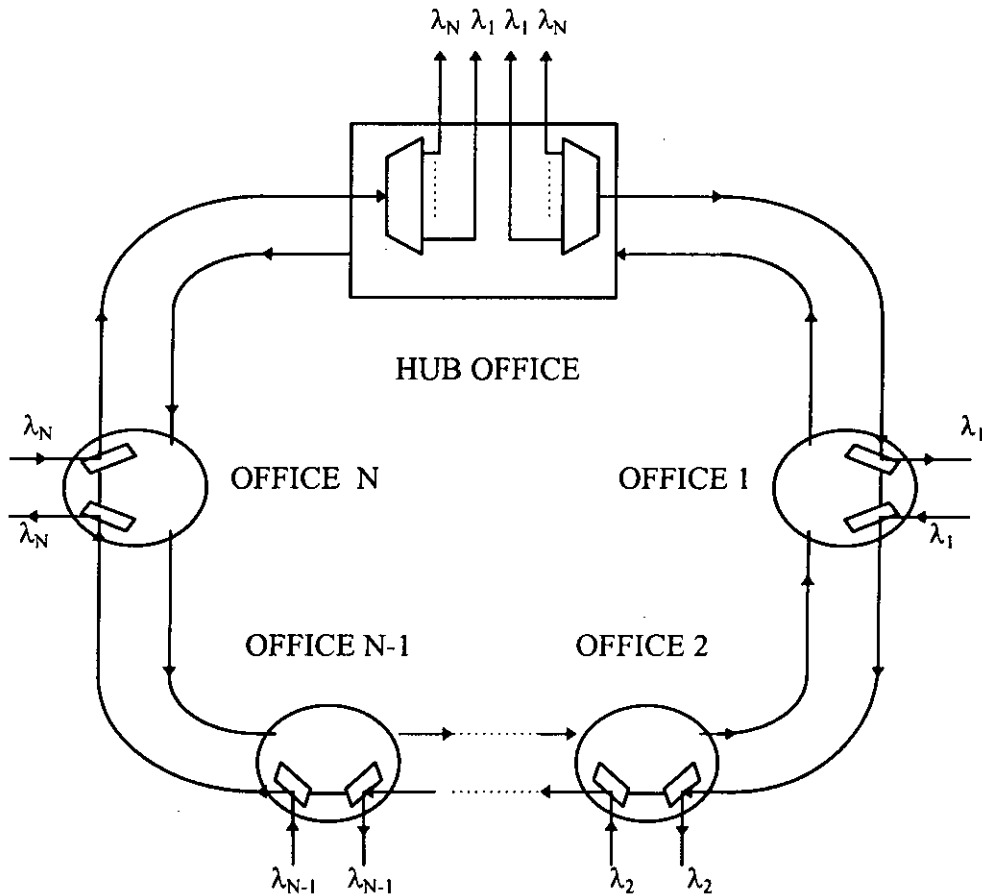


Fig. 2.7 Uni-directional self-healing WDM ring network with a HUB and N local offices.

Transmission on both the fibre rings is identical except for direction of propagation. The counter propagating signal facilitates network survivability during a cable cut. Each of N local offices is assigned a unique wavelength for transmission to and receiving from the Hub. The block diagram of the

equipment at each local office is shown in Fig. 2.8. The block diagram of the equipment in the hub location is shown in Fig 2.9.

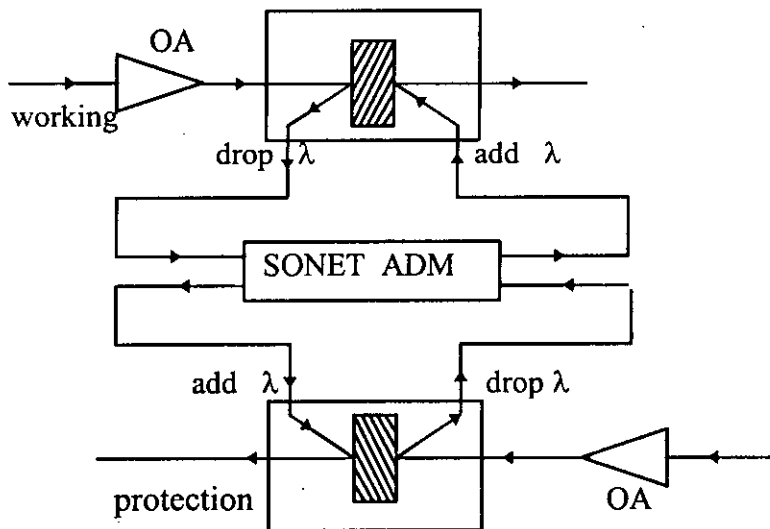


Fig. 2.8 Optical equipment at each local office for the network in Fig. 2.7.

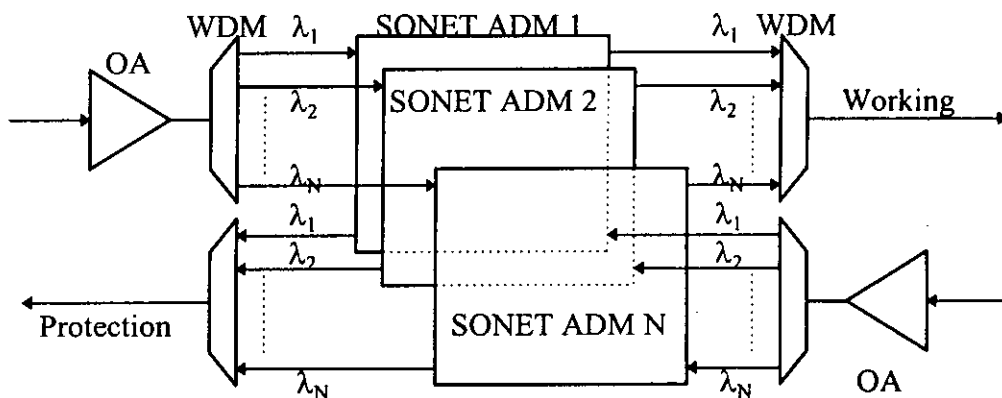


Fig. 2.9 Optical equipment at the hub for the network in Fig. 2.7.

The equipment consists of two optical fibre amplifiers (one in each direction) followed by redundant wavelength demultiplexers and an array of N SONET ADMs, each in the terminal node. The output signals from the SONET ADM arrays are multiplexed using redundant wavelength multiplexers, one for the working ring and one for the protection ring, and sent over the fibres with the signal at each wavelength intended for a different local office. At each office,

the channels would be received by using a heterodyne receiver technology or with optical filters followed by a direct detection receiver.

2.3 The Receiver model :

2.3.1 Mach-Zehnder Interferometer (MZI) :

The block diagram of the FSK direct detection receiver with an MZI considered for analysis is shown in Fig. 2.10 The MZI acts as an optical filter and differentially detects the 'mark' and 'space' of received FSK signal which are then directly fed to a pair of photodetectors. The difference of the two photocurrents are applied to the amplifier which is followed by an equalizer. The equalizer is required to equalize the pulse shape distortion caused by the photodetector capacitance and due to the input resistance and capacitance of the amplifier. After passing through the baseband filter, the signal is detected at the decision circuit by comparing it with a threshold of zero value.

MZI has two input ports, two 3dB couplers and two wave guide arms with length difference ΔL . A thin film heater is placed in one of the arms to act as a phase shifter, because propagation times for the two wave guide arms change due to the change of refractive index. The phase shifter is used for precise frequency tuning. Frequency spacing of the peak to bottom transmittance of the OFD is set equal to the peak frequency deviation $2\Delta f$ of the FSK signal. Consequently the 'mark' and the 'space' appear at the two output ports of the OFD. These outputs are differentially detected by the photo-detectors with balanced configuration.

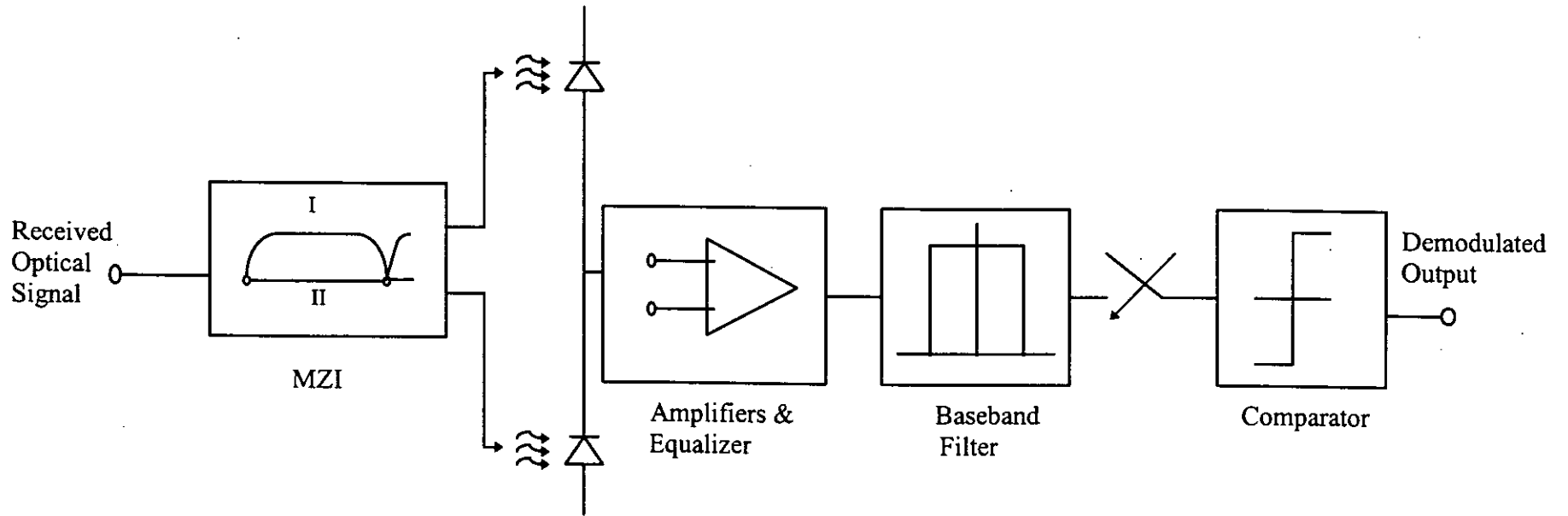


Fig. 2.10 Block diagram of an FSK direct detection receiver with Mach-Zehnder Interferometer (MZI) as an optical frequency discriminator (OFD).

2.3.2. MZI characteristics :

If $E(t)$ represents the signal input to the MZI, then the signals received at the output ports can be expressed as [11,40].

$$|E_2(t)| = |E(t)| \text{Sin} \left[\frac{k(l_2 - l_1)}{2} \right] \quad 2.1$$

and

$$|E_1(t)| = |E(t)| \text{Cos} \left[\frac{k(l_2 - l_1)}{2} \right] \quad 2.2$$

where l_1 and l_2 are the length of two arms of MZI and k is the wave number which can expressed as

$$k = \frac{w}{v} = \frac{2\pi}{\lambda} = \frac{2\pi f \eta_{eff}}{c}$$

η_{eff} , f and c are the effective refractive index of the wave guide, frequency of optical input signal and velocity of light in vacuum, respectively.

The transmittance of arm II of MZI is

$$T_{II}(f) = \frac{|E_2(t)|^2}{|E(t)|^2} = \text{Sin}^2 \left[\frac{k(l_2 - l_1)}{2} \right] = \text{Sin}^2 \theta \quad 2.3$$

and that of arm I of MZI is

$$T_I(f) = \frac{|E_1(t)|^2}{|E(t)|^2} = \text{Cos}^2 \left[\frac{k(l_2 - l_1)}{2} \right] = \text{Cos}^2 \theta \quad 2.4$$

where θ is the phase factor related to the arm path difference $\Delta L = l_2 - l_1$ and can be expressed as

$$\theta = \frac{k\Delta L}{2} = \frac{\pi f \eta_{eff} \Delta L}{c} \quad 2.5$$

Normally ΔL is chosen as

$$\Delta L = \frac{c}{4\eta_{eff} \Delta f} \quad 2.6$$

Therefore, $\theta = \frac{\pi f}{4\Delta f}$

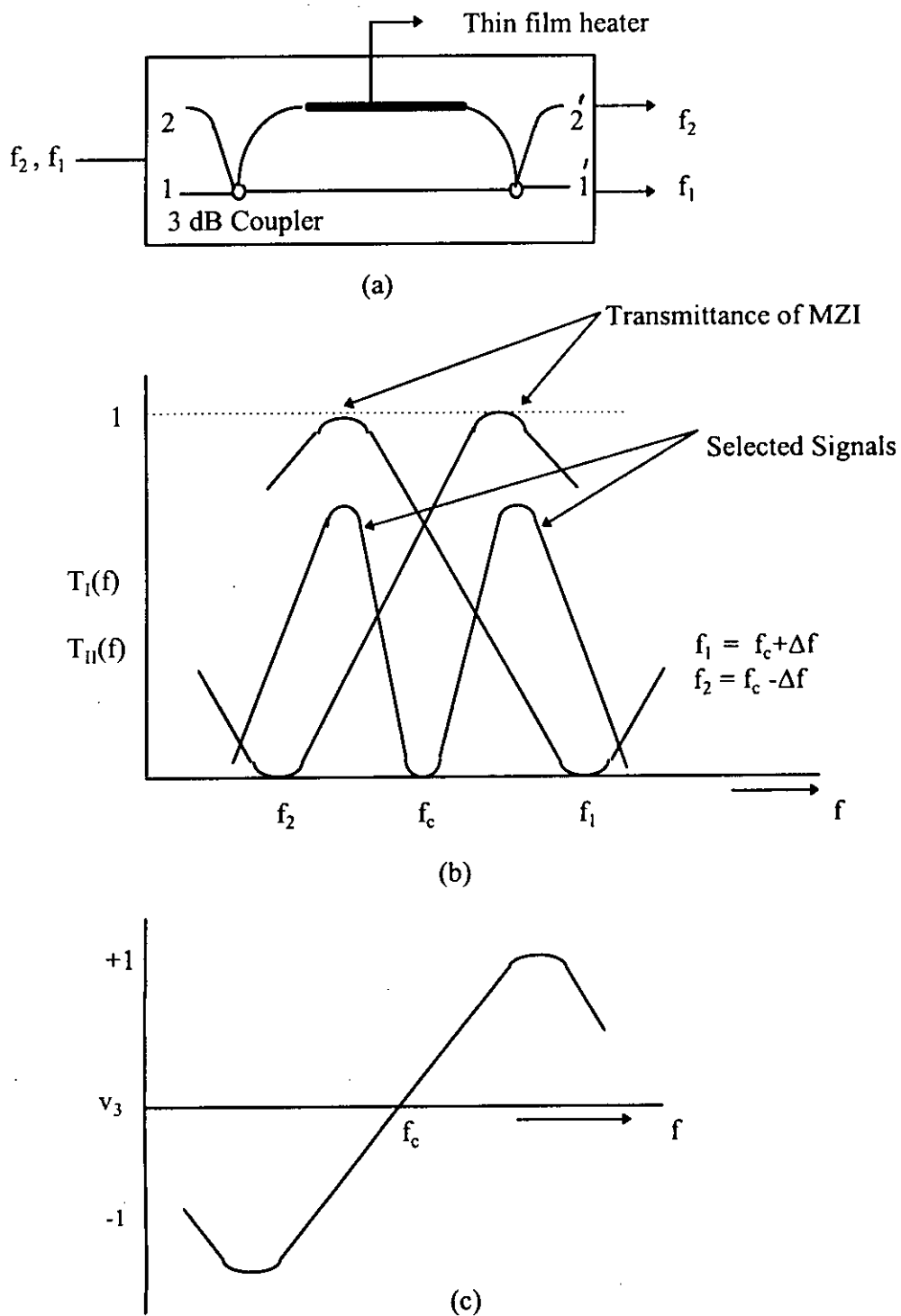


Fig. 2.11 (a) An MZI with large ΔL or narrow wavelength spacing, (b) Transmittance characteristics of an MZI and (c) Differential output of the balanced receiver.

Then we get

$$T_{II}(f) = \text{Sin}^2\left(\frac{\pi f}{4\Delta f}\right) \quad 2.7$$

and

$$T_I(f) = \text{Cos}^2\left(\frac{\pi f}{4\Delta f}\right) \quad 2.8$$

The outputs of the MZI are therefore anti-symmetric and are shown in Fig 2.11.

For an MZI, used as an OFD, Δf is so chosen that [11,40] $\Delta f = \frac{f_c}{2n+1}$, f_c is the carrier frequency of the FSK signal and n is an integer. The 'mark' and 'space' of FSK signals are represented by f_1 and f_2 respectively where $f_1 = f_c + \Delta f$ and $f_2 = f_c - \Delta f$

Therefore when 'mark' is transmitted

$$T_I = 1 \text{ and } T_{II} = 0$$

Similarly, for transmission of 'space'

$$T_I = 0 \text{ and } T_{II} = 1$$

Thus, two different signals f_1 and f_2 can be extracted from two output ports of MZI.

The MZI is used in our analysis as an OFD for a multichannel WDM/FDM system, is fabricated utilizing the periodicity of the transmittance versus frequency characteristic of an MZI [11,40].

2.4 Theoretical Analysis of Optical Direct Detection FSK :

2.4.1 The Optical Signal :

The optical FSK signal input to the fibre is given by

$$x_{in}(t) = \sqrt{2P_k} \exp[j\{2\pi f_k t + \phi_k(t) + \phi_{nk}(t)\}] + \sum_{\substack{i=1 \\ i \neq k}}^N \sqrt{2P_i} \exp[j\{2\pi f_i t + \phi_i(t) + \phi_{in}(t)\}] \quad 2.9$$

where f_k and f_i are the optical frequencies, P_k and P_i represents the transmitted optical signal powers of the k th and i th channel respectively, $\phi_k(t)$ and $\phi_i(t)$ are the angle modulations, $\phi_{nk}(t)$ and $\phi_{in}(t)$ are the phase noise of the transmitting lasers of the k th and i th channel respectively. Here $\phi_k(t)$ is given by

$$\phi_k(t) = 2\pi\Delta f \int_{-\infty}^t I(t) dt \quad 2.10$$

where $I(t) = \sum_k a_k p(t - kT)$; $p(t)$ represents the elementary pulse shape,

$a_k = \pm 1$ is the random bit pattern and Δf is the peak frequency deviation.

The single mode fibre transfer function due to chromatic dispersion is given by [21]

$$H(f) = \exp(-j\alpha f^2) \quad 2.11$$

where $\alpha = \frac{\pi D(\lambda)L\lambda^2}{c}$, $D(\lambda)$ is the fibre chromatic dispersion, λ is the optical wavelength, c is the speed of light and L is the length of fibre. The fibre impulse response $h(t)$ is given by where $h(t) = F^{-1}[H(f)]$ where F denotes Fourier transformation.

The transfer function of a FP filter used in ADM is given by [37]

$$H_f(f) = \frac{1}{1 + j \frac{2(f - f_o)}{f_{FP}}} \quad 2.12$$

where f_{FP} is the 3 dB bandwidth of FP filter, $h_f(t)$ is the impulse response of the FP filter and $h_f(t) = F^{-1} [H_f(f)]$

2.4.2 The output of the FPF :

The optical signal at the output of the fibre at the N-th distant node can be obtained as

$$\begin{aligned} E_o(t) &= x_{in}(t) \otimes [h_1(t) \otimes \dots \otimes h_N(t)] \otimes [h_{f1}(t) \otimes \dots \otimes h_{fm}(t)] \quad 2.13 \\ &= x_{in}(t) \otimes h'(t) \end{aligned}$$

where \otimes denotes convolution, $h_1(t) = h_2(t) = \dots = h_N(t)$ and $h_{f1}(t) = h_{f2}(t) = \dots = h_{fm}(t)$, m is the number of FP filters and N is the number of amplifiers and in worst cases $m=2N$. Here $h'(t)$ is the overall impulse response due to cascaded FP filter and EDFAs and is given by

$$h'(t) = [h_1(t) \otimes \dots \otimes h_N(t)] \otimes [h_{f1}(t) \otimes \dots \otimes h_{fm}(t)].$$

Using (2.9) and (2.12) the output signal $E_o(t)$ can be expressed as

$$\begin{aligned} E_o(t) &= \sqrt{2P_k GL} \exp[j\{2\pi f_k t + \phi(t)\}] \otimes h'(t) \quad 2.14 \\ &+ \sum_{\substack{i=1 \\ i \neq k}}^N \sqrt{2P_i GL} \exp[j\{2\pi f_i t + \phi'_i(t)\}] \otimes h'(t) + E_{sp}(t) \\ &= E_k(t) + \sum_{\substack{i=1 \\ i \neq k}}^N E_i(t) + E_{sp}(t) \end{aligned}$$

where $\phi(t) = \phi_k(t) + \phi_{nk}(t)$ and $\phi'_i(t) = \phi_i(t) + \phi_m(t)$, $E_k(t)$ and $E_i(t)$ represents the signal of the desired channel and the signals of the other channels respectively and $E_{sp}(t)$ is the ASE signal.

Using (2.13), (2.14) and following Ref.[41], the electric field due to the desired signal at the N-th node is given by

$$E_s(t) = \sqrt{2P_s GLI} \exp[j\{2\pi f_o t + \phi_o(t)\}] \quad 2.15$$

where P_s is the signal power, G is the gain of the amplifier and L is the fibre

loss between two nodes, $\phi_o(t)$ is the output phase and I is the cascaded filtering effect which can be expressed as

$$I = \int_{f_c - \frac{\beta_u}{2}}^{f_c + \frac{\beta_u}{2}} |H'(f)|^2 G_{FSK-PN}(f) df \quad 2.16$$

$G_{FSK-PN}(f)$ is the power spectral density (PSD) of the FSK signal corrupted by phase noise and is given by [42]

$$G_{FSK-PN}(f) = 2G_{FSK}(f) \otimes G_{PN}(f) \quad 2.17$$

where
$$G_{PN}(f) = \frac{1}{\pi} \times \frac{\beta_l}{\beta_l^2 + (2f)^2}$$

$G_{FSK}(f)$ is the normalized PSD of the desired FSK signal [43], $G_{PN}(f)$ is the PSD of laser phase noise[43], β_l is the full-width half-maximum (FWHM) linewidth of the transmitting laser.

The output signal phase $\phi_o(t)$ is given by [41]

$$\begin{aligned} \phi_o(t) &= \text{Re} \left[\int_{-\infty}^t h'(\tau) \phi(t-\tau) d\tau \right] + \sum_{n=2}^{\infty} \frac{1}{n!} I_m(j^n f_n) \\ &= \theta_s(t) + \theta_{nc}(t) \end{aligned} \quad 2.18$$

where $\theta_s(t)$ represents the linear filtering term and $\theta_{nc}(t)$ represents the non-linear filtering terms consisting of the cross-term and the intermodulation terms. The linearly filtered phase $\theta_s(t)$ can be rewritten as

$$\begin{aligned} \theta_s(t) &= \text{Re} \left[\int_{-\infty}^t h'(\tau) \phi(t-\tau) d\tau \right] \\ &= \text{Re} \left[\int_{-\infty}^t h'(\tau) \phi_k(t-\tau) d\tau \right] + \text{Re} \left[\int_{-\infty}^t h'(\tau) \phi_{nk}(t-\tau) d\tau \right] \\ &= \theta'_s(t) + \theta'_n(t) \end{aligned} \quad 2.19$$

where $\theta'_s(t)$ and $\theta'_n(t)$ are the filtered output signal phase and phase noise respectively.

2.4.3 The Crosstalk Signal :

To calculate crosstalk we assume crosstalk due only to the adjacent channel only. From (2.13), the crosstalk signal at the N-th node is then given by

$$\begin{aligned} E_c(t) &= \sqrt{2P_c GL} \exp\left[j\{2\pi(f_o + \Delta F)t + \phi_{sc}(t) + \phi_{nc}(t)\}\right] \otimes h'(t) \\ &= \sqrt{2P_c GL I_x} \exp\left[j\{2\pi(f_o + \Delta F)t + \theta(t)\}\right] \end{aligned} \quad 2.20$$

where $\theta(t)$ is the output phase and P_c is the crosstalk channel power, I_x is the crosstalk effect due to adjacent channel which is given by

$$I_x = \int_{f_c - \frac{\beta_o}{2}}^{f_c + \frac{\beta_o}{2}} |H'(f)|^2 G_{FSK-PN}(f + \Delta F) df \quad 2.21$$

Total electric field at the HUB office is then given by

$$E(t) = E_s(t) + E_c(t) + E_{sp}(t) \quad 2.22$$

$E_s(t)$ = Electric field due to signal only;

$E_c(t)$ = Electric field due to adjacent channel crosstalk;

$E_{sp}(t)$ = Electric field due to spontaneous emission noise of cascaded EDFAs.

Following Ref. [29] electric field due to spontaneous emission noise of cascaded EDFAs is given by

$$E_{sp}(t) = \sum_{k=-N}^{k=N} \sqrt{2N_o \Delta \nu G_a} L \text{Cos}[(\omega_o + 2\pi k \Delta \nu)t + \phi_k] \quad 2.23$$

where ϕ_k is a random phase for each component of spontaneous emission, $\Delta \nu$ is the laser linewidth, G_a is the accumulation factor of the ASE noise and is given by

$$G_a \cong N(G_{tot}^{\frac{1}{N}} - 1) \quad 2.24$$

where G_{tot} = total system gain.

$N_o = N_{sp}(G-1)h\nu$; N_{sp} is the spontaneous emission factor, h is Plank's constant and ν is optical frequency.

The total electric field is then expressed as

$$\begin{aligned}
E(t) &= \sqrt{2P_s G L I} \exp[j\{2\pi f_o t + \theta_s(t)\}] \\
&+ \sqrt{2P_c G L I_x} \exp[j\{2\pi(f_o + \Delta F)t + \theta(t)\}] \\
&+ \sum_{k=-N}^{k=N} \sqrt{2N_o \Delta \nu G_a L} \text{Cos}[(\omega_o + 2\pi k \Delta \nu)t + \phi_k] \\
&= E_s(t) + E_c(t) + E_{sp}(t)
\end{aligned} \tag{2.25}$$

2.4.4 The Receiver Output Signal :

The photodetector output current is then obtained as

$$\begin{aligned}
i(t) &= R_d |E_s(t) + E_c(t) + E_{sp}(t)|^2 \\
&= i_s(t) + i_c(t) + i_{s-sp}(t) + i_{c-sp}(t) + i_{sp-sp}(t) + i_{th}(t) + i_{sh}(t)
\end{aligned} \tag{2.26}$$

where $i_s(t)$ represents the signal current, $i_c(t)$ is the current due to crosstalk signal, $i_{s-sp}(t)$ is the current due to signal-spontaneous emission beat noise, $i_{c-sp}(t)$ is the cross-talk spontaneous beat noise, $i_{sp-sp}(t)$ is the spontaneous-spontaneous beat noise, $i_{th}(t)$ is the receiver thermal noise and $i_{sh}(t)$ is the photodetector shot noise. The power spectral density of the different beat-noise components are derived in the Appendix-A and are given by :

$$N_{s-sp} = 4R_d q P_s G(G-1)L^2 I G_a [N_{sp} \otimes G_{FSK-PN}(f)] \tag{2.27}$$

$$N_{sp-sp} = 2q^2 G_a N_{sp}^2 (G-1)^2 L^2 \int_{-\infty}^{\infty} |H'(f)|^2 df \tag{2.28}$$

$$N_{c-sp} = 4qR_d P_c G(G-1)L^2 I_x G_a [N_{sp} \otimes G_{FSK-PN}(f + \Delta F)] \tag{2.29}$$

Output signal of desired channel rewritten as

$$E_s(t) = \sqrt{2P_s G L I} \exp[j\{2\pi f_o t + \theta'_s(t) + \theta_n(t)\}] \tag{2.30}$$

For a 'mark' transmission, the current at output of balanced photodetector is[44]

$$i_m(t) = IR_d P_s \text{Cos}[2\pi f_k \tau + \Delta\theta'_s(t) + \Delta\theta_n(t)] \quad 2.31$$

where $\Delta\theta'_s(t) = \theta'_s(t) - \theta'_s(t - \tau)$, τ is the time delay between the two branches of the MZI and $\Delta\theta_n(t) = \theta_n(t) - \theta_n(t - \tau)$.

From (2.18) $\theta'_s(t)$ can be expressed as

$$\theta'_s(t) = \phi_k(t) \otimes h'(t) \quad 2.32$$

$$\begin{aligned} &= 2\pi\Delta f \int_{-\infty}^t I(t) \otimes h'(t) dt \\ &= 2\pi\Delta f \int_{-\infty}^t \sum_k a_k p(t - kT) \otimes h'(t) dt \\ &= 2\pi\Delta f \int_{-\infty}^t \sum_k a_k g(t - kT) dt \end{aligned}$$

where $g(t) = p(t) \otimes h'(t)$

Thus the chromatic dispersion produces distortion of the optical pulse shape.

Therefore,

$$\Delta\theta'_s(t) = \theta'_s(t) - \theta'_s(t - \tau) \quad 2.33$$

$$= 2\pi\Delta f \int_{t-\tau}^t \sum_k a_k g(t - kT) dt$$

Thus the output of the balanced photodetectors is

$$i(t) = IR_d P_s \text{Cos}\left[2\pi f_k \tau + 2\pi\Delta f \int_{t-\tau}^t \sum_k a_k g(t - kT) dt + \Delta\theta_n(t)\right] \quad 2.34$$

where R_d is the photodetector responsivity. Therefore,

$$\begin{aligned} i(t) &= IR_d P_s \text{Cos}\left[2\pi f_k \tau + 2\pi\Delta f \int_{t-\tau}^t a_o g(t) dt \right. \\ &\quad \left. + 2\pi\Delta f \int_{t-\tau, k \neq 0}^t \sum_k a_k g(t - kT) dt + \Delta\theta_n(t)\right] \end{aligned} \quad 2.35$$

For 'mark' transmission ($a_o = +1$) at any sampling instant, $i(t)$ can be expressed as

$$i_m(t) = IR_d P_s \text{Cos}\left[2\pi f_k \tau + \frac{\pi}{2} - \frac{\pi}{2} + 2\pi\Delta f \tau q(t) + 2\pi\Delta f \int_{t-\tau}^t \sum_{k \neq 0} a_k g(t-kT) dt + \Delta\theta_n(t)\right]$$

$$= IR_d P_s \text{Cos}\left[2\pi f_k \tau + \frac{\pi}{2} - \frac{\pi}{2} + \frac{\pi}{2} q(t) + \frac{\pi}{2} \sum_{k \neq 0} a_k q(t-kT) dt + \Delta\theta_n(t)\right] \quad 2.36$$

where for optimum demodulation : $\tau = \frac{T}{2h}$ and $h(= 2\Delta f T)$ is the modulation index and $q(t)$ is defined as

$$q(t) = \frac{1}{\tau} \int_{t-\tau}^t g(t_1) dt_1 \quad 2.37$$

$$\Delta\theta_n(t) = 2\pi \int_{t-\tau}^t \mu(t_1) dt_1 \quad 2.38$$

$\mu(t)$ is a zero mean Gaussian frequency noise of two sided flat PSD of $\frac{\Delta\nu}{2\pi}$, $\Delta\nu$ being the transmitting laser linewidth.

Denoting the phase noise due to chromatic dispersion by $\Delta\theta_{CD}$ as

$$\Delta\theta_{CD}(t) = -\frac{\pi}{2} + \frac{\pi}{2} q(t) + \frac{\pi}{2} \sum_{k \neq 0} a_k q(t-kT) dt \quad 2.39$$

$$= \bar{\theta}_{CD} + \frac{\pi}{2} \sum_{k \neq 0} a_k q(t-kT) dt$$

where $\bar{\theta}_{CD} = -\frac{\pi}{2} + \frac{\pi}{2} q(t)$, the output current $i_m(t)$ can be expressed as

$$i_m(t) = IR_d P_s \text{Cos}\left[2\pi f_k \tau + \frac{\pi}{2} + \Delta\theta_{CD}(t) + \Delta\theta_n(t)\right] \quad 2.40$$

$\Delta\theta_{CD}(t)$ is induced by the GVD and $\Delta\theta_n(t)$ is accounts for the phase distortion due to laser phase noise.

2.4.5 Bit Error Rate Expression :

Under ideal CPFSK demodulation condition $w_k \tau = (2n + 1) \frac{\pi}{2}$ where n is an integer and $2\pi\Delta f\tau = \frac{\pi}{2}$ for NRZ data, the output signal corresponding to the 'mark' and 'space' transmission are

$$i_m(t) = IR_d P_s [x(t)] \text{ and } i_s(t) = -IR_d P_s [x(t)] \quad 2.41$$

where $x(t) = \text{Cos}[\Delta\phi(t)]$ describe the phase noise induced interferometric intensity noise and $\Delta\phi(t) = \Delta\theta_{CD}(t) + \Delta\theta_n(t)$

The output of the low-pass filter for 'mark' transmitted at a sampling time t is

$$i(t) = IR_d P_s \text{Cos}[\Delta\phi(t)] + n(t) \quad 2.42$$

where $n(t)$ is total noise power consists of the filtered output noise contributed by the photodetector quantum shot noise, the interferometric noise due to input intensity fluctuation, receiver thermal noise and other beat noise components.

The total noise power spectral density is given by [44]

$$S_n(f) = S_{pd}(f) + S_{pdi}(f) + S_{th}(f) + S_{s-sp}(f) + S_{c-sp}(f) + S_{sp-sp}(f) + S_c(f) \quad 2.43$$

where

$$S_{pd}(f) = qR_d P_s \quad 2.44$$

$$S_{pdi}(f) = 0.5R_d P_s \left[S_x(f) - \bar{x}^2 \delta(f) \right] \quad 2.45$$

$$S_{th}(f) = i_{th}^2 S_x(f) \quad 2.46$$

$$S_c(f) = P_c I_x GL / B \quad 2.47$$

and x represent the PSD and the mean value of $x(t)$ respectively.

The total noise power is then obtained as

$$\sigma_m^2 = \sigma_s^2 = \int_{-\frac{B_c}{2}}^{\frac{B_c}{2}} S_n(f) |H_{LP}(f)|^2 df \quad 2.48$$

where $H_{LP}(f)$ represents the transfer function of the receiver low-pass filter which is assumed to be Gaussian having bandwidth $B_c = 0.75B_r$.

$$\text{Let } Q = \frac{i_m - i_s}{\sigma_m + \sigma_s} \quad 2.49$$

Then the conditional bit error rate can be expressed as

$$P(e|\Delta\phi) = 0.5 \operatorname{erfc}\left(\frac{Q}{\sqrt{2}}\right) \quad 2.50$$

The average bit error rate of a direct detection CPFSK system is then

$$BER = 0.5 \int_{-\infty}^{\infty} \operatorname{erfc}\left(\frac{Q}{\sqrt{2}}\right) P_{\Delta\phi}(\Delta\phi) d(\Delta\phi) \quad 2.51$$

where $P_{\Delta\phi}(\Delta\phi)$ is the probability density function of $\Delta\phi$

Using Gauss-quadrature rule, the BER can be computed as

$$BER = 0.5 \sum_{i=1}^N \int_{-\infty}^{\infty} w_i \operatorname{erfc}\left[\frac{2\left\{R_d P_s \cos\left(\Delta\theta^i + \Delta\theta_n\right)\right\}}{\sqrt{2}\sigma}\right] P_{\Delta\theta}(\Delta\theta_n) d(\Delta\theta_n) \quad 2.52$$

where the weights w_i and the nodes $\Delta\theta^i_{CD}$ are evaluated from the knowledge of moments of the random process $\Delta\theta_{CD}(t)$ and $P_{\Delta\theta}(\Delta\theta_n)$ is the Gaussian pdf of the laser phase noise at the output with zero mean and variance $\sigma^2_{ph} = 2\pi\Delta\nu\tau$.

CHAPTER-3

RESULTS AND DISCUSSIONS

Following the theoretical analysis presented in Chapter-2 the performance results for a WDM ring network consisting of concatenated EDFAs and MUX/DMUX are evaluated at a bit rate of 10 Gb/s with different filter bandwidths, channel spacing, node separations, other receiver and system parameters. The parameters of the single mode fibre used for numerical computations are: chromatic dispersion co-efficient $D_c = 15 \text{ ps/km.nm}$ for wavelength $\lambda = 1550 \text{ nm}$ and fibre attenuation = 0.2dB/km .

The bit error rate (BER) performance of WDM ring network is depicted in Fig. 3.1 in presence of fibre chromatic dispersion, accumulated ASE noise due to the cascaded EDFAs, noise due to crosstalk from adjacent channels and receiver noises without considering the effect of laser phase noise. The BER is plotted as a function of the received optical power $P_s(\text{dBm})$ for several values of FP filter bandwidth. The receiver sensitivity is defined as the optical power required to achieve a BER of 10^{-9} . In this figure, results are given for $D_c=15\text{ps/km.nm}$, $L=40\text{km}$, $N=2$ when the modulation index $h(=2\Delta fT)=1.0$ and channel spacing $\Delta F=1.0\text{nm}$. The figure reveals that the BER decreases with increase in input power and when the value of FP filter bandwidth $B=0.45\text{nm}$ the receiver sensitivity is found to be -23.25dBm . At increased and decreased value of FP filter bandwidth from $B=0.45\text{nm}$ (i.e. when $B>0.45\text{nm}$ & $B<0.45\text{nm}$) the required amount of signal power is higher to achieve the same BER. The additional signal power compared to the case of $D_c=0.0$ may be termed as the power penalty at $\text{BER}=10^{-9}$ due to the effect of fibre chromatic dispersion.

When the fibre length $L=120\text{km}$ for same number of node and channel spacing, as in Fig. 3.1, the BER performance results are plotted in Fig. 3.2 with B as a

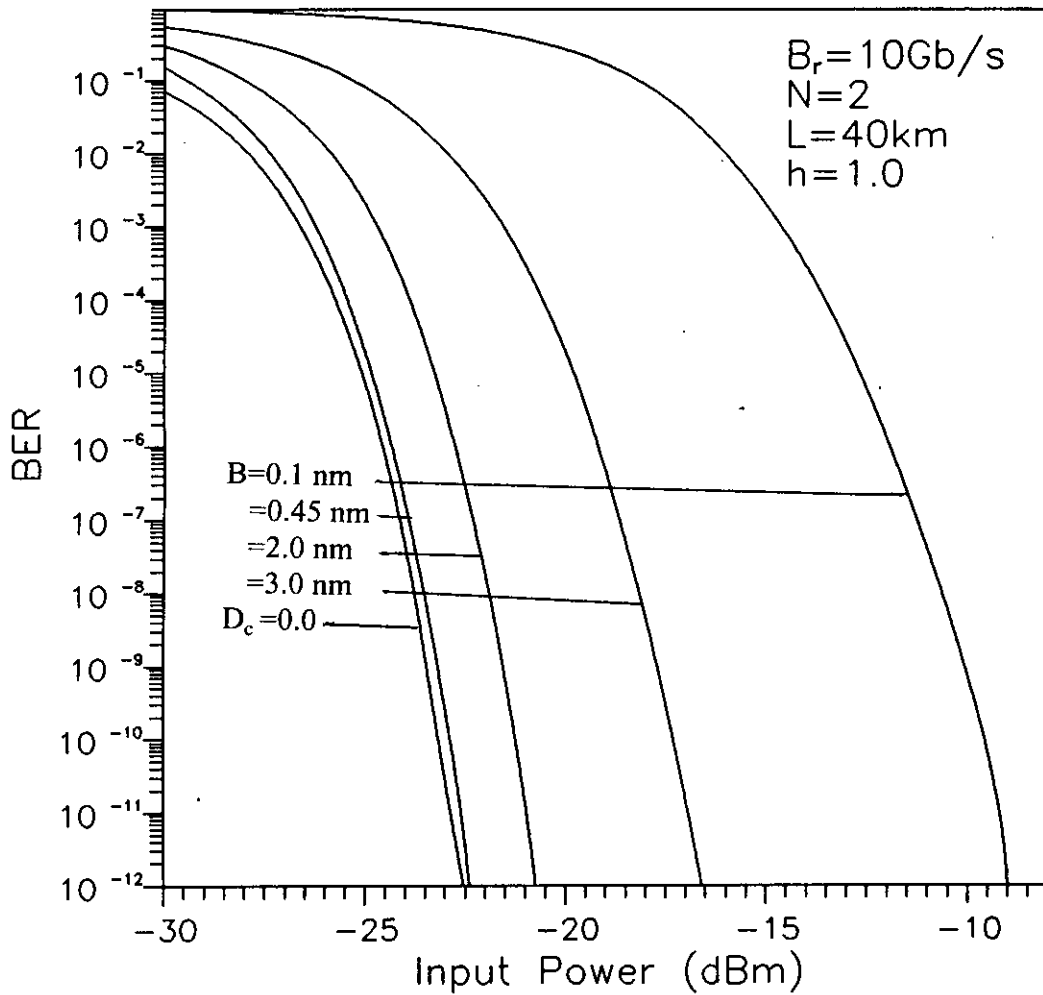


Fig. 3.1 The bit error rate (BER) performance of a WDM optical ring network using direct detection optical FSK system at a bit rate 10 Gb/s with fibre chromatic dispersion $D_c = 15 \text{ ps/km.nm}$, fibre length $L = 40 \text{ km}$, number of node $N = 2$, channel spacing $\Delta F = 1.0 \text{ nm}$ at an wavelength of 1550 nm and modulation index $h = 1.0$ for several values of FP filter bandwidth.

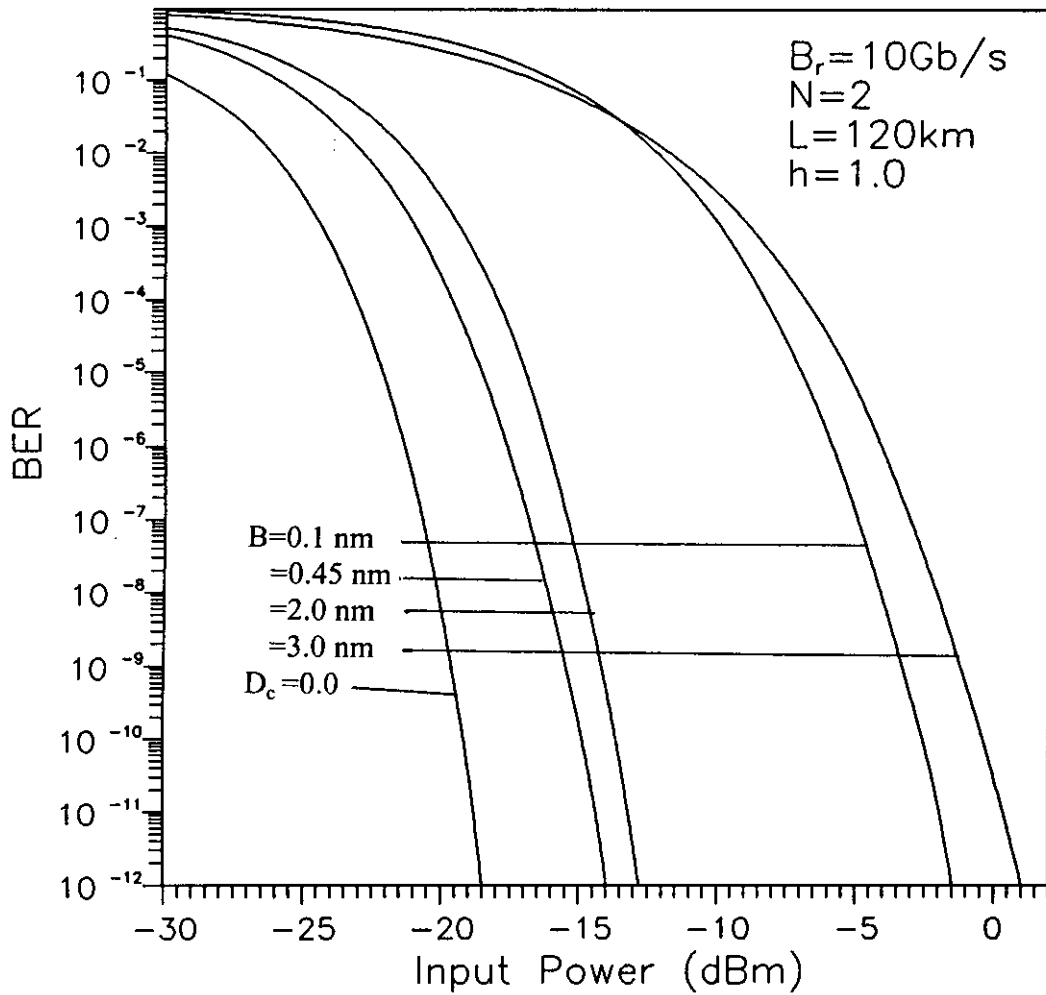


Fig. 3.2 The bit error rate (BER) performance of a WDM optical ring network using direct detection optical FSK system at a bit rate 10 Gb/s with fibre chromatic dispersion $D_c = 15 \text{ ps/km.nm}$, fibre length $L = 120 \text{ km}$, number of node $N = 2$, channel spacing $\Delta F = 1.0 \text{ nm}$ at an wavelength of 1550 nm and modulation index $h = 1.0$ for several values of FP filter bandwidth.

parameter. Comparing Fig. 3.2 with Fig. 3.1 it is clear that performance of the system degraded due to fibre chromatic dispersion for higher fibre length. The BER performance results are plotted in Fig. 3.3 for $N=8$, $L=40\text{km}$ and same channel spacing for different filter bandwidths. It is observed from the Fig. 3.3 comparing with Fig. 3.1 that receiver sensitivity is degraded due to increase in the number of nodes or channels. This is due to the fact that the number of cascaded EDFAs and MUX/DMUX increase with the number of channels and as a result the accumulated spontaneous emission noise (ASE) increases and signal magnitude decreases due to cascading filtering effect.

When the modulation index is decreased to $h=0.5$, the BER performance results are plotted in Fig. 3.4 for $D_c=15\text{ps/km.nm}$, $N=8$, and $L=40\text{km}$ with FP filter bandwidths as a parameter. Compared to Fig 3.3 it becomes evident that the power penalty suffered by the network due to fibre chromatic dispersion is slightly decreased when h is decreased from 1.0 to 0.5. This is due to the fact that as h decreases the difference between 'mark' and 'space' frequencies in the FSK signal spectrum decreases. As a consequence intersymbol interference caused by fibre chromatic dispersion is less at decreased values of modulation index h .

In presence of laser phase noise with fibre chromatic dispersion the BER performance of a WDM ring network is shown in Fig. 3.5 for fibre length $L=40\text{km}$, number of node $N=4$ and modulation index $h=1.0$ with same dispersion co-efficient and channel spacing taking FP filter bandwidths as a parameter for $\Delta\nu T=0.001$. The performance results for same parameters without laser phase noise ($\Delta\nu T=0.0$) are given in Fig. 3.6. It is noticed from the figures that BER performance is degraded due to the effect of laser phase noise caused by non-zero linewidth compared to the Fig 3.6. Phase noise causes the spectrum of the FSK signal to be broadened and for a given receiver bandwidth, the signal power is less at output of the receiver bandpass filter. As a result

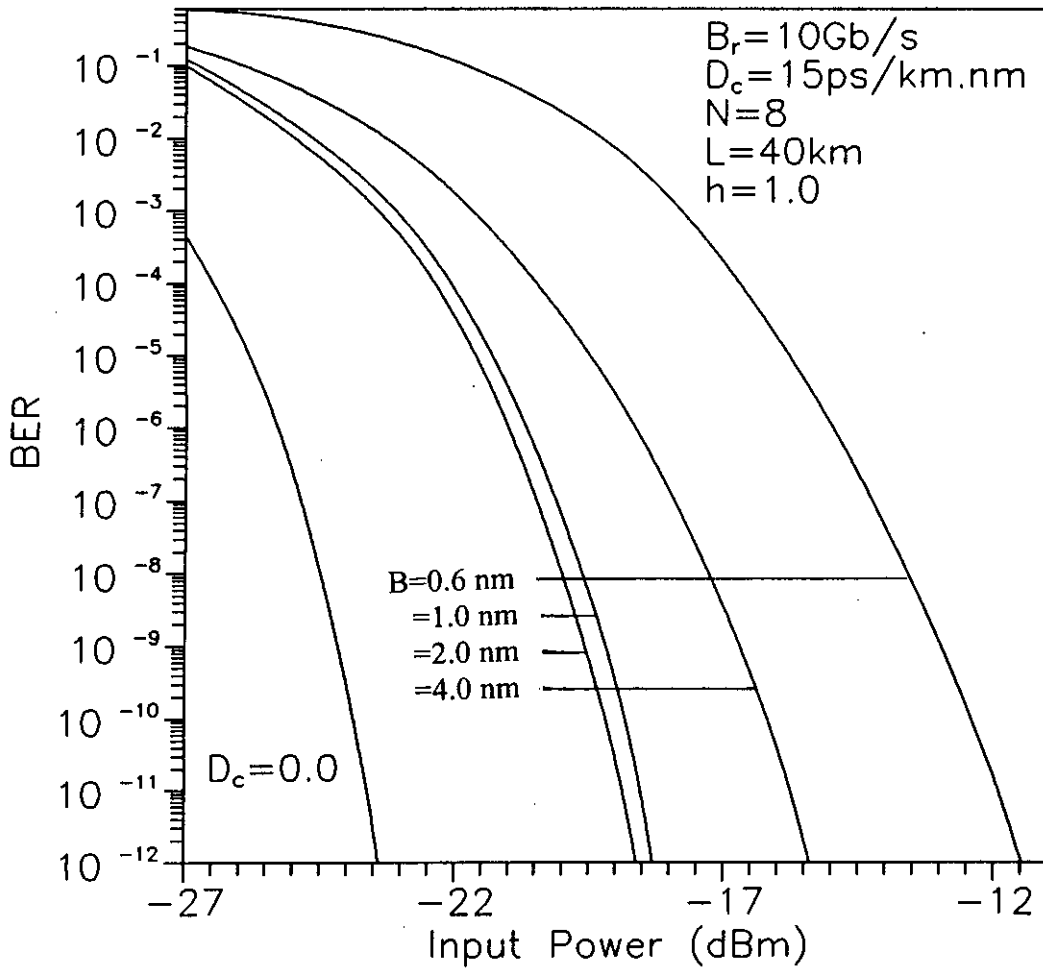


Fig. 3.3 The bit error rate (BER) performance of a WDM optical ring network using direct detection optical FSK system at a bit rate 10 Gb/s with fibre chromatic dispersion $D_c = 15 \text{ ps/km.nm}$, fibre length $L = 40 \text{ km}$, number of node $N = 8$, channel spacing $\Delta F = 1.0 \text{ nm}$ at an wavelength of 1550 nm and modulation index $h = 1.0$ for several values of FP filter bandwidth.

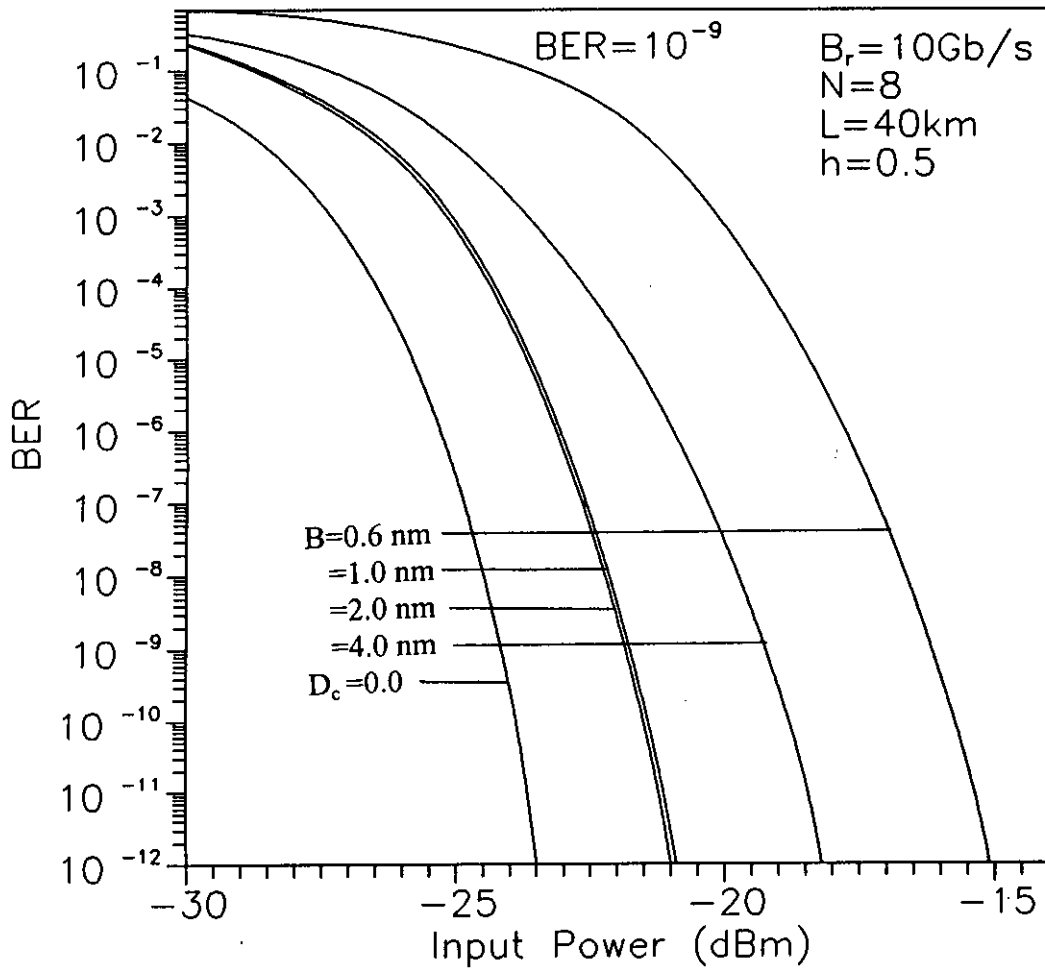


Fig. 3.4 The bit error rate (BER) performance of a WDM optical ring network using direct detection optical FSK system at a bit rate 10 Gb/s with fibre chromatic dispersion $D_c = 15 \text{ ps/km.nm}$, fibre length $L = 40 \text{ km}$, number of node $N = 8$, channel spacing $\Delta F = 1.0 \text{ nm}$ at an wavelength of 1550 nm and modulation index $h = 0.5$ for several values of FP filter bandwidth.

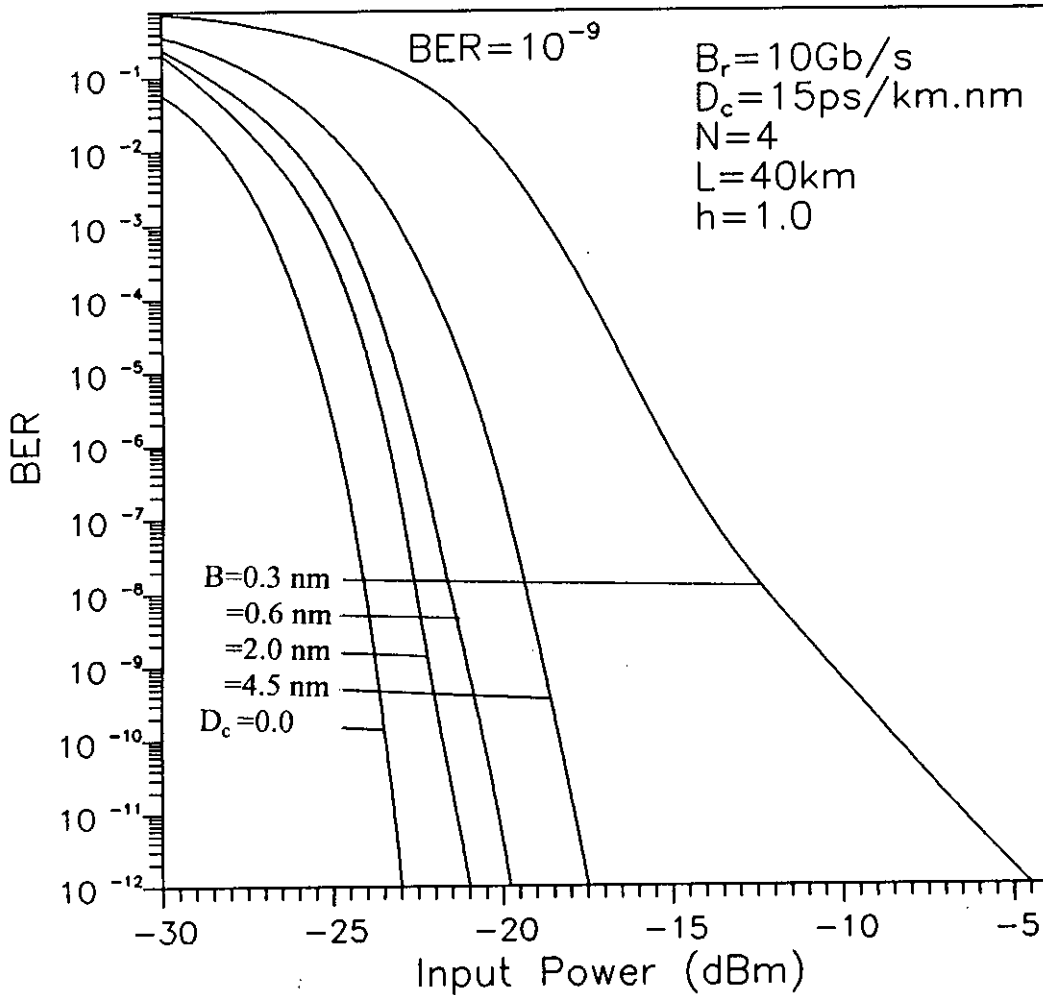


Fig. 3.5 The bit error rate (BER) performance of a WDM optical ring network using direct detection optical FSK system at a bit rate 10 Gb/s with combined effect of fibre chromatic dispersion $D_c = 15 \text{ ps/km.nm}$ and laser phase noise $\Delta\nu T = 0.001$, fibre length $L = 40 \text{ km}$, number of node $N = 4$, channel spacing $\Delta F = 1.0 \text{ nm}$ at a wavelength of 1550 nm and modulation index $h = 1.0$ for several values of FP filter bandwidth.

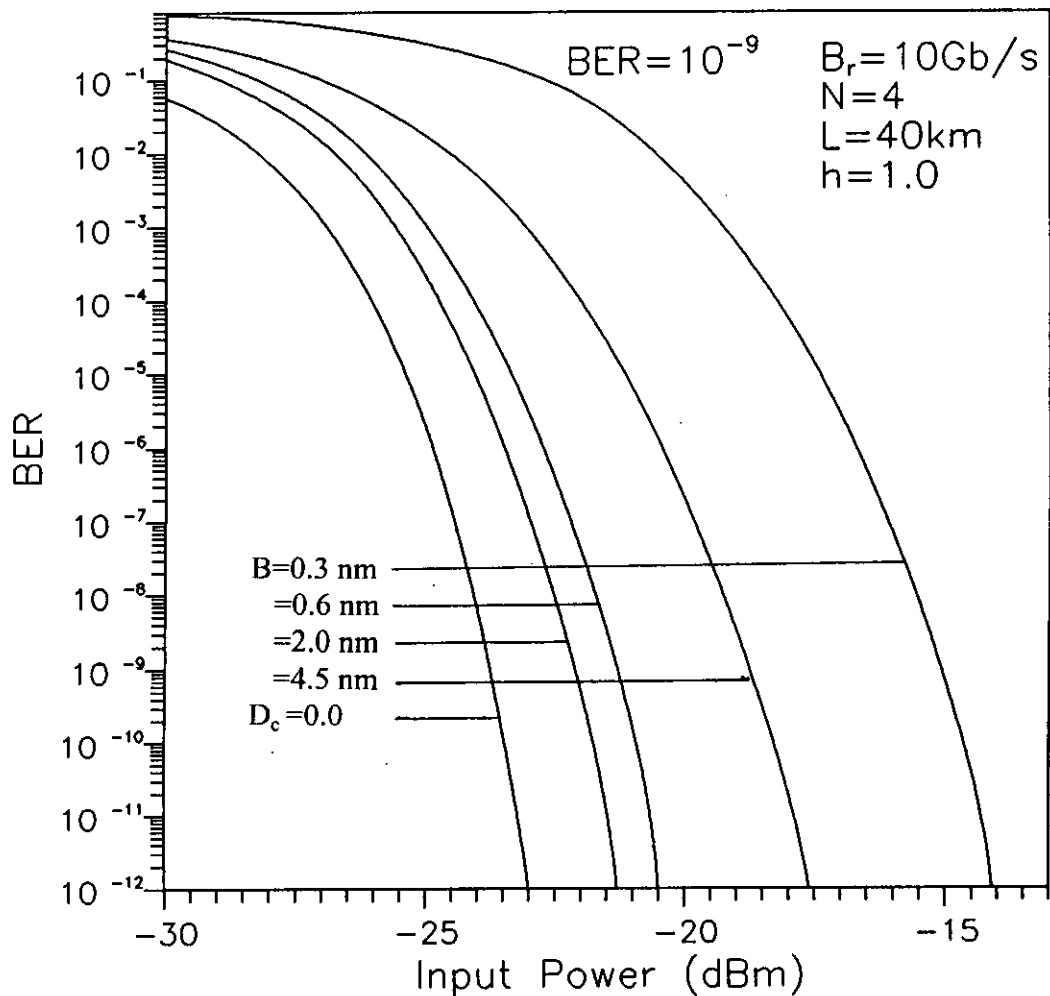


Fig. 3.6 The bit error rate (BER) performance of a WDM optical ring network using direct detection optical FSK system at a bit rate 10 Gb/s with fibre chromatic dispersion $D_c = 15 \text{ ps/km.nm}$, fibre length $L = 40 \text{ km}$, number of node $N = 4$, channel spacing $\Delta F = 1.0 \text{ nm}$ at a wavelength of 1550 nm and modulation index $h = 1.0$ for several values of FP filter bandwidth.

more signal power is required to achieve the same BER. The effect of phase noise is more at higher values of linewidth and lower values of filter bandwidth.

At a given input power the BER is higher in the presence of dispersion compared to the case when there is no dispersion. The receiver sensitivity thus degrades and there is additional penalty due to the effect of dispersion. From figures it is also observed that the receiver sensitivity is optimum at a particular filter bandwidth but severely degrades with filter bandwidths corresponding to a specified node. For example, the receiver sensitivity to achieve $BER=10^{-9}$ is -23.75 dBm when there is no dispersion ($D_c=0.0$) whereas in presence of dispersion with $D_c=15\text{ps/km.nm}$, the receiver sensitivity is found to be -21.5 dBm (from Fig. 3.6) at $B=0.6$ nm but at $B=4.5$ nm and 5.0 nm the receiver sensitivity is found to be -18.8 dBm and -15.2 dBm respectively. The sensitivity degradation is found to be more pronounced in the presence of both dispersion and laser phase noise. For $\Delta\nu T=0.001$, the receiver sensitivity is -23.7 dBm when $D_c=0.0$ and it is found to be -21.15 dBm when $D_c=15\text{ps/km.nm}$ (from Fig. 3.5) at $B=0.6$ nm whereas at $B=4.5$ nm the sensitivity is found to be -18.75 dBm.

The values of penalty in signal power suffered by the system due to fibre chromatic dispersion are determined from bit error rate (BER) curves at $BER=10^{-9}$. The plots of power penalty versus FP filter bandwidth (nm) are shown in Fig. 3.7 and Fig. 3.8 with modulation index $h=1.0$ for several values of channel spacing and fibre span $L=40\text{km}$ and $L=120\text{km}$ respectively. The figure depicts the variation of power penalty with filter bandwidth B and it is revealed that for small values of the filter bandwidth the penalty is higher and decreases with increase in B . At a particular filter bandwidth the penalty is minimum. Further increase in the filter bandwidth causes the penalty to increase rapidly. The FP filter bandwidth at which we obtained the minimum penalty for a specific node called optimum filter bandwidth for that node.

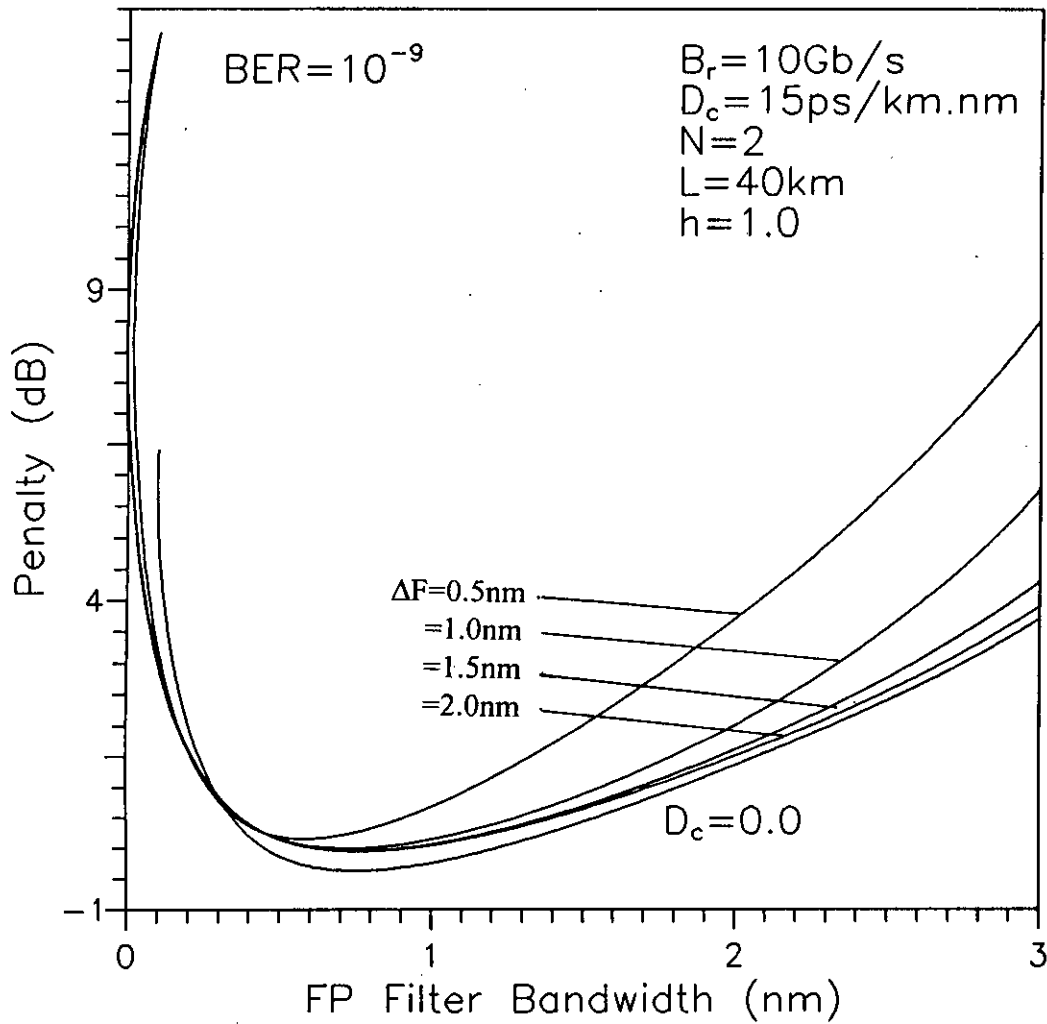


Fig. 3.7 Plots of penalty in signal power due to fibre chromatic dispersion at $BER=10^{-9}$ versus FP filter bandwidth (nm) with fibre length $L=40$ km, number of node $N=2$ and modulation index $h=1.0$ for several values of channel spacing ΔF (nm).

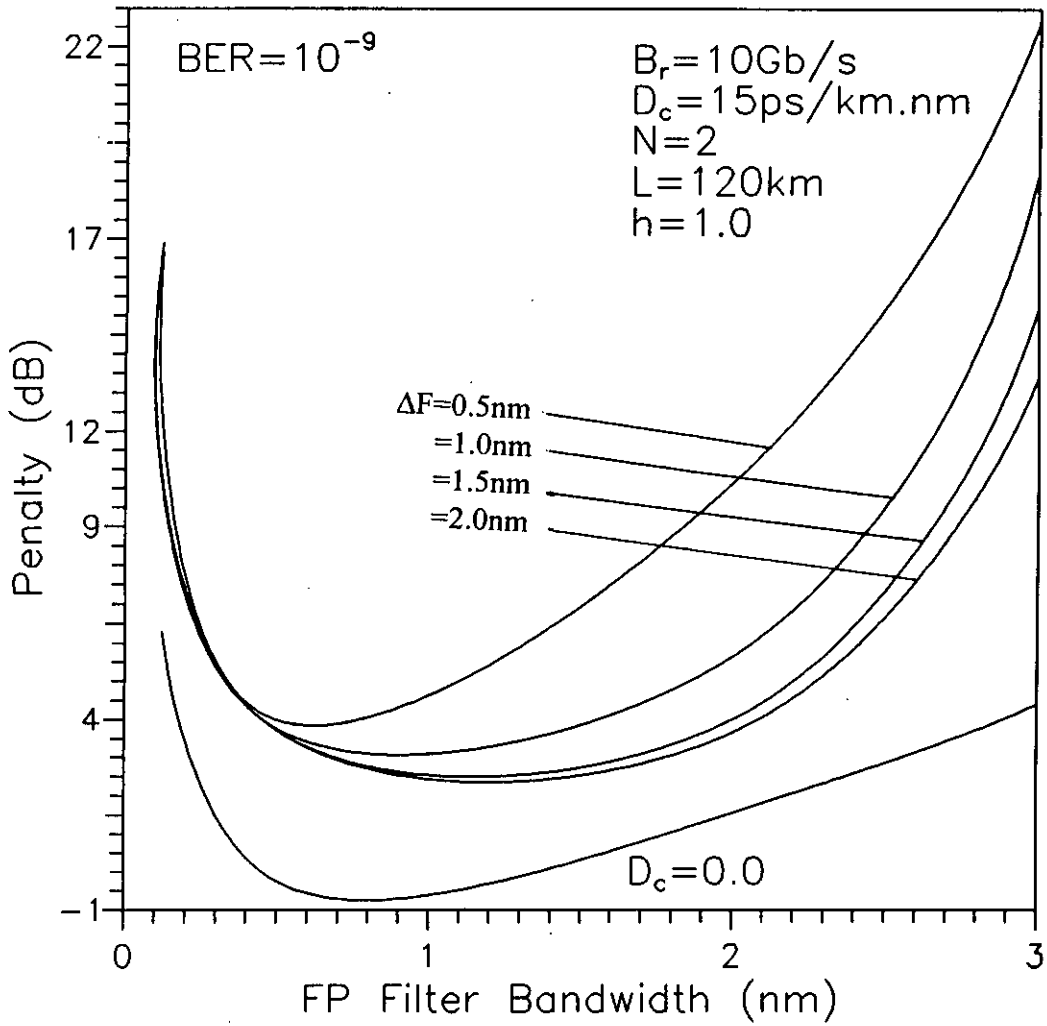


Fig. 3.8 Plots of penalty in signal power due to fibre chromatic dispersion at $\text{BER} = 10^{-9}$ versus FP filter bandwidth (nm) with fibre length $L = 120$ km, number of node $N = 2$ and modulation index $h = 1.0$ for several values of channel spacing ΔF (nm).

Further, it is also observed that for channel spacing $\Delta F=2.0$ nm, the penalty is below 0.15 dB when fibre length $L=40$ km and number of node $N=2$ at filter bandwidth $B=0.5$ nm. When channel spacing is decreased from 2.0nm, the penalty becomes more than 0.15 dB. Comparing Fig. 3.7 and Fig. 3.8 we also found that for the same node and filter bandwidth, the penalty is more for larger fibre span. As seen from the figures, the penalty is approximately 0.15 dB (for $B=0.5$ nm and $\Delta F=2.0$ nm) corresponding to fibre length $L=40$ km whereas it increases to 3.35 dB when L is increased to 120km.

It is also noticed from the similar plots in Fig. 3.9 and Fig. 3.10 for node $N=4$ with fibre length $L=40$ km and $L=120$ km the penalty in signal power is higher comparing with Fig. 3.7 and Fig. 3.8 and minimum power penalty is obtained at filter bandwidth $B=1.5$ nm for channel spacing 2.0 nm. When there is no dispersion (ie. $D_c=0.0$), the optimum filter bandwidth is approximately 0.75 nm. It is further observed from the figures that the penalty becomes higher when filter bandwidth is decreased or increased from its optimum value. Similar results is found from the plots in Fig. 3.11 and Fig. 3.12 for node $N=8$ with fibre length $L=80$ km and $L=120$ km. The penalty in signal power increases with number of node and fibre length. The optimum filter bandwidth in case of node $N=8$ is approximately 2.0 nm. For number of nodes $N=10$ the similar results is noticed in Fig. 3.13 and Fig. 3.14 with fibre length $L=40$ km and $L=80$ km. Comparing with the previous results plotted for different nodes, it is observed that the power penalty is very high for $N=10$ at larger fibre span due to the effect of chromatic dispersion which degrades system performance at larger fibre span. Further the accumulated ASE noise is also dominant when number of nodes increases. The optimum filter bandwidth is found to be 3.0 nm for number of nodes $N=10$.

The variation of power penalty with B by considering the combined effect of dispersion and laser phase noise for $\Delta\nu T=0.001$ is shown in Fig. 3.15 for

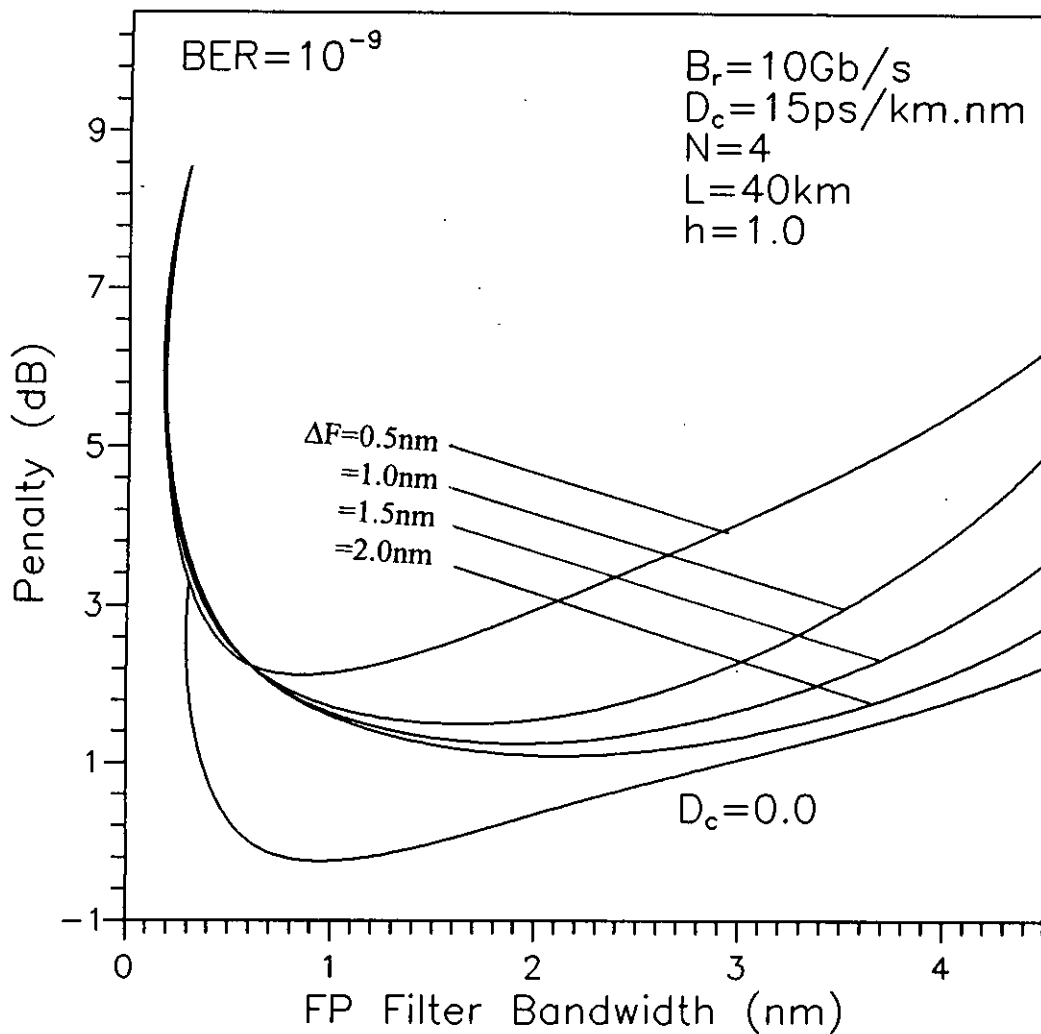


Fig. 3.9 Plots of penalty in signal power due to fibre chromatic dispersion at $\text{BER} = 10^{-9}$ versus FP filter bandwidth (nm) with fibre length $L = 40$ km, number of node $N = 4$ and modulation index $h = 1.0$ for several values of channel spacing ΔF (nm).

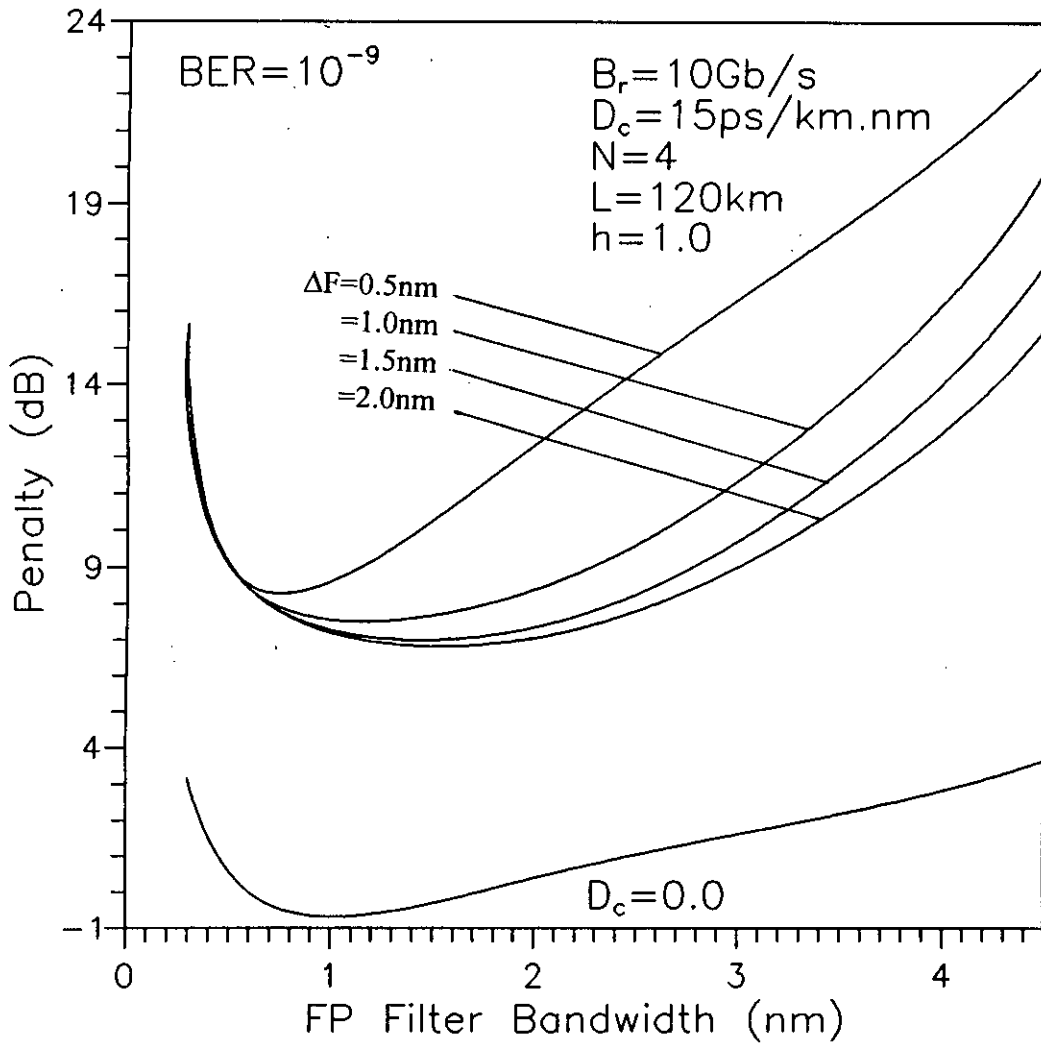


Fig. 3.10 Plots of penalty in signal power due to fibre chromatic dispersion at $\text{BER} = 10^{-9}$ versus FP filter bandwidth (nm) with fibre length $L = 120$ km, number of node $N = 4$ and modulation index $h = 1.0$ for several values of channel spacing ΔF (nm).

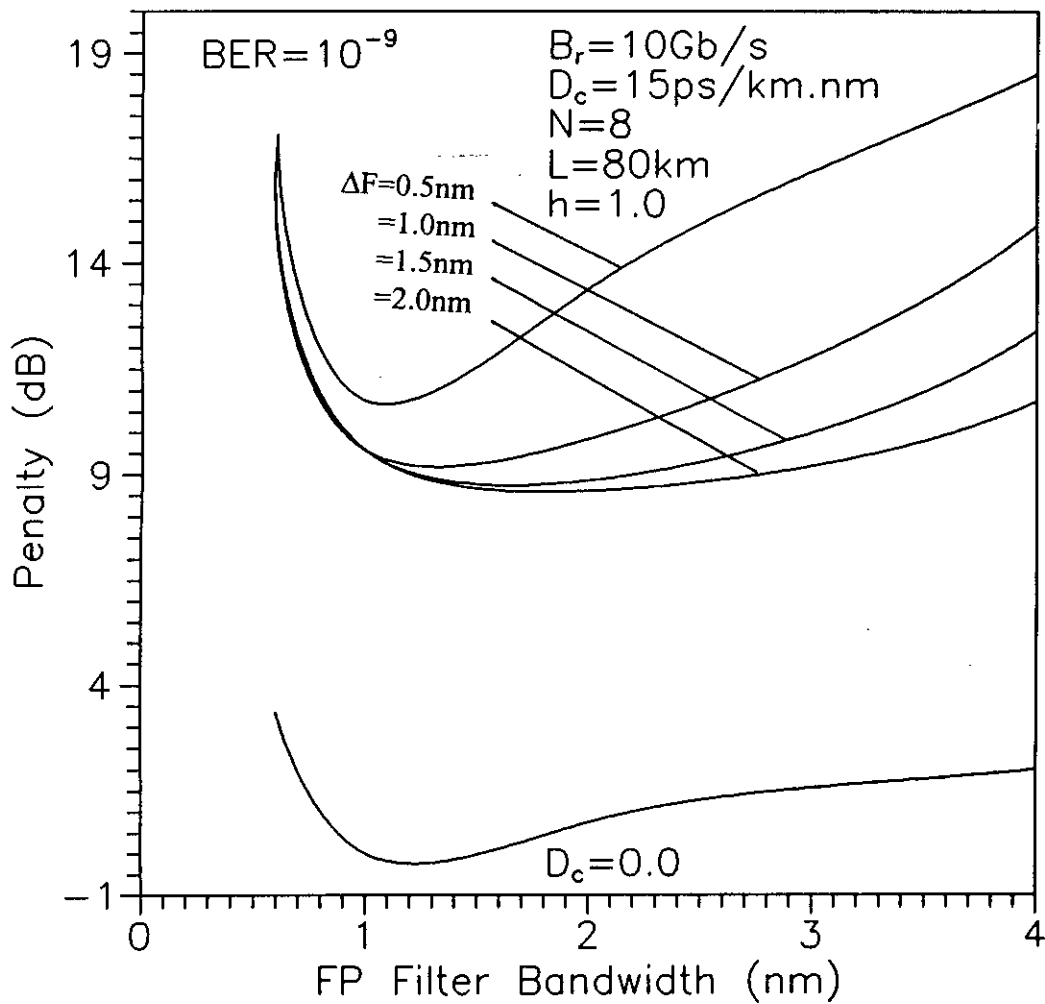


Fig. 3.11 Plots of penalty in signal power due to fibre chromatic dispersion at $\text{BER} = 10^{-9}$ versus FP filter bandwidth (nm) with fibre length $L = 80$ km, number of node $N = 8$ and modulation index $h = 1.0$ for several values of channel spacing ΔF (nm).

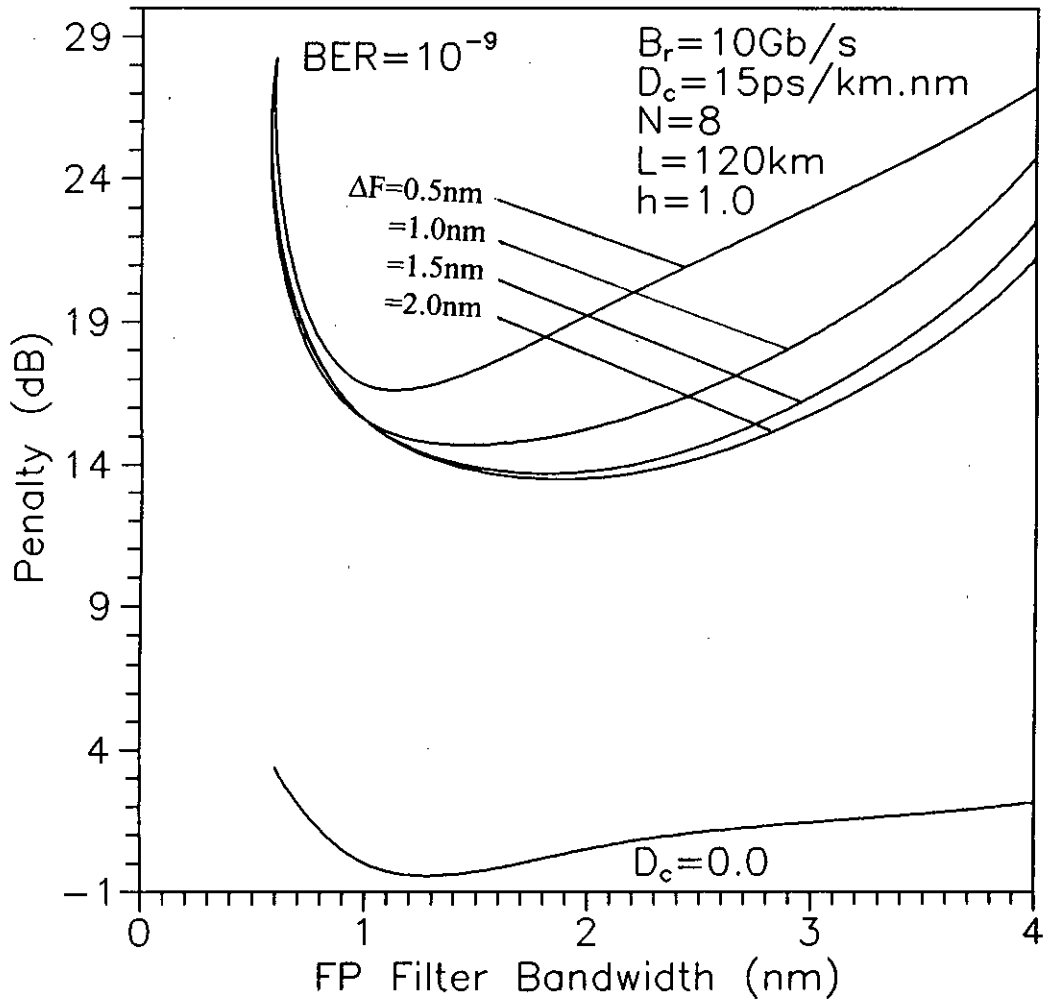


Fig. 3.12 Plots of penalty in signal power due to fibre chromatic dispersion at $\text{BER} = 10^{-9}$ versus FP filter bandwidth (nm) with fibre length $L = 120$ km, number of node $N = 8$ and modulation index $h = 1.0$ for several values of channel spacing ΔF (nm).

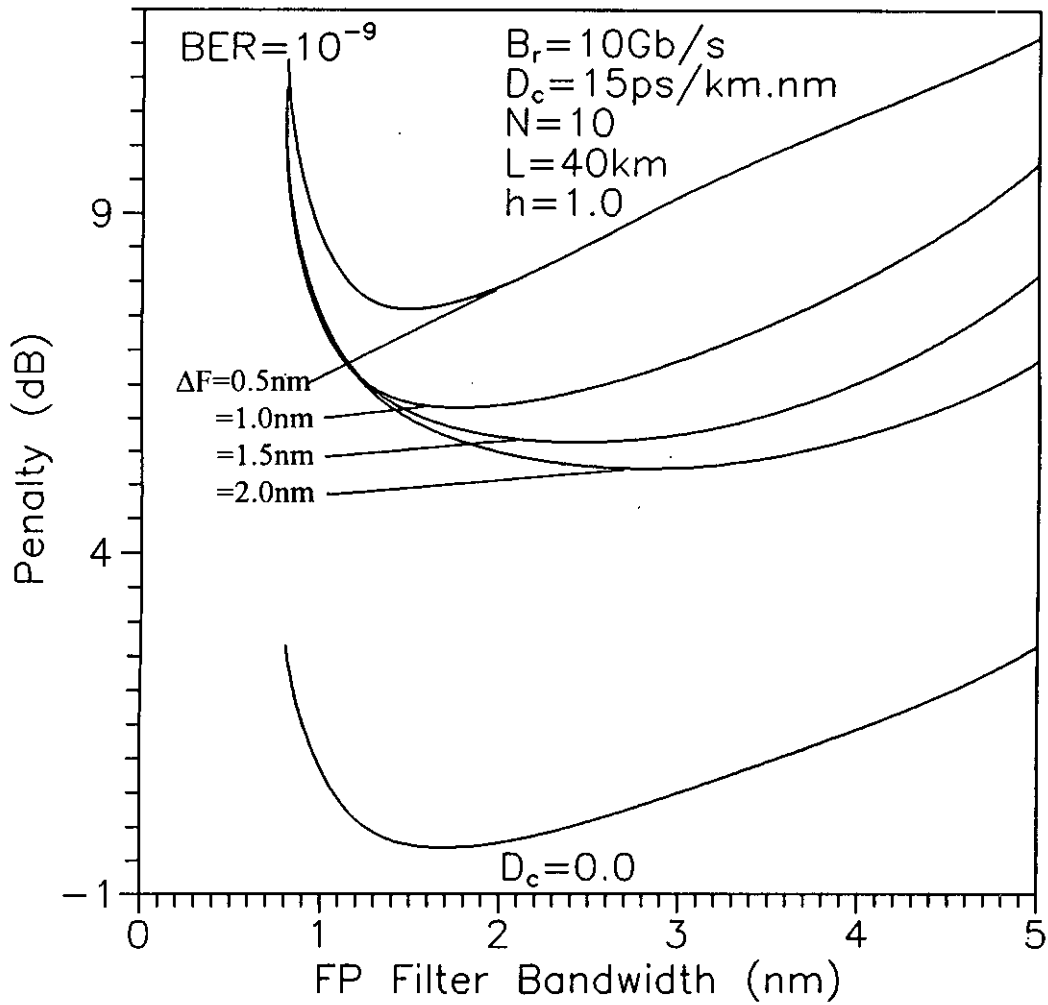


Fig. 3.13 Plots of penalty in signal power due to fibre chromatic dispersion at $\text{BER} = 10^{-9}$ versus FP filter bandwidth (nm) with fibre length $L = 40$ km, number of node $N = 10$ and modulation index $h = 1.0$ for several values of channel spacing ΔF (nm).

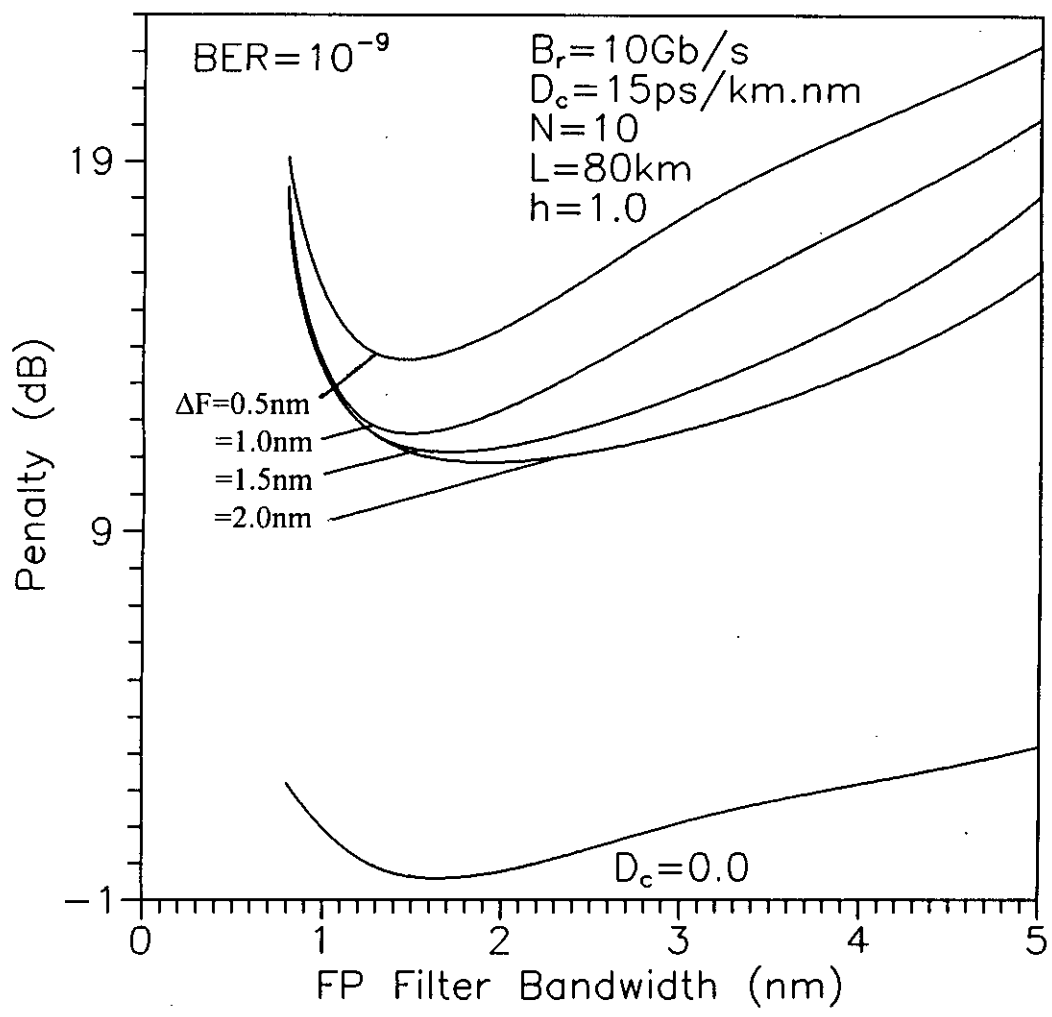


Fig. 3.14 Plots of penalty in signal power due to fibre chromatic dispersion at $\text{BER} = 10^{-9}$ versus FP filter bandwidth (nm) with fibre length $L = 80$ km, number of node $N = 10$ and modulation index $h = 1.0$ for several values of channel spacing ΔF (nm).

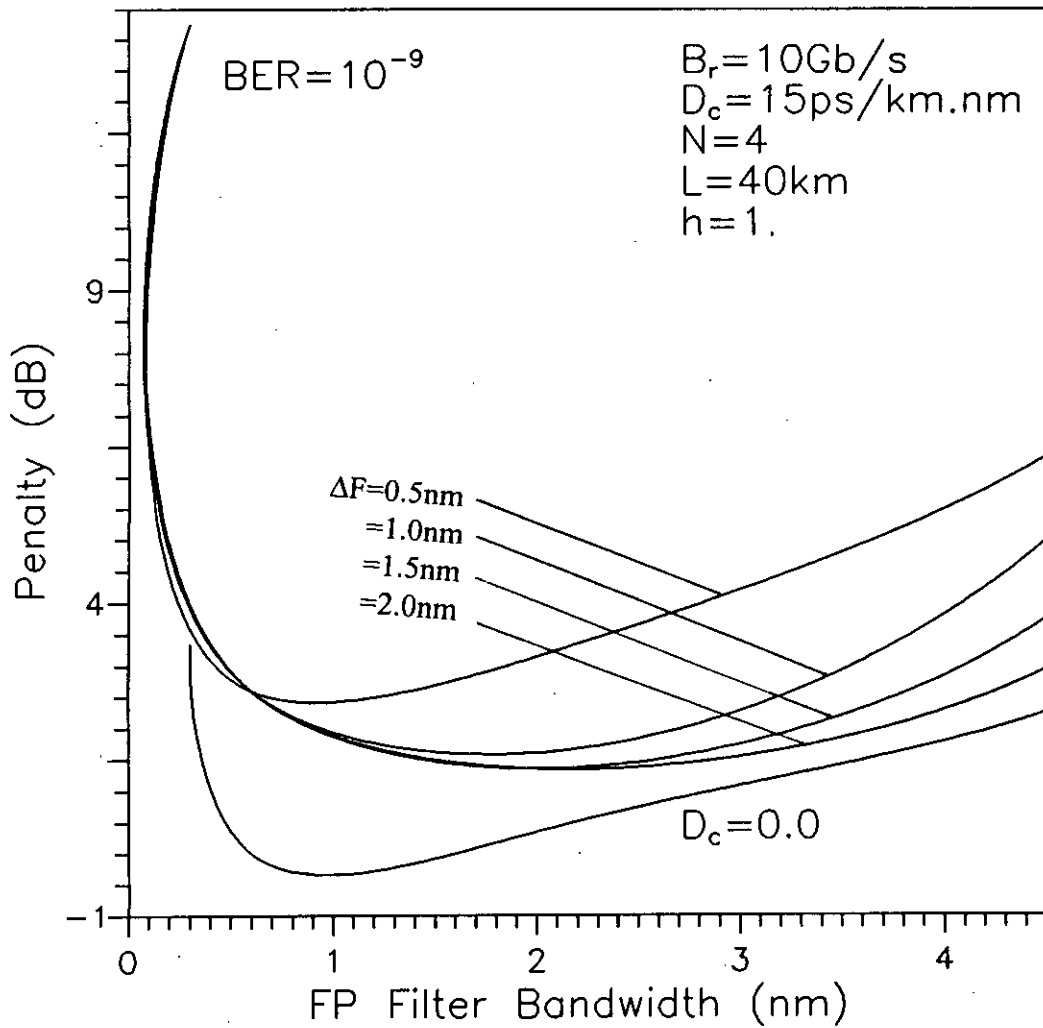


Fig. 3.15 Plots of penalty in signal power due to combined effect of laser phase noise and fibre chromatic dispersion at $\text{BER} = 10^{-9}$ versus FP filter bandwidth (nm) with fibre length $L = 40 \text{ km}$, number of node $N = 4$, normalized laser linewidth $\Delta\nu T = 0.001$ and modulation index $h = 1.0$ for several values of channel spacing ΔF (nm).

$L=40\text{km}$, $N=4$. Comparing Fig. 3.15 with Fig. 3.9 additional power penalty is observed due to laser phase noise in Fig. 3.15. For $L=40\text{ km}$, $\Delta F=2.0\text{ nm}$, $B=2.0\text{ nm}$ the penalty is 1.25 dB (Fig. 3.9) when only fibre chromatic dispersion is present whereas the penalty is approximately 1.35 dB when combined effect of laser phase noise and fibre chromatic dispersion is present (Fig. 3.15). This is due to the fact that phase noise causes the spectrum of the FSK signal to be broadened and for a given receiver bandwidth, the signal power is less at the output of the receiver bandpass filter.

Similar plots of penalty versus FP filter bandwidth B are also shown in Fig. 3.16 and Fig. 3.17 for $h=0.5$. comparing Fig. 3.11 and Fig. 3.17 we note that for same fibre span and same values of filter bandwidth and channel spacing, the penalty is lower for lower values modulation index. This may due to the fact that the effect of chromatic dispersion is lower at lower spectral bandwidth of FSK signal at decreased modulation index. For $L=80\text{ km}$, $\Delta F=2.0\text{ nm}$, $B=2.0\text{ nm}$ the penalty is 8.75 dB (Fig. 3.11) when $h=1.0$ whereas the penalty is approximately 3.93 dB when h is decreased to 0.5 (Fig. 3.17).

To get more insight in to the effect of dispersion on the system performance, the penalty in signal power at $\text{BER}=10^{-9}$ is plotted as a function of channel spacing ΔF in Fig. 3.18 and Fig. 3.19 for node $N=2$ with FP filter bandwidth B as a parameter. For fibre length $L=40\text{km}$ (Fig. 3.18) it is found that penalty in signal power with filter bandwidth $B=0.5\text{ nm}$ is approximately equal for different channel spacing. Because at lower filter bandwidth crosstalk noise power is less dominant over other noises. Whereas at filter bandwidth $B=1.0\text{nm}$ penalty is very high at channel spacing 0.5nm and it is decreased when channel spacing is increased and minimum penalty is obtained at channel spacing 2.0nm . This is due to the fact that at lower values of channel spacing and higher values of filter bandwidth crosstalk noise power is larger. Crosstalk noise power become reduced for a particular filter bandwidth when channel spacing

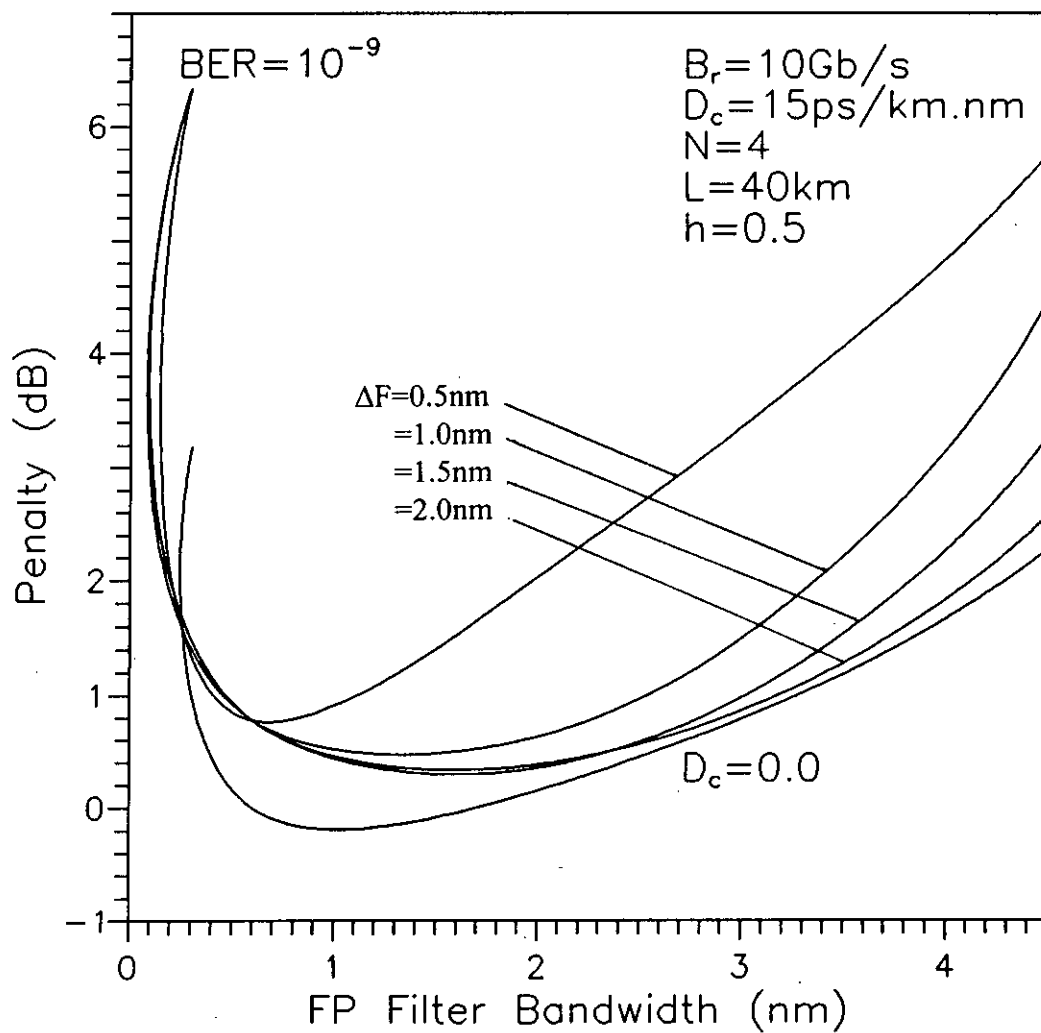


Fig. 3.16 Plots of penalty in signal power due to fibre chromatic dispersion at $\text{BER} = 10^{-9}$ versus FP filter bandwidth (nm) with fibre length $L = 40$ km, number of node $N = 4$ and modulation index $h = 0.5$ for several values of channel spacing ΔF (nm).

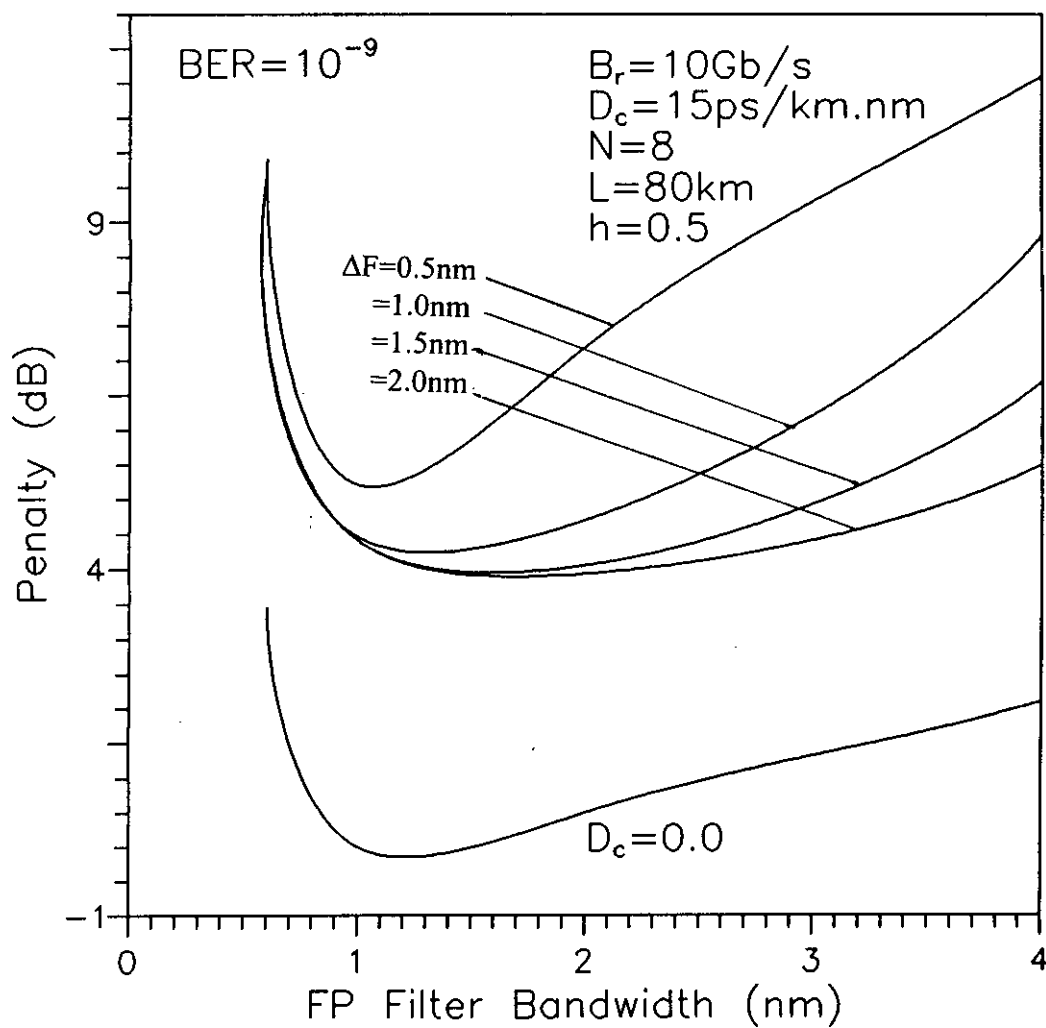


Fig. 3.17 Plots of penalty in signal power due to fibre chromatic dispersion at $\text{BER} = 10^{-9}$ versus FP filter bandwidth (nm) with fibre length $L = 80$ km, number of node $N = 8$ and modulation index $h = 0.5$ for several values of channel spacing ΔF (nm).

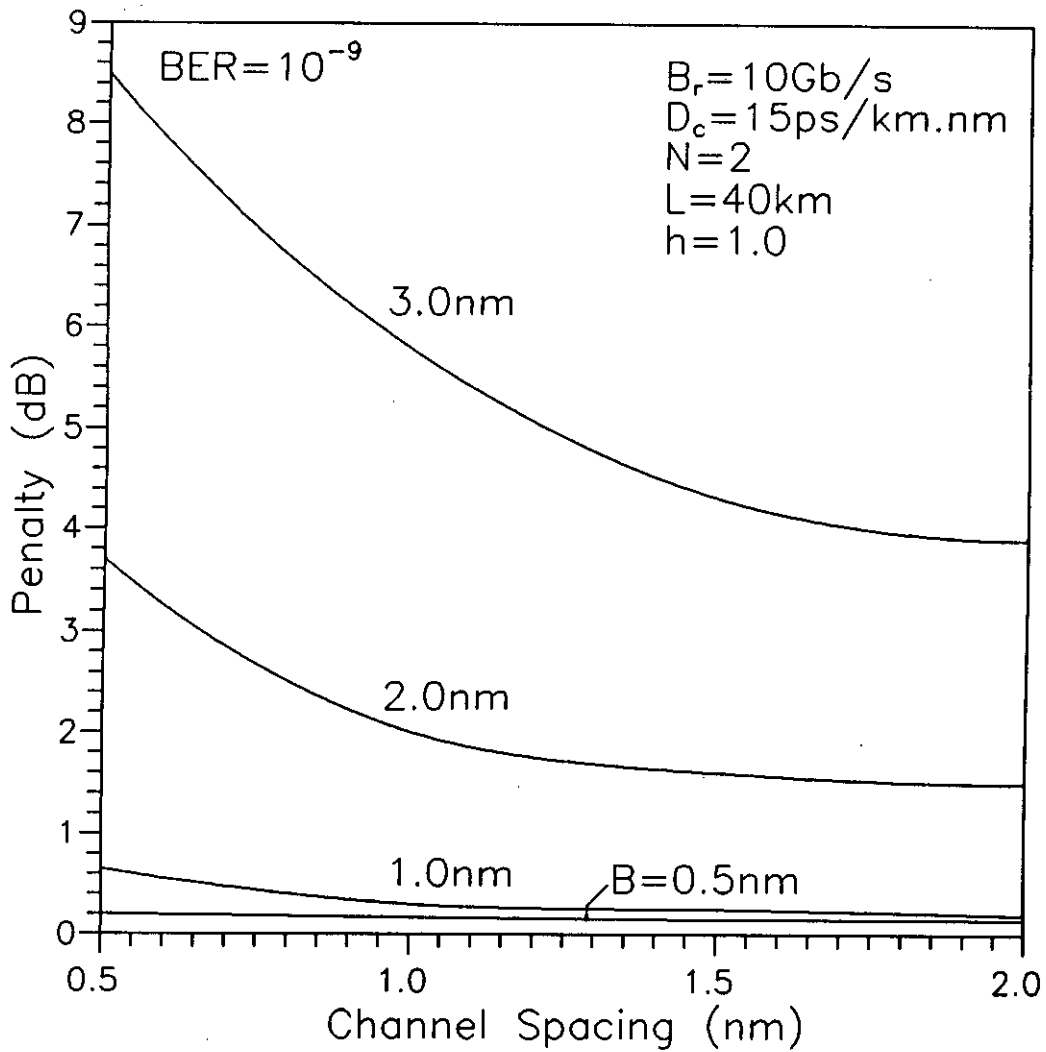


Fig. 3.18 Variation of power penalty in signal power due to fibre chromatic dispersion at $BER=10^{-9}$ versus channel spacing ΔF (nm) with fibre length $L=40$ km, number of node $N=2$ and modulation index $h=1.0$ for several values of FP filter bandwidth (nm).

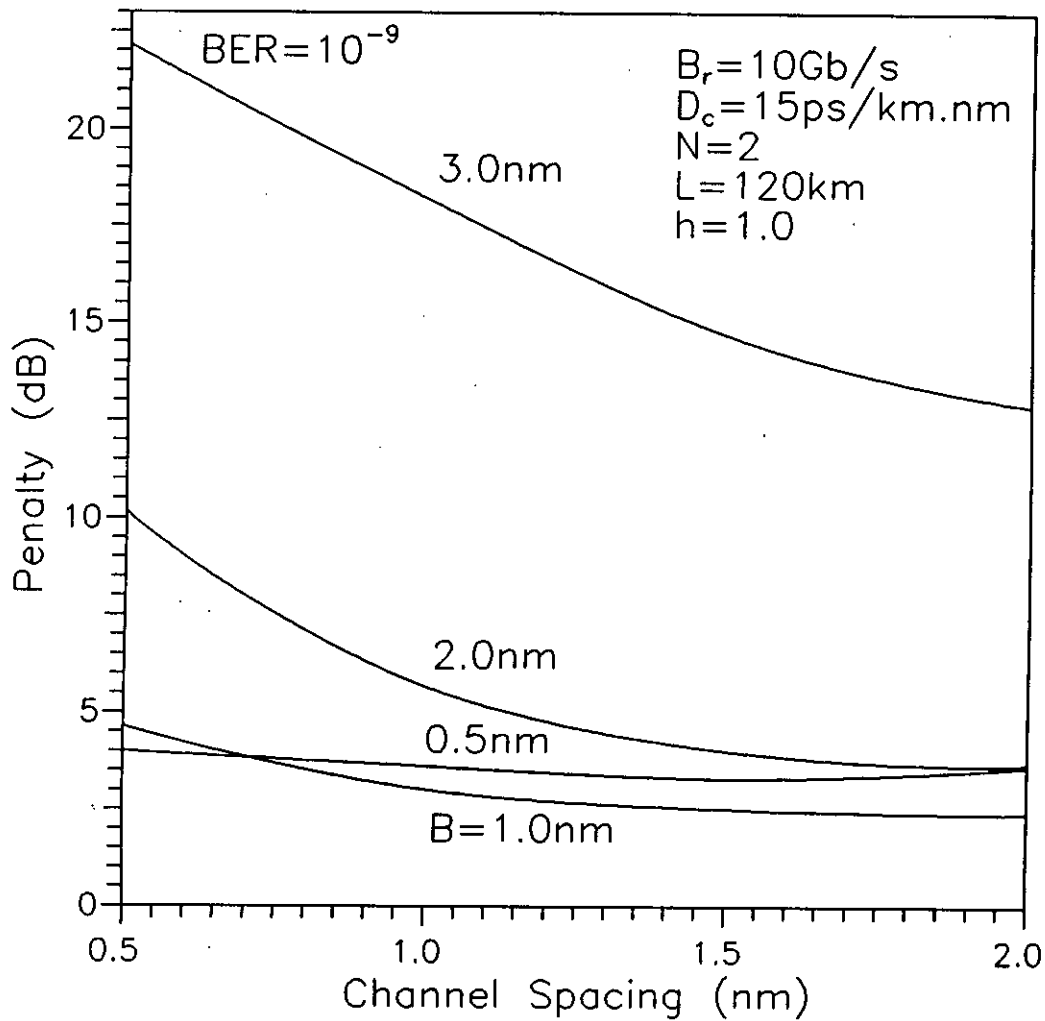


Fig. 3.19 Variation of power penalty in signal power due to fibre chromatic dispersion at $\text{BER} = 10^{-9}$ versus channel spacing ΔF (nm) with fibre length $L = 120 \text{ km}$, number of node $N = 2$ and modulation index $h = 1.0$ for several values of FP filter bandwidth (nm).

is increased from lower to higher values (0.5nm to 2.0nm). The power penalty is more pronounced when filter bandwidth is further increased as shown in Fig. 3.18. Similar results are also observed from Fig. 3.19 plotted for fibre length $L=120\text{km}$. Comparing Fig. 3.19 with Fig. 3.18 it is evident that more power penalty is found due to fibre chromatic dispersion for higher fibre length.

The variation of power penalty versus channel spacing is plotted in Fig. 3.20 at FP filter bandwidth $B=2.0\text{nm}$ with fibre length $L=40\text{km}$ and $L=80\text{km}$ for different number of nodes with modulation index $h=1.0$. It is noticed from the figure that for node $N=2$ the power penalty is higher at $B=2.0\text{nm}$ because optimum filter bandwidth for $N=2$ is 0.5nm . At $B=2.0\text{nm}$ crosstalk due to adjacent channel is very large in case of $N=2$. For node $N=4$ and $N=8$ the penalty is minimum because optimum filter bandwidth for these nodes are approximately 1.5nm and 2.0nm respectively. For node $N=10$ power penalty is higher because at filter bandwidth $B=2.0\text{nm}$ the signal magnitude at the output of the receiver is small so higher penalty is occurred at lower filter bandwidth. When filter bandwidth is increases then penalty becomes minimum and at $B=3.0\text{nm}$ the minimum penalty is obtained for $N=10$. The penalty is higher for $L=80\text{km}$ due to the effect of fibre chromatic dispersion for long node separation. Similar plots is shown in Fig 3.21 when $B=3.0\text{nm}$ for different number of nodes. Higher penalty is found for $N=2,4$ and 8 at $B=3.0\text{nm}$ because crosstalk noise power is very dominant at $B=3.0\text{nm}$ for these nodes. Whereas minimum penalty is obtained at $B=3.0\text{nm}$ for $N=10$.

The variation of power penalty with $h=0.5$ is plotted in Fig. 3.22 for $L=40\text{km}$ and $L=80\text{km}$ at $B=2.0\text{nm}$ for $N=4$. Comparing Fig. 3.22 with Fig. 3.20 it is noticed that at lower value of modulation index the penalty is very less.

The variation of minimum power penalty (corresponding to optimum filter bandwidth and $\text{BER}=10^{-9}$) versus fibre length is plotted in Fig. 3.23 for

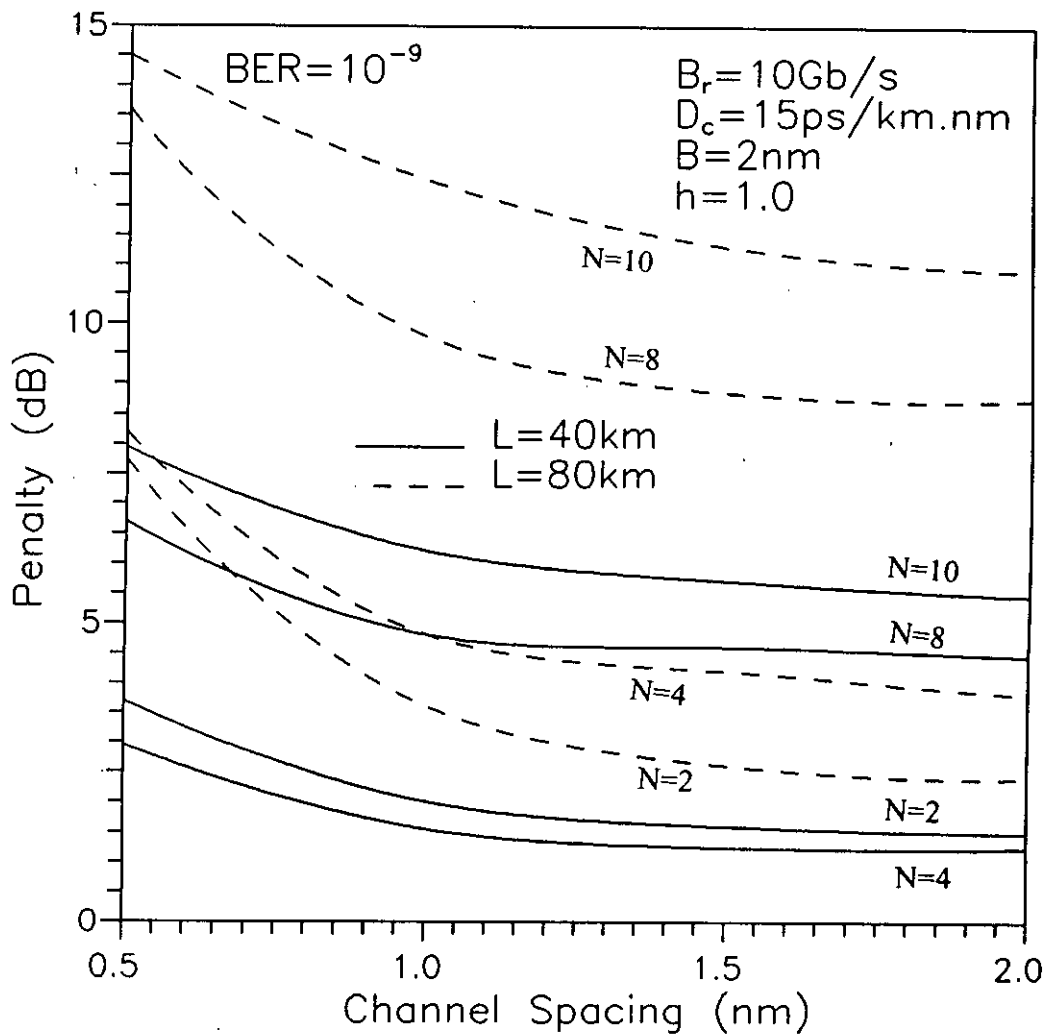


Fig. 3.20 Variation of power penalty in signal power due to fibre chromatic dispersion at $\text{BER} = 10^{-9}$ versus channel spacing ΔF (nm) with fibre length $L = 40 \text{ km}$, and $L = 80 \text{ km}$ at FP filter bandwidth $B = 2.0 \text{ nm}$ and modulation index $h = 1.0$ for different number of nodes.

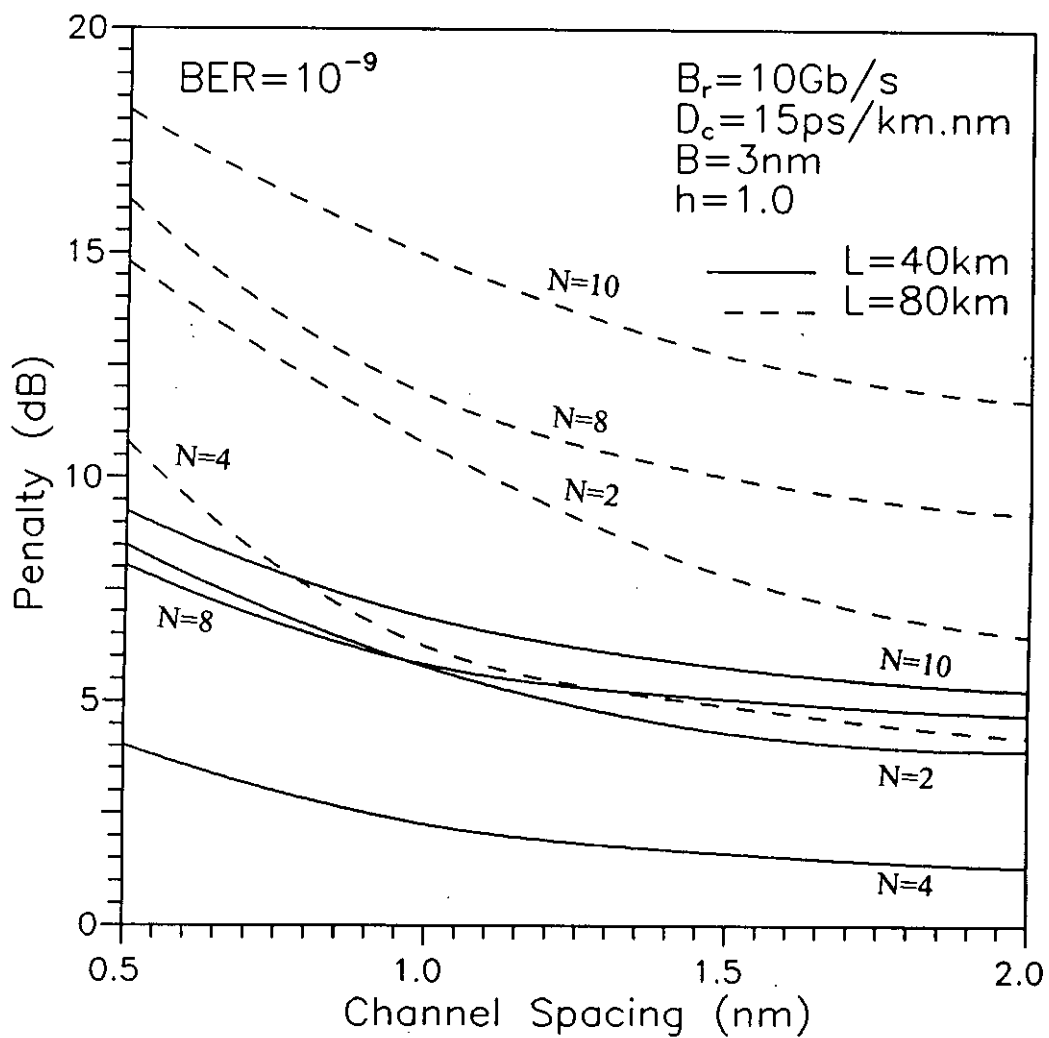


Fig. 3.21 Variation of power penalty in signal power due to fibre chromatic dispersion at $\text{BER} = 10^{-9}$ versus channel spacing ΔF (nm) with fibre length $L = 40 \text{ km}$, and $L = 80 \text{ km}$ at FP filter bandwidth $B = 3.0 \text{ nm}$ and modulation index $h = 1.0$ for different number of nodes

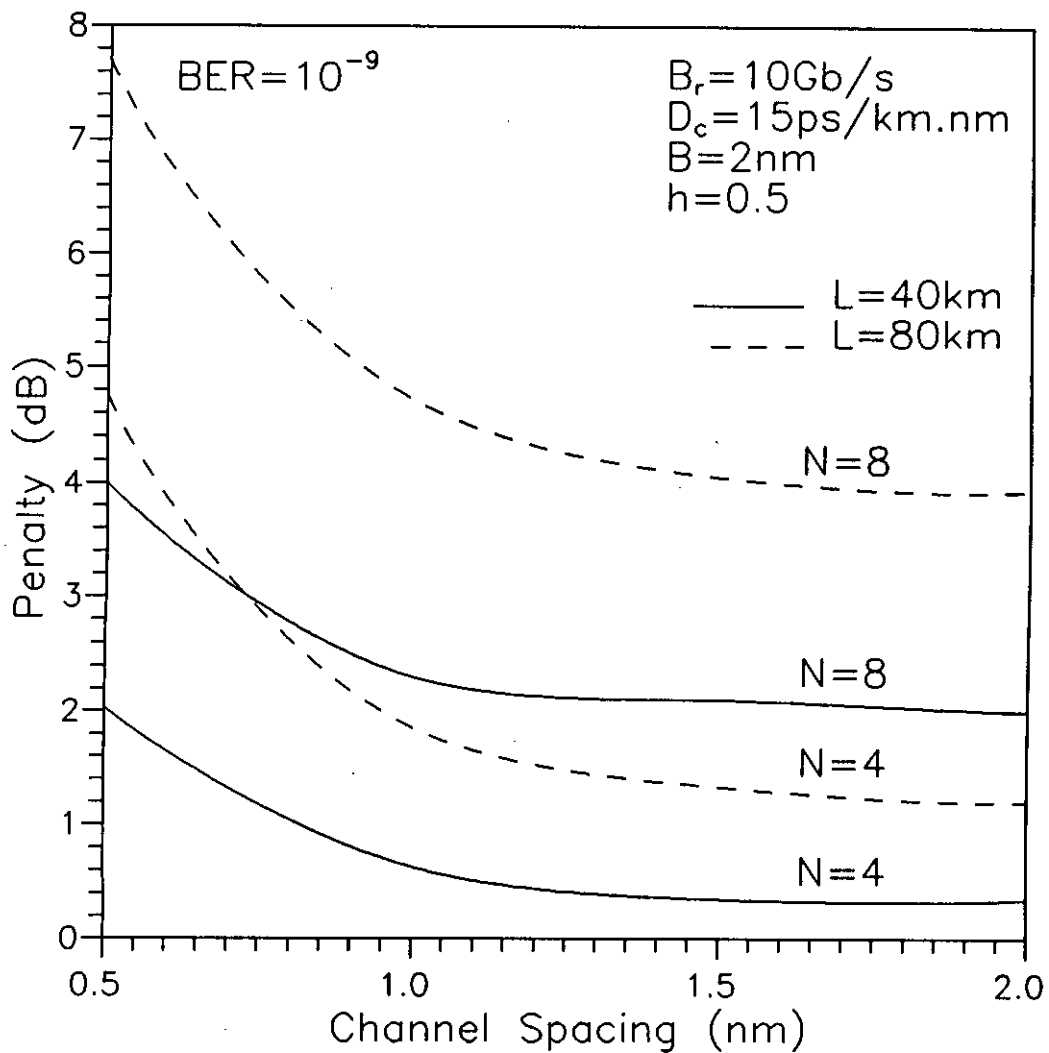


Fig. 3.22 Variation of power penalty in signal power due to fibre chromatic dispersion at $\text{BER} = 10^{-9}$ versus channel spacing ΔF (nm) with fibre length $L = 40 \text{ km}$, and $L = 80 \text{ km}$ at FP filter bandwidth $B = 2.0 \text{ nm}$ and modulation index $h = 0.5$ for different number of nodes $N = 4$ and $N = 8$.

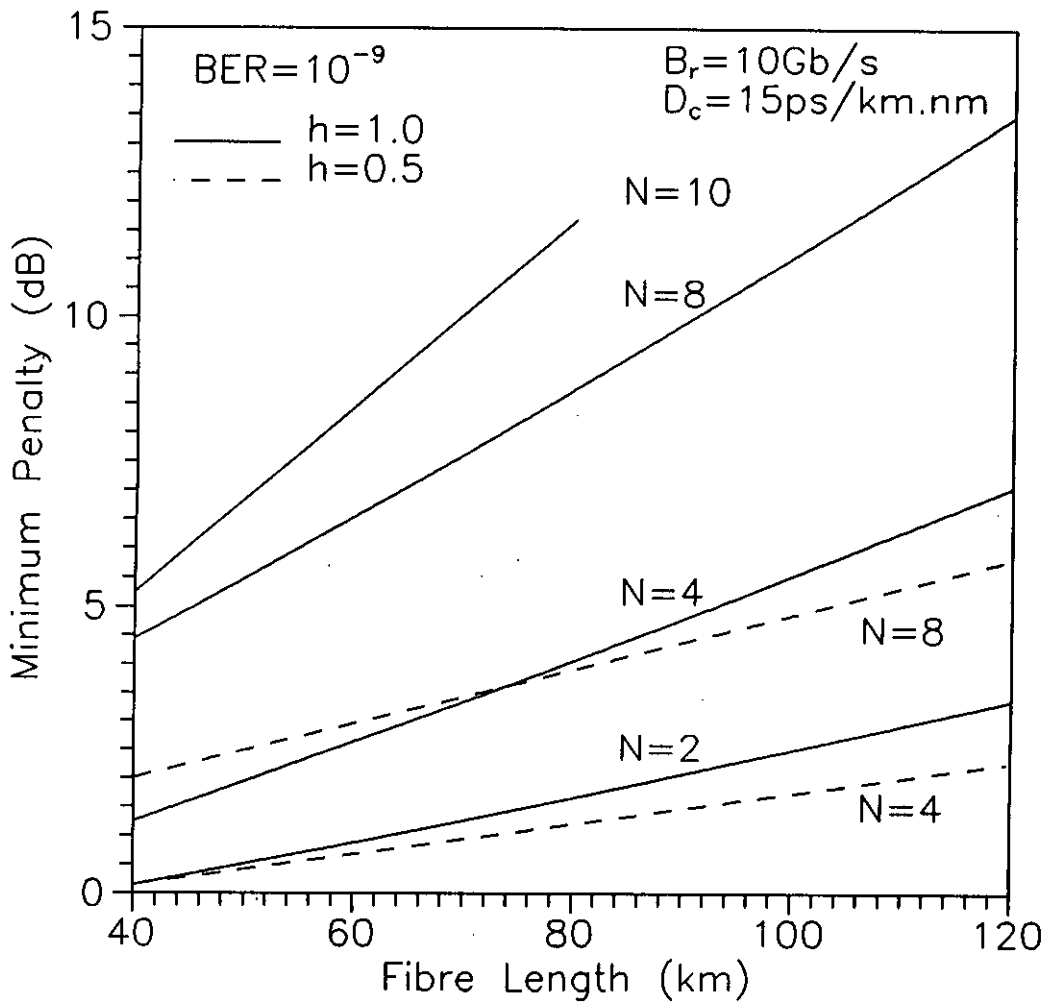


Fig. 3.23 Variation of minimum power penalty in signal power due to fibre chromatic dispersion at $BER=10^{-9}$ versus fibre length (km) with modulation index $h=0.5$ and $h=1.0$ for different number of nodes.

different number of nodes with modulation index $h=1.0$ and $h=0.5$. However, as mentioned before the penalty is found to be higher at higher values of modulation index. It is observed that the penalty increases linearly with fibre length because of the effect of fibre chromatic dispersion. From figure it is concluded that for $L=40$ km the penalty is minimum when number of node $N=2$ but with increase in number of node the penalty becomes higher and highest penalty is obtained when $N=10$. This is due to the fact that with increase in the number of nodes the number of cascaded MUX/DMUX increases as twice the number of EDFAs. So the accumulated ASE noise increases as well as signal magnitude is reduced due to increased filtering effect. As a result system performance is degraded in case of large number of nodes. Similar results are obtained from Fig. 3.24 plotted as a function of nodes for different fibre length when modulation index is $h=1.0$ and $h=0.5$.

For 1 dB power penalty at $BER=10^{-9}$, the allowable channel spacing is plotted in Fig. 3.25 as a function of FP filter bandwidth (nm) for number of node $N=2$, and $h=1.0$. It is observed that the allowable filter bandwidth is higher for larger channel spacing. At channel spacing 0.5nm, allowable filter bandwidth is 1.12 nm for 1.0 dB power penalty but at channel spacing 2.0nm the corresponding $B=1.72$ nm for same power penalty.

The allowable channel spacing is plotted in Fig. 3.26 as a function of FP filter bandwidth (nm) when number of node $N=4$ with modulation index $h=0.5$ and $h=1.0$ for 1.5 dB power penalty at $BER=10^{-9}$. It is noted earlier that at $\Delta F=0.5$ nm for $N=4$ and $h=1.0$ power penalty is higher than 1.5 dB. So no allowable filter bandwidth is available corresponding to 1.5 dB penalty at $\Delta F=0.5$ nm when $h=1.0$. This is because at small channel spacing crosstalk noise power severely degrades system performance. It is also noticed from figure that when h is decreased to 0.5 then allowable filter bandwidth is available at $\Delta F=0.5$ nm for 1.5 dB penalty because for lower values of h penalty

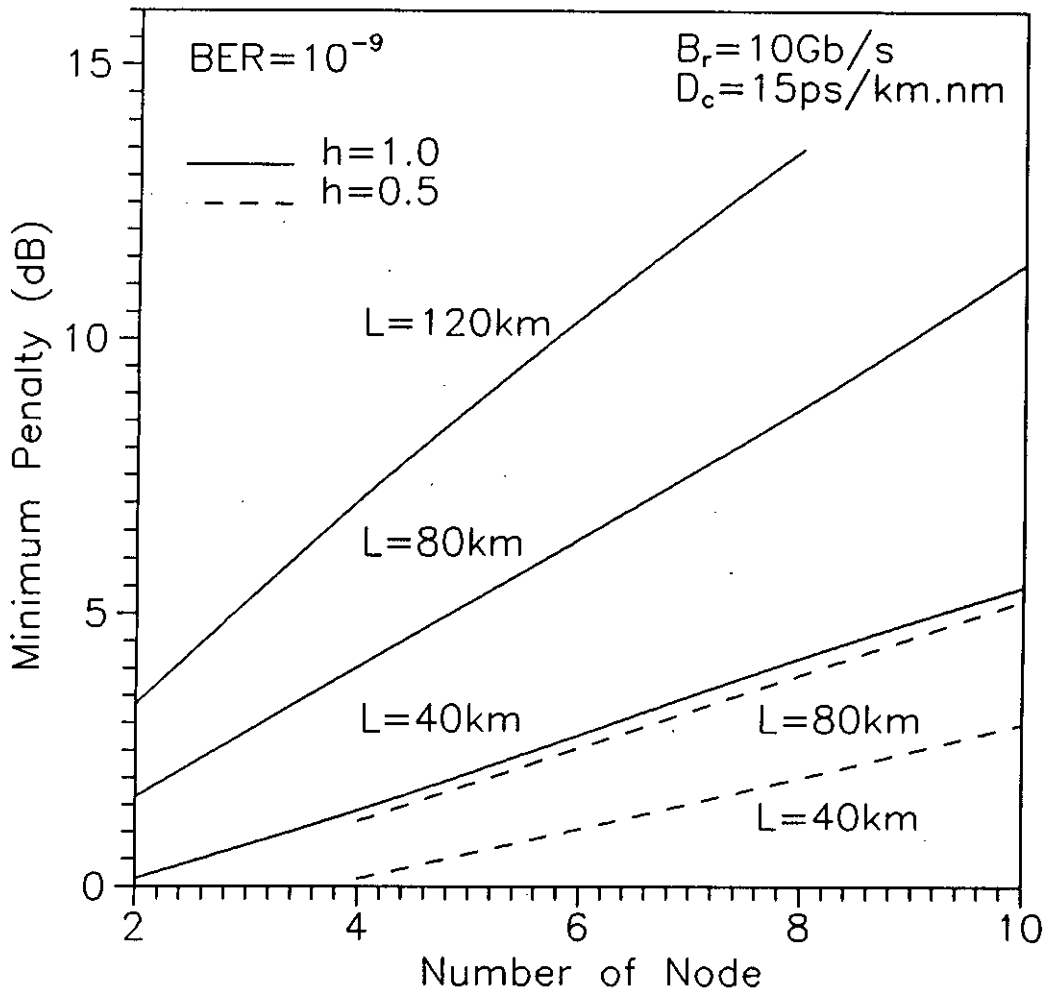


Fig. 3.24 Variation of minimum power penalty in signal power due to fibre chromatic dispersion at BER = 10^{-9} versus number of nodes with channel spacing $\Delta F = 2$ nm and modulation index $h = 0.5$ and $h = 1.0$ for several values of fibre length (km).

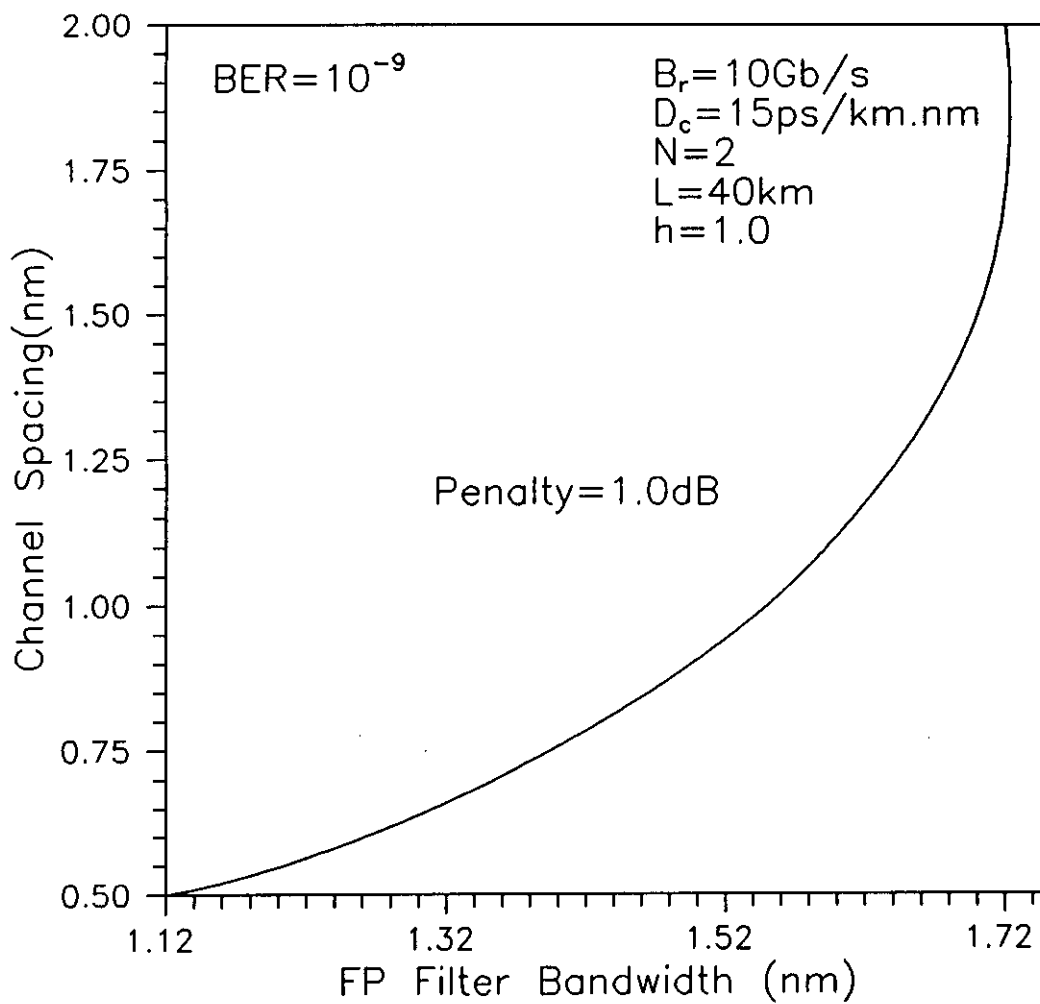


Fig. 3.25 Plots of allowable channel spacing (nm) corresponding to 1dB penalty at $\text{BER} = 10^{-9}$ as a function of FP filter bandwidth (nm) for modulation index $h = 1.0$ number of nodes $N = 2$ and fibre length $L = 40\text{km}$.

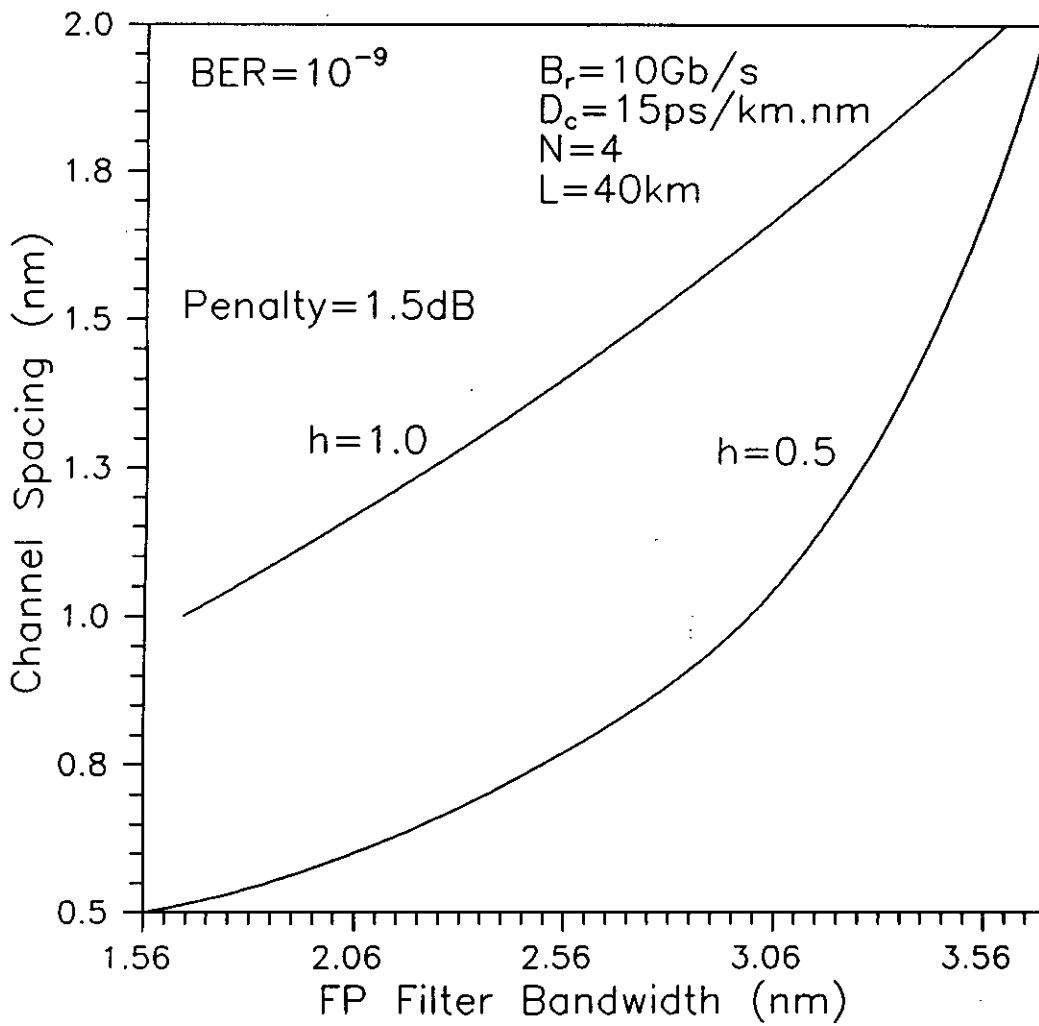


Fig. 3.26 Plots of allowable channel spacing (nm) corresponding to 1.5 dB penalty at $\text{BER} = 10^{-9}$ as a function of FP filter bandwidth (nm) for modulation index $h=0.5$ and 1.0 , number of nodes $N=4$ and fibre length $L=40 \text{ km}$.

bandwidth is 1.56 nm when $h=0.5$ but at channel spacing 1.5 nm the corresponding filter bandwidth is 2.76 nm when $h=0.5$ and 3.46 nm when $h=1.0$ respectively.

CHAPTER-4

CONCLUSION AND SUGGESTIONS FOR FUTURE WORKS

4.1 Conclusion :

A theoretical analysis is provided for an optical WDM ring network consisting of cascaded add-drop MUX/DMUX and EDFAs with direct detection FSK receiver using Mach-Zehnder Interferometer (MZI) as an optical frequency discriminator (OFD). The analysis is carried out to include the combined influence of cascaded filtering effect, ASE noise by the EDFAs, receiver noise, impact of fibre chromatic dispersion and laser phase noise on the system performance. The probability density function of the random phase fluctuation due to effect of fibre chromatic dispersion and laser phase noise is determined from its moments and the expression for bit error probability is developed.

Following the theoretical analysis the bit error rate performance results are evaluated at a bit rate of 10 Gb/s with single mode fibre at an wavelength of 1550 nm for different sets of values of channel spacing, filter bandwidth, number of node and modulation index with fibre chromatic dispersion co-efficient 15 ps/nm.km and fibre attenuation 0.2 dB/km etc.

The results show that in the absence of laser phase noise, the performance of optical WDM ring network is highly degraded due to the combined effect of fibre chromatic dispersion, cascaded filtering and accumulated spontaneous emission noise of EDFAs. For smaller values of filter bandwidth and channel spacing the system suffers penalty in signal power at a specified BER of 10^{-9} , compared to the case of no dispersion. In the presence of laser phase noise, the system performance is more degraded and the penalty is higher. For example in the absence of laser phase noise the penalty suffered by the system at BER= 10^{-9} is approximately 1.25 dB for channel spacing $\Delta F=2.0$ nm when number of node $N=4$ and filter bandwidth $B= 2.0$ nm with fibre span $L=40$ km

and modulation index $h=1.0$. In presence of phase noise, the above penalty is found to be 1.35 dB for same parameters. It is further noticed that the penalty is lower for lower values of modulation index h . For $L=40$ km, $N=4$, $\Delta F=2.0$ nm the penalty is found to be 0.38 dB at filter bandwidth $B=2.0$ nm when $h=0.5$. The penalty in signal power is increased with increased number of node. It is observed that when number of node $N=2$ then penalty is below 1 dB for fibre length $L=40$ km, at $B=2.0$ nm with $h=1.0$. When number of nodes $N>2$ the penalty is more than 1 dB for similar condition.

It is also found that at a particular filter bandwidth the penalty is higher when channel spacing is small for a specific node. The penalty is decreased when channel spacing is further increased for that filter bandwidth and minimum penalty is obtained when channel spacing is optimum. When filter bandwidth is increased or decreased from optimum value, the penalty is significantly increased.

For example, when number of nodes $N=8$, fibre span $L=40$ km, modulation index $h=1.0$, the minimum penalty is found to be 4.5 dB corresponding to optimum optical bandwidth $B=1.0$ nm with $D_c=15$ ps/km.nm. When there is no there is no dispersion ($D_c=0.0$) the penalty in the above case is found to be only 0.25 dB.

When number of nodes N is reduced to 2, the penalty is found to be 2.75 dB with $L=80$ km, $h=1.0$, $B=1.0$ nm and channel separation $\Delta F=0.5$ nm. When ΔF is increased to 1.0 nm, the penalty reduces to 1.7 dB. Further, for $BER=10^{-9}$ corresponding to 1 dB penalty, for $N=4$, $L=40$ km and $h=0.5$, the required values of B are found to be 1.1 nm and 2.15 nm with corresponding channel separation of $\Delta F=0.5$ nm and 0.8 nm respectively.

It is also concluded from our study that the optimum filter bandwidth varies with number of channels. For example when only two channels is propagated through the network then optimum filter bandwidth is $B=0.5$ nm whereas optimum filter bandwidth

is found to be 1.5 nm, 2.0 nm and 3.0 nm when number of propagated channels is increased to four, eight and ten respectively.

Further, we also noticed that for a given value of filter bandwidth B , at $\text{BER}=10^{-9}$ there is an upper limit on channel spacing ΔF at which power penalty is minimum for different number of nodes and fibre length. The penalty is significant when effect of dispersion is considered for $h=1.0$ and is considerably less when h is decreased. But more higher penalty is observed for combined effect of phase noise and dispersion.

For 1 dB power penalty at $\text{BER}=10^{-9}$, the maximum allowable filter bandwidth is higher at higher values of channel spacing. For example, corresponding to $N=2$, $L=40$ km and modulation index $h=1.0$ we observed that when channel spacing $\Delta F=0.5$ nm then allowable filter bandwidth is $B=1.12$ nm and when $\Delta F=2.0$ nm the corresponding filter bandwidth is $B=1.72$ nm. Further, corresponding to 1.5 dB penalty at $\text{BER}=10^{-9}$, for $N=4$, $L=40$ km, it is found that for $\Delta F=0.5$ nm allowable filter bandwidth is $B=1.56$ nm for $h=0.5$ but no filter bandwidth is obtained when $h=1.0$ for same channel spacing. When $\Delta F=2.0$ nm the allowable filter bandwidth is $B=3.7$ nm and $B=3.3$ nm for $h=0.5$ and $h=1.0$ respectively. Thus fibre chromatic dispersion imposes restriction on the filter bandwidths in terms of allowable channel spacing for a specified system penalty at a given BER. At larger number of channels the penalty is much more higher than 1.0 dB.

It is further observed that the allowable fibre length corresponding to 2 dB penalty at $\text{BER}=10^{-9}$ is more than 90 km for $N=2$ and 50 km for $N=4$ when $h=1.0$. When h is decreased to 0.5, the allowable fibre length increases to around 110 km for $N=4$. Further, we also observed that in case of $N=8$ the allowable fibre length reduces to $L=40$ km when $h=0.5$. The allowable fibre length exponentially decreases with increasing number of nodes. Thus, there is considerable reduction in the allowable fibre length due to the effect of fibre chromatic dispersion.

It is concluded that the number of channels of a WDM ring network is limited by the effect of fibre chromatic dispersion, laser phase noise, cascaded EDFAs and FP filters. The node separation is decreased with increased number of nodes. When number of node $N=2$ then larger node separation is possible. The maximum node separation $L=120$ km is observed when number of channels is ten. Further, an increase in number of channels results in decrease of node separation because fibre chromatic dispersion severely degrades the system performance for larger fibre length between nodes. When the number of channel is increased to 15 the maximum node separation is approximately 40 km.

4.2 Suggestions for Future Works:

Further research related to this work can be carried out to investigate the influence of fibre chromatic dispersion on optical bi-direction ring network. The maximum number of channels, optimum channel separation, maximum fibre span limited by the combined effect of fibre chromatic dispersion and laser phase noise at a bit rate 10 Gb/s or higher are to be determine.

Further research works can also be carried out to evaluate the impact of fibre non-linear effect such as fibre Four-Wave-Mixing (FDM), Cross-Phase-Modulation (XPM) and Self-Phase-Modulation (SPM) on the performance of a WDM optical ring network.

Further works of importance are to determine dispersion compensation techniques to reduce the power penalty due to fibre chromatic dispersion so as to increase the repeaterless transmission distance and number of transmittted channels in multichannel WDM optical ring network with single-mode fibres.

References :

- [1] G. Prati, "Coherent Optical Communications and Photonic Switching", Proceedings of the Fourth Tirrenia International Workshop on Digital Communications , Tirrenia, Italy, September 19-23, 1989.
- [2]. F. M. Knox, W. Forysiak and N. J. Doran, "10 Gb/s Soliton Communication Systems over standard fiber at 1550 nm and the use of dispersion compensation," Journal of Lightwave Technology, vol.13, no.10, October 1995, pp. 1955-1962.
- [3]. B. L. Patel, E. M. Kimber, M. G. Taylor, A. N Robinson, I. Hardcastle, A. Hadjifotiou, S. J. Wilson, R. Keys and J. E. Righton, "High performance 10 Gb/s optical transmission system using Erbium-doped fibre amplifier", Electronic Letters vol. 27 no. 23, pp. 2179-2180, Nov. 1991.
- [4]. G. Jacobsen, K. Emura, T. Ono and S. Yamazaki, "Requirements for LD FM characteristics in an optical CPFSK system", Journal of Lightwave Technology, vol. 9, 1991, pp. 1113-1123.
- [5] R. A. Linke and A. H. Granuck, "High-capacity coherent lightwave systems", Journal of Lightwave Tech., Vol.6, pp. 1750-1769, Nov. 1988.
- [6] S. Kobayashi, Y. Yamamoto, M. Saito and T. Kimura, "Direct Frequency modulation in AlGaAs semiconductor lasers", IEEE Journal of Quantum Electron, vol. QE-18, no.4, 1982, pp. 582-595.

- [7]. K. Iwashita and T. Matsumoto, "Modulation and detection characteristics of optical continuous phase FSK transmission system", *Journal of Lightwave Technology*, vol. LT-5, April 1987, pp. 452-260.
- [8]. R .S. Vodhanel, J. L. Gimlet, N. K. Cheung and S. Tsuji, "FSK heterodyne transmission experiments at 560 Mbit/s and 1 Gbit/s", *Journal of Lightwave Technology*, vol. LT-5, April 1987, pp.561-468.
- [9] E. L. Goldstein et al. "Multiwavelength fibre amplifiers cascaded in unidirectional interoffice ring networks", in *Proc. Conf. Opt. Fibre Commun.*, 1992, paper Th1-2.
- [10]. D. J. Malyon and W. A. Stallard, "565 Mb/s FSK direct detection system operating with four cascaded photonic amplifiers", *Electronics Letters*, vol.25, no.8, 1989, pp. 495-496.
- [11] C. Rolland, R. S. Moore, F. Shepherd and G. Hillier, "10 Gb/s. 1560 nm multi quantum well InP/InGaAsP Mach-Zender optical modulator", *Electronic Letters*, vol. 29, no.5, March 1993, pp. 471-472.
- [12] A. R. Charplyvy, "Limitations on Lightwave communication imposed by optical fiber nonlinearities", *Journal of Lightwave Technology*, vol.8, no. 10, October 1990, pp. 1548-1557.
- [13] N. Shibata, K. Nosu, K. Iwashita and Y. Azuma, "Transmission Limitation due to fiber nonlinearities in optical FDM systems", *IEEE Journal on Selected Areas in Communications*, vol.8, no.6, August 1990, pp. 1068-1077.

- [14] D. Cotter, "Stimulated Brillouin scattering in mono mode optical fiber", *J. Opt. Communications*, vol.4, 1983, pp. 10-19.
- [15] K. O. Hill, D. C. Johnson, B. S. Kawasaki and I. R. MacDonald, "CW three-wave mixing in single mode optical fibers", *J. Appl. Phys.*, vol.49, 1978, pp. 5098-5106.
- [16] N. Kikuchi and S. Sasaki "Analytical Evaluation Technology of Self-Phase-Modulation Effect on the Performance of Cascaded Optical Amplifier System", *Journal of Lightwave Technol.* vol. 13, No. 5, pp. 868-878, May 1995.
- [17] M. E. Marhic, N. Kagi, T. K. Chiang and L. G. Kazovsky "Optimizing the Location of Dispersion Compensators Periodically Amplified Fibre Links in the Presence of Third-Order Nonlinear Effects", *IEEE Photon. Technol. Lett.* vol. 8. No. 1, pp.145-147, January 1996.
- [18] B. Glance, K. Pollock, C. A. Burrus, B. L. Kasper, G. Eisenstein and L. W. Stulz, "Density spaced WDM coherent optical star network", *Electronic Letters*, vol.23, 1987, pp. 875-876.
- [19] H. Toba, K. Oda, K. Nosu, N. Takato and H. Miyazawa. "5 GHz spaced eight channel optical FDM transmission experiment using guided wave tunable demultiplexer", *Electronic Letters*, vol.24, 1988, pp. 78-80.
- [20] R. S. Vodhanel, A. F. Elrefaie, M. Z. Iqbal, R. E. Wagner, J.L. Gimlett and S. Tsuji, "Performance of directly modulated DFB lasers in 10 Gb.s ASK, FSK and DPSK Lightwave systems", *Journal of Lightwave Technology*, vol. 8, no. 9, September 1990, pp. 1379-1385.

- [21] A. F. Elrefaie and R. E. Wagner, "Chromatic dispersion limitations for FSK and DPSK systems with direct detection receivers," *IEEE Photonics Technology Letters*, vol.8, no.1, January 1991.
- [22] T. Okoshi, "Heterodyne and coherent optical fiber communications: Recent progress", *IEEE Transactions Microwave Theory Technology*, vol. MTT-30, August 1982, pp. 1138-1149.
- [23] M. Tamburrini, P. Spano and S. Piazzolla, "Influence of semiconductor laser phase noise on coherent optical communication systems", *Optics Letters*, vol.8, no.3, March 1983, pp.174-176.
- [24] J. Salz, "Coherent Lightwave communications," *AT&T Tech. Journal*, vol.64, no.10, Dec. 1985. pp. 2153-2209.
- [25]. I. Garrett and G. Jacobsen, "Theoretical analysis of heterodyne optical receivers for transmission systems using (semiconductor) lasers with non-negligible line width," *Journal of Lightwave Technology*, vol. LT-4, March 1986, pp. 323-334.
- [26] J. Franz, C. Rapp and G. Soder, "Influence of baseband filtering on laser phase noise in coherent optical transmission systems," *Journal of Optical Communications*, vol.7, no.1, March 1986, pp. 15-20.
- [27] K. Emura, S. Yamazaki, S. Fujita, M. Shikida, I. Mito and K. Minemura, "Over 300 km transmission experiment on an optical FSK heterodyne dual filter detection system", *Electronic Letters*, vol.22, no.21, October 9, 1986, pp. 1096-1097.

- [28] I. Garrett and G. Jacobsen, "The effect of laser line width on coherent optical receivers with non-synchronous demodulation", *Journal of Lightwave Technology*, vol. LT-5, April 1987, pp. 551-560.
- [29]. N. A. Olsson, "Lightwave systems with Optical Amplifiers", *Journal of Lightwave Technology*, Vol.7, pp. 1071-1082, July 1989.
- [30]. S. Shigeru, A. Mamorsu and I. Takeshi "System Performance of Coherent Transmission Over Cascaded In-Line Fibre Amplifiers", *Journal of Lightwave Technology*, Vol.11, No.2 February 1993.
- [31]. T. Hidenori "Long Distance Transmission Experiments Using the WDM Technology", *Journal of Lightwave Technology*, Vol.14, No.6, June 1996.
- [32]. N. Antoniadis, I. Roudas, R.E. Wagner, and S.F. Habiby, "Simulation of ASE noise accumulation in a wavelength add/drop Multiplexer Cascaded". *IEEE Photonics Technology Letters*, Vol.9, No.9, September 1997.
- [33]. J. Zhou, R. Cadeddu, E. Casaecia, C. Cavazzoni, and M. J. O'Mahony, "Cross-talk in Multiwavelength Optical Cross-Connect Networks", *Journal of Lightwave Technolgy*, Vol.14, No.6, June 1996.
- [34]. S. D. Dods, P. R. Lacey and R. S. Tucker, "Homodyne Crosstalk in WDM Ring and Bus Networks", *IEEE photonics Technology Letters*, Vol.9, No.9, September 1997.

- [35]. P. J. Legg, M. Tur, and I. Andonovic, "Solution paths to Limit Interferometric Noise Induced Performance Degradation in ASK/Direct Detection Lightwave Networks", *Journal of Lightwave Technology*, Vol.14, No. 9, September 1996.
- [36]. K. Inoue, H. I. Toba, "Fibre Four-Wave-Mixing in Multi-Amplifier Systems with Nonuniform Chromatic Dispersion", *Journal of Lightwave Technology*, Vol.13, No.1, January 1995.
- [37]. A. A. Al-Orainy, "Analysis of Crosstalk in WDM-Ring Networks", *IEEE Photonics Technology Letters*, Vol. 5, No.12, December 1993.
- [38]. A. F. Elrefaie "Multiwavelength Survivable Ring Network Architectures", *IEEE International Conference on Communication ICC'93*, May 1993, Paper 48.7.
- [39]. B. Glance, C. R. Doerr, I. P. Kaminow, and R. Montagne "Optically Restorable WDM Ring Network Using Simple Add/Drop Circuitry", *Journal of Lightwave Technology*, Vol.14, No. 11, November 1996.
- [40] N. Takato, T. Kominato, A. Sugita, K. Jinguji, H. Toba and M. Kawachi "Silica- Based Integrated Optic Mach-Zender Multi/Demultiplexer Family with Channel Spacing of 0.01-250 nm", *IEEE Journal on Selected areas in Communications* Vol. 8 No. 6, August 1990.
- [41] E. Bedrosian and S. O. Rice, "Distortion and crosstalk of linearly filtered, angle-modulated signals", *Proc. IEEE* vol. 56, pp. 2-13, Jan. 1968.

- [42] L. G. Kazovsky, "Multichannel Coherent Optical Communications Systems", J. Lightwave Technol., vol. LT-5, no. 8, pp. 1050-1102, Aug. 1987.
- [43] L. G. Kazovsky and J. Gimlett , "Sensitivity Penalty in Multichannel Coherent Optical Communication", J. Lightwave Technol., vol. LT-6, no. 8, pp. 1353-1365, Aug. 1988.
- [44] R. Gangopadhyay, S. P. Majumder , P. Cochrane and E. Forestieri "Performance Analysis of a Direct Detection Receiver for AMI coded CPFSK Signals", IEEE Photon. Technol. Lett., vol.7, pp. 552-554, May 1995.

APPENDIX-A

Output of PD :

Generated photo-current at the output of photodetector is given by

$$\begin{aligned}
 i(t) &= R_d \bar{E}^2(t) \\
 &= R_d \left\{ \sqrt{2P_s GLI} \exp[j\{2\pi f_o t + \theta_s(t)\}] \right. \\
 &\quad + \sqrt{2P_c GLI_x} \exp[j\{2\pi(f_o + \Delta F)t + \theta(t)\}] \\
 &\quad \left. + \sum_{k=-N}^{k=N} \sqrt{2N_o \Delta \nu G_a L} \text{Cos}[(w_o + 2\pi k \Delta \nu)t + \phi_k] \right\}^2 \\
 i(t) &= R_d \left[2P_s GLI \text{Cos}^2(w_o t + \theta_s(t)) + 2P_c GLI_x \text{Cos}^2\{(w_o + 2\pi \Delta F)t + \theta_s(t)\} \right. \\
 &\quad + \sum_{k=-N}^K 2N_o \Delta \nu G_a L \text{Cos}^2\{(w_o + 2\pi k \Delta \nu)t + \phi_k\} \\
 &\quad + 2\sqrt{2P_s GLI} \sqrt{2P_c GL_x} \text{Cos}\{w_o t + \theta_s(t)\} \text{Cos}\{(w_o + 2\pi \Delta F)t + \theta_s(t)\} \\
 &\quad + 2\sqrt{2P_s GLI} \sum_{k=-N}^N \sqrt{2N_o \Delta \nu G_a L} \text{Cos}\{w_o t + \theta_s(t)\} \text{Cos}\{(w_o + 2\pi k \Delta \nu)t + \phi_k\} + \\
 &\quad \left. 2\sqrt{2P_c GLI_x} \sum_{k=-n}^N \sqrt{2N_o \Delta \nu G_a L} \text{Cos}\{2\pi(f_o + \Delta F)t + \theta_s(t)\} \text{Cos}\{(w_o + 2\pi k \Delta \nu)t + \phi_k\} \right]
 \end{aligned}$$

$$i(t) = i_s(t) + i_c(t) + i_{s-sp}(t) + i_{c-sp}(t) + i_{sp-sp}(t) + i_{th}(t) + i_{sh}(t)$$

where $i_s(t)$ represents the signal current, $i_c(t)$ is the current due to crosstalk signal, $i_{s-sp}(t)$ is the current due to signal-spontaneous emission beat noise, $i_{c-sp}(t)$ is the cross-talk spontaneous beat noise, $i_{sp-sp}(t)$ is the spontaneous-spontaneous beat noise, $i_{th}(t)$ is the receiver thermal noise and $i_{sh}(t)$ is the photodetector shot noise.

Signal-spontaneous Beat Noise :

$$\begin{aligned}
 i_{s-sp}(t) &= 2R_d \sqrt{2P_s G L I} \sum_{k=-N}^N \sqrt{2N_o \Delta \nu G_a L} \text{Cos}\{w_o t + \theta_s(t)\} \cdot \text{Cos}\{(w_o + 2\pi k \Delta \nu)t + \phi_k\} \\
 &= 2R_d \sqrt{4P_s G L I N_o G_a L \Delta \nu} \sum_{k=-N}^N \frac{1}{2} \left[\text{Cos}(2\pi k \Delta \nu t + \phi_k + \theta_s(t)) + \right. \\
 &\quad \left. \text{Cos}\{(2w_o + 2\pi k \Delta \nu)t + \phi_k + \theta_s(t)\} \right]
 \end{aligned}$$

$\text{Cos}2w_o t$ term averages to zero. For each frequency, $2\pi k \Delta \nu$ the sum has two components but with a random phase. Therefore, the power spectrum of $i_{s-sp}(t)$ is uniform in the frequency interval $0 - B_o/2$ and has a density of

$$N_{s-sp} = \left\{ 2R_d \sqrt{P_s G L I G_a N_o \Delta \nu L} \right\}^2 \frac{1}{2} \times 2$$

$$N_{s-sp} = 4R_d q P_s G (G-1) L^2 I G_a [N_{sp} \otimes G_{FSK-PN}(f)]$$

where $R = \frac{\eta q}{h \nu}$, let $\eta = 1$ and $N_o = N_{sp} (G-1) h \nu$, $G_{FSK-PN}(f)$ is the normalized PSD of FSK signal corrupted by phase noise.

The single-sided power spectral density (PSD) of the FSK modulated signal without laser phase noise is given by [43]

$$G_{FSK}(f) = \frac{T}{8} \left[\sum_{i=1}^2 A_i(\nu) + \sum_{i=1}^2 \sum_{j=1}^2 A_i(\nu) \cdot A_j(\nu) \cdot B_{ij}(\nu) \right] \quad 0 < f < \infty$$

where $T = \frac{1}{B_r}$ is the bit duration $\nu = fT$ and $G_{FSK}(f)$ is the normalized PSD

of the FSK signal.

where

$$A_i(\nu) = P(\alpha_i)$$

with

$$\alpha_i = [f - (2i-3)\Delta f]T$$

and

$$B_{ij}(\nu) = \frac{\text{Cos}(2\pi\nu - \gamma_{ij}) - \psi \text{Cos}(\gamma_{ij})}{1 + \psi^2 - 2\psi \text{Cos}(2\pi\nu)}$$

with $\psi = \text{Cos}(\pi\delta)$, $\gamma_{11} = -\pi\delta$, $\gamma_{12} = \gamma_{21} = 0$ and $\gamma_{22} = \pi\delta$ respectively

Spontaneous crosstalk Beat Noise :

$$\begin{aligned} i_{r-sp}(t) &= 2R_d \sqrt{2P_c G L I_x} \sum_{k=-N}^N \sqrt{2N_o \Delta\nu G_a L} \text{Cos}\{2\pi(f_o + \Delta F)t + \theta_i(t)\} \\ &\quad \text{Cos}\{(w_o + 2\pi k \Delta\nu)t + \phi_k\} \\ &= 2R_d \sqrt{4P_c G L I_x N_o \Delta\nu G_a L} \sum_{k=-N}^N \frac{1}{2} [\text{Cos}\{(2f_o + \Delta F + k\Delta\nu)2\pi t + \phi_k + \theta_i(t)\} \\ &\quad + \text{Cos}\{(k\Delta\nu + \Delta F)2\pi t + \theta_i(t) + \phi_k\}] \end{aligned}$$

For each frequency $2\pi k \Delta\nu$ has two components therefore PSD is uniform and density is given by

$$\begin{aligned} N_{c-sp} &= \left\{ 2R_d \sqrt{P_c G L^2 I_x G_a N_o \Delta\nu} \right\}^2 \frac{1}{2} \times 2 \\ N_{c-sp} &= 4qR_d P_c G(G-1)L^2 I_x G_a [N_{sp} \otimes G_{FSK-PN}(f + \Delta F)] \end{aligned}$$

Spontaneous - Spontaneous Beat Noise :

$$\begin{aligned} i_{sp-sp}(t) &= R_d \sum_{k=-N}^K 2N_o \Delta\nu G_a L \text{Cos}^2\{(w_o + 2\pi k \Delta\nu)t + \phi_k\} \\ &= 2N_o \Delta\nu G_a L R_d \left[\sum_{k=-N}^K \text{Cos}^2\{(w_o + 2\pi k \Delta\nu)t + \phi_k\} \right] \\ &= 2N_o \Delta\nu G_a L R \left[\sum_{k=-N}^N \text{Cos}(B_k) \sum_{j=-N}^N \text{Cos}(B_j) \right] \end{aligned}$$

where $B_k = (w_o + 2\pi k \Delta\nu)t + \phi_k$ and $B_j = (w_o + 2\pi k \Delta\nu)t + \phi_k$

So, above equation can be written as

$$i_{sp-sp}(t) = 2N_o \Delta \nu G_a LR \left[\sum_{k=-N}^K \sum_{j=-N}^N \frac{1}{2} \{ \text{Cos}(B_k - B_j) + \text{Cos}(B_k + B_j) \} \right]$$

But terms $\text{Cos}(B_k + B_j)$ have frequencies $2\omega_o$ and averages to zero.

So, we can write

$$i_{sp-sp}(t) = N_o \Delta \nu G_a LR_d \left[\sum_{k=0}^{2K} \sum_{j=0}^{2N} \text{Cos}\{(k-j)2\pi k \Delta \nu t + \phi_k - \phi_j\} \right]$$

The DC term is obtained for $k=j$ and there are $2M$ such terms.

$$I_{sp}^{dc} = 2G_a LR_d N_o \Delta \nu N = N_{sp} (G-1) q G_a L$$

Therefore, the power spectrum of the spontaneous-spontaneous beat noise extends from 0 to B_o with a triangular shape and a power spectral density near dc is

$$N_{sp-sp} = 2q^2 G_a N_{sp}^2 (G-1)^2 L^2 \int_{-\infty}^{\infty} |H'(f)|^2 df$$

